OUKA
The University of Osaka
Institutional Knowledge Archive

Title	Research on Bionanosensor Networks for Target Detection and Tracking
Author(s)	岡家, 豊
Citation	大阪大学, 2015, 博士論文
Version Type	VoR
URL	https://doi.org/10.18910/52030
rights	
Note	

The University of Osaka Institutional Knowledge Archive : OUKA

https://ir.library.osaka-u.ac.jp/

The University of Osaka

Research on Bionanosensor Networks for Target Detection and Tracking

January 2015

Yutaka OKAIE

Research on Bionanosensor Networks for Target Detection and Tracking

Submitted to
Graduate School of Information Science and Technology
Osaka University

January 2015

Yutaka OKAIE

Lisf of Publications

1. Journal Papers

1. Y. Okaie, T. Nakano, T. Hara, T. Obuchi, K. Hosoda, Y. Hiraoka and S. Nishio, "Cooperative Target Tracking by a Mobile Bionanosensor Network," *IEEE Transactions on NanoBioscience*, Vol. 13, No. 3, pp. 267 - 277, Sept. 2014.

2. Y. Okaie, T. Nakano, T. Hara and S. Nishio, "Autonomous Mobile Bionanosensor Networks for Target Tracking: A Two-dimensional Model," *Nano Communication Networks*, Vol. 5, Issue 3, pp. 63 - 71, Sept. 2014.

3. Y. Okaie, T. Nakano, T. Hara and S. Nishio, "Distributing Nanomachines for Minimizing Mean Residence Time of Molecular Signals in Bionanosensor Networks," *IEEE Sensors Journal*, Vol. 14, No. 1, pp. 218 - 227, Jan. 2014.

2. International Conference Papers

1. Y. Okaie, T. Nakano, T. Obuchi, T. Hara and S. Nishio, "Bacterium-based Mobile Bionanosensor Networks for Target Tracking: A Biologically Realistic Model," *in Proceedings of 8th International Conference on Bio-Inspired Information and Communications Technologies*, Massachusetts, U.S.A., Dec. 2014.

2. T. Nakano, T. Hara, Y. Okaie, T. Obuchi and S. Nishio, "Mobile bionanosensor networks through molecular communication," *in Proceedings of Asia-Pacific Microwave Conference (APMC 2014)*, pp. 525 - 527, Miyagi, Japan, Nov. 2014.

3. Y. Okaie, T. Nakano, T. Hara, K. Hosoda, Y. Hiraoka and S. Nishio, "Modeling and Performance Evaluation of Mobile Bionanosensor Networks for

Target Tracking," *in Proceedings of IEEE International Conference on Communications (ICC 2014)*, pp. 3969 - 3974, Sydney, Australia, June 2014.

4. Y. Okaie, T. Nakano, T. Hara and S. Nishio, "Single Target Tracking in Bionanosensor Networks: Preliminary Simulation Results," *in Proceedings of International Conference on Body Area Networks (BodyNets 2013)*, pp. 476 - 477, Massachusetts, U.S.A., Sept. 2013.

5. T. Nakano, M. J. Moore, Y. Okaie, A. Enomoto and T. Suda, "Cooperative Drug Delivery through Molecular Communication among Biological Nanomachines," *in Proceedings of IEEE International Workshop on Molecular and Nanoscale Communications (MoNaCom 2013)*, pp. 809 - 812, Budapest, Hungary, June 2013.

6. T. Nakano, M. J. Moore, Y. Okaie, A. Enomoto and T. Suda, "Swarming Biological Nanomachines Through Molecular Communication for Targeted Drug Delivery," *in Proceedings of 6th International Conference on Soft Computing and Intelligent Systems & The 13th International Symposium on Advanced Intelligent Systems (SCIS-ISIS 2012)*, pp. 2317 - 2320, Kobe, Japan, Nov. 2012.

7. Y. Okaie and T. Nakano, "Sensor Placement Strategies for Detecting Brownian Molecules in Nanonetworks," *in Proceedings of IEEE Wireless Communications and Networking Conference (WCNC 2012)*, pp. 1777 - 1781, Paris, France, Apr. 2012.

8. Y. Okaie, M. J. Moore and T. Nakano, "Propagation Delay of Brownian Molecules in Nano-biosensor Networks," *in Proceedings of 6th International Conference on Bio-Inspired Models of Network, Information, and Computing Systems (BIONETICS 2011)*, York, England, Dec. 2011.

3. Oral Presentations

1. Y. Okaie, "Nanomachine Distribution Problems in Nanonetworks: Optimization and Heuristics," *IEEE International Workshop on Molecular and Nanoscale Communication (MoNaCom 2012)*, Ottawa, Canada, June 2012.

Abstract

Recent decades have witnessed remarkable progress in research and development of *bionanosensors*, nano-to-microscale devices made of biomaterials. A bionanosensor implements a set of simple functionalities to manipulate molecules in the environment. Examples of bionanosensors include DNA molecules designed to perform logical operations, motor proteins reconstructed to transport molecules in an engineered environment, and genetically engineered cells capable of sensing biochemical conditions of the environment.

Since bionanosensors are made of biomaterials and operate based on chemical energy, applications in biomedical domains are highly anticipated. Due to their small size, however, individual bionanosensors are limited in operational ranges and functionalities; bionanosensors need to form a network to cover larger areas and to perform complex functionalities for specific applications. This gives birth to a new interdisciplinary research area, called *bionanosensor networks*.

The area of bionanosensor networks aims at establishing methodologies to form robust and functional networks from spatially distributed bionanosensors. It also aims at developing innovative applications of such networks that are not readily realizable with existing network technologies (e.g., wireless communication technologies).

In this thesis, we consider two major classes of problems in nanomedical applications of bionanosensor networks: *target detection* and *target tracking*. Targets in such applications can be disease sites or infectious microorganisms that represent potential threat to the environment, and timely detection of targets and tracking of targets are important to provide immediate treatments or further analysis of the environment. In this thesis, we design two types of bionanosensor networks: *static* and *dynamic* to attack the target detection or tracking problem. Here a static bionanosensor network consists of bionanosensors that are immobilized to perform application functionality, while a dynamic bionanosensor network consists of bionanosensors that autonomously migrate to perform application functional-

ity.

This thesis consists of five chapters. In Chapter 1, we first describe the background of bionanosensor network research. We then introduce research challenges in bionanosensor networks and define objectives of this thesis. We also illustrate an architecture of bionanosensor networks and review related work to highlight contributions of this thesis.

In Chapter 2, we consider a static bionanosensor network for target detection application. In this type of bionanosensor network, bionanosensors are statically placed in the monitoring environment to detect targets that randomly walk in the environment. We formulate the target detection problem as an optimization problem to find a spatial distribution of bionanosensors that can minimize mean residence time of targets. We then mathematically analyze the problem under the condition that target arrival locations follow the uniform distribution: for one-dimensional environment, we find the optimal solution, and for n-dimensional environment ($n \geq 2$), we provide the lower bound expression. Furthermore, in a two-dimensional environment, where analytical approaches are not available, we assume that target arrival locations follow the normal distribution and conduct simulation experiments to compare the performance of several placement schemes in terms of mean residence time.

In Chapter 3, we consider a dynamic bionanosensor network for target tracking. In this type of bionanosensor network, autonomous mobile bionanosensors use repellents and attractants to detect and track a moving target. Bionanosensors release repellents to spread over the monitoring environment in search of targets, while they release attractants to gather around a target location. We develop a mathematical model to describe the spatio-temporal dynamics of bionanosensors, repellents, and attractants, and demonstrate through numerical experiments that the dynamic bionanosensor network is able to locate and track a moving target under varieties of settings.

In Chapter 4, we investigate through in silico experiments the feasibility of using bacteria as bionanosensors to form a dynamic bionanosensor network. A

bacterium is a microscale organism capable of sensing environmental conditions, producing chemical substances, and actively moving in the environment. Also, it can be genetically engineered to modify these functionalities. We first develop a mobility model of bacterium-based bionanosensors, and then evaluate the ability of bacterium-based bionanosensors to locate and track moving targets. Simulation results demonstrate that a group of bacterium-based bionanosensors is able to track a moving target when the combined use of attractants and repellents is employed, indicating that bacteria are promising materials to implement bionanosensors for target tracking.

Finally, Chapter 5 discusses future research challenges to conclude this thesis.

Contents

1 Introduction **1**

1.1 Background 1

1.2 Research Challenges and Objectives 2

1.3 Architecture of Bionanosensor Networks 3

1.3.1 Monitoring Environment 3

1.3.2 Targets 3

1.3.3 Bionanosensors 4

1.3.4 External Devices 5

1.4 Related Work 6

1.4.1 Wireless Sensor Networks (WSNs) 6

1.4.2 Molecular Communication and Nanonetworks 7

1.4.3 Drug Delivery Systems 8

1.4.4 Systems/Synthetic Biology 9

1.5 Thesis Organization 10

1.5.1 Static Bionanosensor Networks for Target Detection . . . 11

1.5.2 Dynamic Bionanosensor Networks for Target Tracking . . 11

1.5.3 Bacterium-based Bionanosensor Networks for Target Tracking 12

2 Static Bionanosensor Networks for Target Detection **13**

2.1 Overview 13

2.2 Problem Formulation 16

2.2.1 Mean Residence Time in One Dimension 18
2.2.2 Mean Residence Time in Higher Dimensions 21
2.3 Analysis of Mean Residence Time 21
2.3.1 Mean Residence Time in One Dimension 21
2.3.2 Mean Residence Time in Higher Dimensions 22
2.4 Simulation Experiments 24
2.4.1 Bionanosensor Placement Approaches 24
2.4.2 Simulation Model and Configurations 25
2.4.3 Simulation Results 26
2.5 Summary 33

3 Dynamic Bionanosensor Networks for Target Tracking 35
3.1 Overview 35
3.2 PDE-based Model 37
3.2.1 Dynamics of Bionanosensor Concentration 39
3.2.2 Dynamics of Attractant Concentration 41
3.2.3 Dynamics of Repellent Concentration 42
3.3 Numerical Experiments 43
3.3.1 Numerical Method 43
3.3.2 Impact of Attractants 44
3.3.3 Impact of Repellents 50
3.3.4 Target Tracking 51
3.4 Summary 59

4 Bacterium-based Bionanosensor Networks for Target Tracking 65
4.1 Overview 65
4.2 Model of Bacterium-based Bionanosensors 68
4.2.1 Mobility Model 68
4.2.2 Interactions among Bionanosensors 71
4.3 Simulation Experiments 73
4.3.1 Simulation Algorithms 73

4.3.2 Impact of Repellents 74
4.3.3 Impact of Attractants 78
4.3.4 Target Tracking 85
4.4 Summary 89

5 Conclusion **91**
5.1 Summary of Thesis 91
5.2 Future Work 93
5.2.1 Wet Laboratory Experiments 93
5.2.2 Robust Molecular Communication Methods 93
5.2.3 Protocols and Architectures 94
5.2.4 Interfaces with External Devices 94
5.2.5 Noise Effects 95

Acknowledgment **97**

Chapter 1

Introduction

1.1 Background

Recent decades have witnessed remarkable progress in research and development of *bionanosensors*, nano-to-microscale devices made of biomaterials. A bionanosensor implements a set of simple functionalities to manipulate molecules in the environment. Examples of bionanosensors include nanoscale molecular complexes such as DNA molecules designed to perform logical operations [12] and motor proteins reconstructed to transport molecules in an engineered environment [30]. Examples of bionanosensors also include micro-scale, genetically engineered cells that are capable of simple tasks such as sensing biochemical conditions of the environment [75].

Since bionanosensors are made of biomaterials and operate based on chemical energy, applications in biomedical domains are highly anticipated. Due to their small size, however, individual bionanosensors are limited in operational ranges and functionalities; bionanosensors need to form a network to cover larger areas and to perform complex functionalities for target applications. This gives birth to a new interdisciplinary research area, called *bionanosensor networks* [1, 3, 8, 56].

The area of bionanosensor networks aims at establishing methodologies to form robust and functional networks from spatially distributed bionanosensors.

It also aims at developing innovative applications of such networks that are not readily realizable with existing network technologies (e.g., wireless communication technologies). Envisioned applications of bionanosensor networks include (1) targeted drug delivery where bionanosensors storing drug molecules cooperatively spread in the human body to locate disease sites and deliver drug molecules to disease sites, (2) immune system support where bionanosensors communicate location information of foreign agents and cooperatively track and attack foreign agents, and (3) tissue engineering where bionanosensors coordinately distribute over a cellular environment and control developmental processes to form a desired tissue structure.

1.2 Research Challenges and Objectives

Bionanosensor networks are expected to face several challenges that are encountered in Wireless Sensor Networks (WSNs) such as placement of sensor nodes and algorithm design to coordinate the behavior of sensor nodes. Existing techniques and algorithms for WSNs may apply to address such challenges in bionanosensor networks, however, new constraints need to be considered. First, approaches for bionanosensor networks need to be biologically implementable and compatible with bionanosensor design. Second, it is crucial to consider the noise effect on the behavior of bionanosensors and their network, since bionanosensor networks are deployed in a small-scale aqueous environment. Third, interactions among bionanosensors and the environment are based on physical contact and chemical reactions, requiring the need of new computational or mathematical models to design such networks.

Under the aforementioned constraints, in this thesis, we consider two major classes of nanomedical applications of bionanosensor networks: *target detection* and *target tracking*. Target detection is a functionality of bionanosensor networks to detect a target in a given environment, while target tracking is another functionality to detect targets and track targets as they move. In nanomedical applications,

targets can be disease sites, pathogens, infectious micro-organisms, or biochemical weapons that represent potential threat to the environment, and timely detection of targets and tracking of targets are important to provide immediate treatments or further analysis of the environment. Further, in this thesis, we consider two types of bionanosensor networks: *static* and *dynamic*. A static bionanosensor network consists of bionanosensors that are immobilized to perform application functionality, while a dynamic bionanosensor network consists of bionanosensors that autonomously move in the environment to perform application functionality.

1.3 Architecture of Bionanosensor Networks

Fig. 1.1 shows a reference architecture of bionanosensor networks considered in this thesis. The key components include the monitoring environment, targets, bionanosensors, and external devices. In the following subsections, we define these components, describe our assumptions, and give some examples for each of these components.

1.3.1 Monitoring Environment

The monitoring environment is where bionanosensor networks are deployed for target detection and tracking. It is typically a nano-to-micro scale and aqueous environment. It may contain molecules and energy sources for bionanosensor networks to operate. It may also contain noise sources such as thermal noise and molecules that may interfere with the operation of bionanosensor networks. An example of the monitoring environment is the internal environment of the human body.

1.3.2 Targets

Targets are biochemical objects that appear in the monitoring environment. Targets perform particular motion in the environment. For instance, they may move

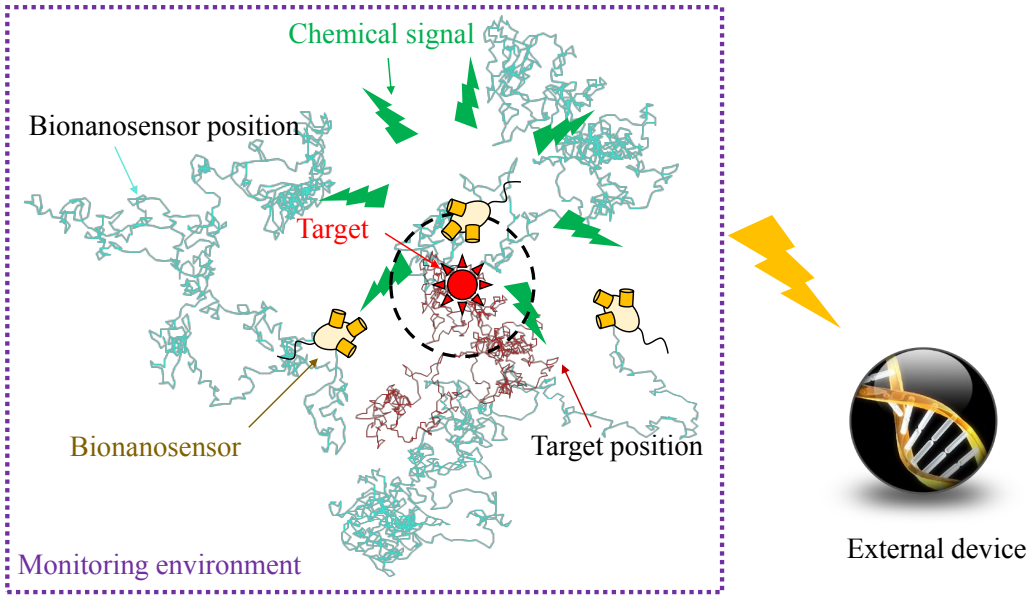


Figure 1.1: Architecture of bionanosensor networks

randomly due to the thermal noise in the environment; they may also move directionally by using chemical energy or by following the flow (e.g., blood flow) in the environment. Targets are chemically identifiable. For instance, targets may express specific proteins on their surface, and bionanosensors may physically contact with the surface receptors of targets to identify the targets. Targets may also secrete biomarkers, indicating the presence of the targets, and bionanosensors in the vicinity of targets may use receptors for the biomarkers to learn the presence of the targets. Examples of targets include pathogens, infectious micro-organisms, or chemical weapons.

1.3.3 Bionanosensors

A bionanosensor is defined based on three criteria: material, size and functionality [51, 56, 61]. A bionanosensor is composed of biomaterials (e.g., proteins, nucleic acids, lipids, biological cells) with or without non-biomaterials (e.g., magnetic particles and gold nanorods). The size of a bionanosensor ranges from the

size of a macromolecule to that of a biological cells (i.e., dimensions of 1 – 100 nm). A bionanosensor implements a set of simple functionalities to manipulate molecules, such as detecting, modifying and releasing molecules. Examples of bionanosensors include:

- DNA sequences capable of detecting a complementary or partially complementary DNA sequence in the environment and cutting and releasing a segment of the detected DNA sequence using enzymes [12],
- Protein motors capable of binding to a specific type of molecules, moving along protein filaments carrying the molecules, and unbinding the molecules when certain environmental conditions are met [30],
- Liposomes capable of storing and releasing certain types of molecules [83] (Fig. 1.2 (a)),
- Single cell organisms and genetically engineered cells capable of actively moving in the environment [90], performing logical operations [87], or detecting a range of concentration of a certain type of molecules in the environment [11] (Fig. 1.2 (b)), and
- Biological cells surface-coated with non-biological materials (e.g., magnetic particles and gold nanorods) to perform non-cell-native functions (e.g., absorbing mercury) [28].

1.3.4 External Devices

An external device is a micro or larger scale conventional device that replies on "traditional" signals such as electrical and optical signals that are not directly compatible with chemical signals used by bionanosensors. An external device may be made from materials that are not compatible with the monitoring environment, and may be orders of magnitude larger than bionanosensors. An external device

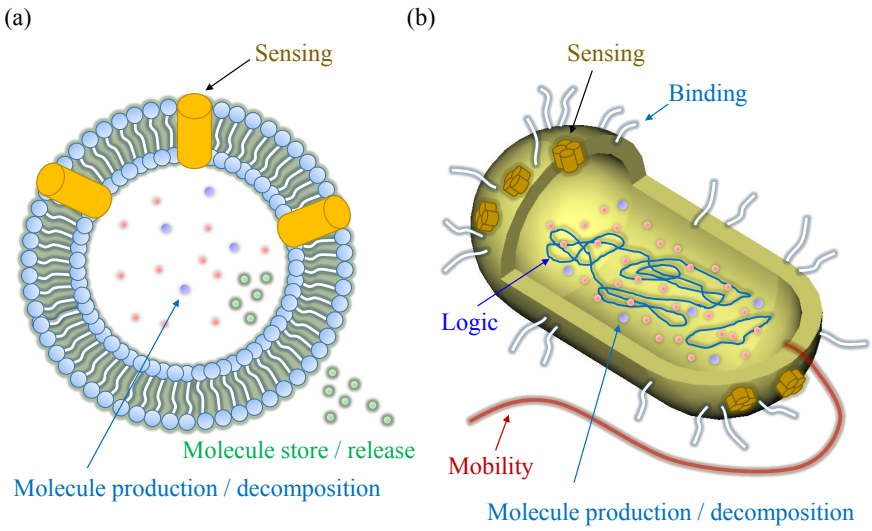


Figure 1.2: Examples of bionanosensors. (a) Liposomes and (b) genetically engineered cells.

functions as a gateway that interconnects a bionanosensor network with external networks such as body area networks [3,10]. Examples of external devices include implantable medical devices [41].

1.4 Related Work

1.4.1 Wireless Sensor Networks (WSNs)

The area of wireless sensor networks (WSNs) leverages data collected from spatially distributed sensors for monitoring, analyzing and controlling environments such as battle fields, chemical factories, and ocean environments [38]. A variety of design strategies are developed to improve performance of WSNs [93], such as coverage (how well the area of interest is monitored by sensors), network connectivity (how efficiently or robustly sensors can relay data to the neighboring sensors and base stations), lifetime longevity (how long time a WSN can be managed guaranteeing some requirements, such as coverage and network connec-

tivity), and data fidelity (how precise and reliable the sensed data in the area of interest).

One of the killer applications of WSNs is target detection and tracking, which involves detecting targets (e.g., animals) entering a monitoring area, estimating their positions, and notifying sink nodes (i.e., data collection points) of their positions as they move [38]. Types of sensor networks for such applications can be either *static* or *dynamic*. In a static sensor network [42], for example, static sensors are hierarchically organized in order to relay location information about targets along the hierarchy toward its root node. In other examples of static sensor networks [89, 94], statically deployed sensors are activated or deactivated dynamically to track moving targets in an energy efficient manner. On the other hand, in dynamic sensor networks, mobile sensors move to detect and track moving targets [76, 95]. Such dynamic sensor networks may utilize a controller node to navigate mobile sensors [88], or they are fully decentralized and self-organized to detect and track moving targets [44].

Bionanosensor networks considered in this thesis are expected to face several challenges that are being addressed in the area of WSNs such as placement of sensor nodes, mechanisms to coordinate the behavior of sensor nodes, and routing and processing of sensor readings [79]. Existing techniques and algorithms in WSNs may apply to address issues in bionanosensor networks, however, new constraints need to be considered in designing solutions to bionanosensor networks (Section 1.2).

1.4.2 Molecular Communication and Nanonetworks

The area of molecular communication and nanonetworks employs communication engineering approaches to investigate the use of molecules as the basis for communication among microscale or nanoscale bionanosensors [2, 34, 56]. In its simplest form, molecular communication consists of *encoding*, in which sender encodes information onto molecules, *sending* in which sender emits information-encoded molecules into the environment, *propagation* in which the environment

propagates information-encoded molecules, *receiving* in which receiver captures information-encoded molecules, and *decoding* in which receiver induces biochemical reactions.

Major efforts in this area are focused on physical layer issues of various types of molecular communication media. In these efforts, information capacity and physical characteristics (e.g., delay, signal attenuation, amplification, and energy requirements) of molecular communication are studied, whose communication mechanisms fall into random walk [24, 50, 59], random walk with drift [37, 80], diffusion-based [6, 7, 45, 73, 74], diffusion- reaction-based [55, 60], active transport [25, 50], and a collision-based [32]. In addition, recent efforts address higher layer and other important issues in molecular communication, such as a beacon coordinate system [47], diffusion-based mechanisms of synchronization [48], distance measurement protocols [49], and a routing system [20].

Unlike these efforts, in this thesis, we perform application oriented studies of molecular communication and nanonetworks, in which bionanosensors form a network to detect and track moving targets. At the time of writing this thesis, application oriented studies in this area are limited to [15, 85, 86], in which a group of bacteria coordinately achieves a high spatial occupancy in a biological environment (e.g., inside the human body) for nanomedical applications.

1.4.3 Drug Delivery Systems

The area of drug delivery systems (DDS) pursues efficient methods of drug administration considering the pharmaceutical aspects related to the absorption, distribution, metabolism, and excretion (ADME). Absorption is the process of drug entry to the blood circulation after the drug administration, distribution is the dissemination of drug to the tissues or cells of the body, metabolism is the chemical transformations of drug, and excretion is the elimination of drug from the body. Research efforts in this area are carried out to embody drug carriers that can be targeted to disease sites in the human body and that can release drug molecules only at disease sites, in order to reduce the risk of side effects on non-disease sites.

Two key functionalities in DDS are spatial control of drug carriers and temporal control of drug release.

Spatial control of drug carriers is to deliver drug carriers to disease sites, aiming at increasing the level (concentration) of drug molecules only around the disease sites while decreasing the level around other sites, thereby reducing the risk of side effects. There are two types of methodologies for the spatial control of drug carriers: active and passive targeting. Active targeting takes advantages of specific interactions between targets and drug carriers based on chemical or physical properties. For example, active targeting uses ligands attached to drug carriers that selectively bind with specific receptors expressed on the membrane surface of targets. Passive targeting makes use of passive phenomena resulting from anatomical or physiological properties. For example, passive targeting uses the blood flow that can deliver drug carriers in a weight-dependent manner, so that drug carriers are accumulated in target organs and tissues such as the kidney and cancerous tissues [46].

Temporal control of drug release is to release drug molecules only when needed, aiming at regulating drug molecule level in accordance with chemical or physical signals. There are two types of signals that function as triggers for temporal control of drug release: chemical and physical properties specific to disease sites (e.g., concentration of glucose [39], temperature [91], pH level [9]) and physical stimulus artificially and externally applied (e.g., heat [33], light [36], magnetic field [19], microwave).

Bionanosensor networks considered in this thesis have potential to advance the area of DDS. Bionanosensors in bionanosensor networks may store drug molecules, coordinate their behavior to detect and track targets, and release drug molecules.

1.4.4 Systems/Synthetic Biology

The area of systems biology uses computational and mathematical tools for the understanding of biological systems as a system. The common approach employed in this area is to develop mathematical models of biological systems and math-

ematically analyze the robustness of biological systems [5]. Another approach developed in this area is to define the architecture and protocols for biological systems to operate. In [23], for example, a graph-theoretic approach is applied to identify the common organizational architecture in biological systems.

The area of synthetic biology aims at designing and constructing biological systems for useful purposes. Examples of synthetic biological systems demonstrated in this area include a logic operation system that performs basic logic operations [87], a cell density control system that maintains a certain level of population [92], and a pattern-forming system that produces various patterns of cell differentiation [11].

Knowledge and techniques developed in these two areas of biology are highly useful for our studies of bionanosensor networks. Computational and mathematical tools in systems biology can be used to design bionanosensor networks, and engineering techniques in synthetic biology can be used to implement bionanosensor networks from biological materials.

1.5 Thesis Organization

The remainder of this thesis is organized as follows. Chapter 2 describes static bionanosensor networks for target detection, which is based on our work published in [57, 63, 64, 65, 70]. Chapter 3 describes dynamic bionanosensor networks for target tracking, which is based on our work published in [58, 67, 69]. Chapter 4 describes bacterium-based bionanosensor networks for target tracking, which is based on our work published in [52, 66, 68, 71]. Finally, Chapter 5 describes future work to conclude this thesis.

In the following, we give an overview of our contributions in each chapter (Chapters 2 to 4).

1.5.1 Static Bionanosensor Networks for Target Detection

In Chapter 2, we consider a static bionanosensor network for target detection application. In this type of bionanosensor network, bionanosensors are statically placed in the monitoring environment to detect targets that randomly walk in the environment. We formulate the target detection problem as an optimization problem to find a spatial distribution of bionanosensors that can minimize mean residence time of targets. We then mathematically analyze the problem under the condition that target arrival locations follow the uniform distribution: for one-dimensional environment, we find the optimal solution, and for n-dimensional environment ($n \geq 2$), we provide the lower bound expression. Furthermore, in a two-dimensional environment, where analytical approaches are not available, we assume that target arrival locations follow the normal distribution and conduct simulation experiments to compare the performance of several placement schemes in terms of mean residence time.

1.5.2 Dynamic Bionanosensor Networks for Target Tracking

In Chapter 3, we consider a dynamic bionanosensor network for target tracking application. In this type of bionanosensor network, autonomous mobile bionanosensors use repellents and attractants to detect and track a moving target. Bionanosensors release repellents to spread over the monitoring environment in search of targets, while they release attractants to gather around a target location. We use a set of partial differential equations to describe the spatial-temporal dynamics of the concentrations of bionanosensors. We then numerically integrate the set of partial differential equations to demonstrate the ability of the dynamic bionanosensor network to locate and track targets under varieties of settings.

1.5.3 Bacterium-based Bionanosensor Networks for Target Tracking

In Chapter 4, we investigate through in silico experiments the feasibility of using bacteria as bionanosensors to form a dynamic bionanosensor network. A bacterium is an microscale organism capable of sensing environmental conditions, producing chemical substances, and actively moving in the environment. Also, it can be genetically engineered to modify these functionalities. We first develop a mobility model of bacterium-based bionanosensors, and then evaluate the ability of bacterium-based bionanosensors to locate and track moving targets. Simulation results demonstrate that a group of bacterium-based bionanosensors is able to track a moving target when the combined use of attractants and repellents is employed, indicating that bacteria are promising materials to implement bionanosensors for target tracking.

Chapter 2

Static Bionanosensor Networks for Target Detection

2.1 Overview

In this chapter, we consider a static bionanosensor network for target detection application. A bionanosensor network considered in this chapter is static in that bionanosensors are immobilized in the environment for detecting targets. The target detection problem is a primary concern in bionanosensor networks for nanomedical applications, where bionanosensors placed deep inside the human body need to detect targets such as toxic substances, disease-indicating molecules, viruses, or pathogens. In such applications, only a limited number of bionanosensors are deployable due to possible side effects with the environment, and thus these bionanosensors need to be placed at appropriate locations to enable timely detection of targets.

Fig. 2.1 shows a model of the static bionanosensor network to be investigated in this chapter. Bionanosensors are statically placed in the monitoring environment where a single target arrives and propagates via Brownian motion. A bionanosensor detects the target through chemically reacting with the target. The specific task of the static bionanosensor network considered in this chapter is to

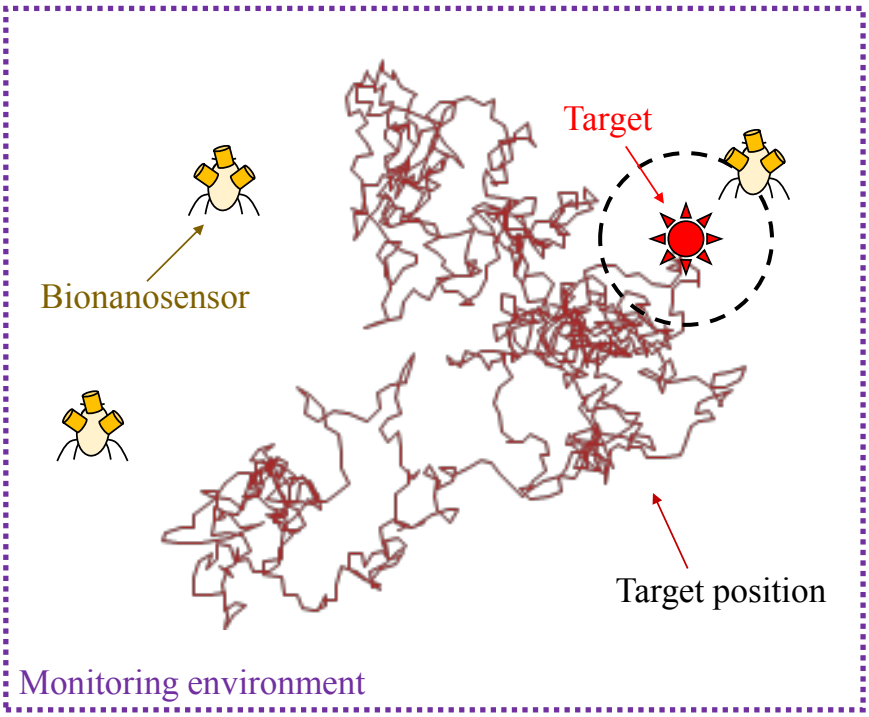


Figure 2.1: A static bionanosensor network [65]

detect a target as early as possible (i.e., to minimize the mean residence time of targets). For more detail of these model components, see Section 1.3.

A bionanosensor network considered in this chapter is static in that bionanosensors are immobilized in the monitoring environment (e.g., they are bound to the surface of the environment). Here spatial distribution of bionanosensors is important for timely detection of targets. In this chapter, we consider three placement schemes that determines the special distribution of bionanosensors: random (RAND), proportional (PROP), and regular (REG). RAND places bionanosensors in random locations, PROP places bionanosensors in locations where target signals appear with higher probability, and REG places bionanosensors into a regular lattice pattern. These placement schemes may be implemented using an external device that generates an electric field [35] or a magnetic field [19] to control the spatial distribution of bionanosensors. These techniques possess the potential abil-

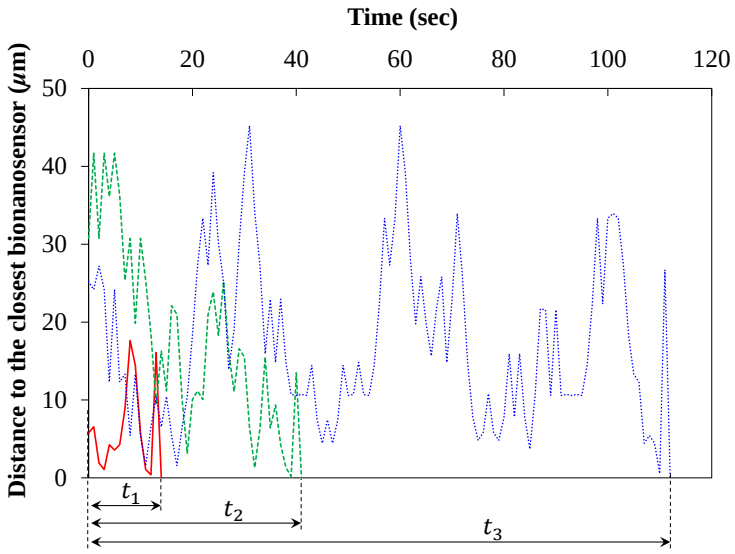


Figure 2.2: Target detection process.

ity to manipulate thousands of bionanosensors in parallel with the single-cell resolution to form a variety of patterns in a static manner. These placement schemes may also be implemented without using an external device. For example, bionanosensors may autonomously move to form a specific spatial distribution and maintain the distribution by adhering to the surface of the environment. Many cells in the body exist in groups binding to surfaces of other cells. Therefore, it is possible to form a static placement by using bionanosensors derived from cells in the body [31].

Fig. 2.2 illustrates how targets are detected by a static bionanosensor network. Here three targets are assumed to arrive at time 0 in a two-dimensional bounded area 100×100 containing 225 bionanosensors that are distributed in a reticular lattice. The three targets randomly walk in the area and are detected and removed by a bionanosensor. The x-axis represents time, and the y-axis the Euclidean distance to the closest bionanosensor. The amount of time from when a target appears in the environment to when it is detected by a bionanosensor, defined as the residence time in this chapter, is $t_1 = 14$, $t_2 = 41$, and $t_3 = 112$, respectively.

Table 2.1: Notations

Notation	Description
n	Dimension of system considered
A	Area in which targets can travel
A_{sig}	Area in which targets arrive
A_{nm}	Area in which bionanosensors are placed
D_T	Diffusion coefficient
L	Length in one dimension
a	Probability density function for target arrival locations
S	Index set of bionanosensors
$\boldsymbol{x}_p$	Position vector of bionanosensor p
x_{pj}	j-th coordinate of bionanosensor p's placement
$\boldsymbol{X}_S$	Placement matrix of a set of bionanosensors S
$w(\boldsymbol{x}, \boldsymbol{X}_S)$	Mean residence time for a target arriving at x when bionanosensor placement is $\boldsymbol{X}_S$
$\lvert\cdot\rvert$	Cardinality of a set given

The remainder of this chapter is organized as follows. In Section 2.2, we formulate the target detection problem as an optimization problem to minimize the mean residence time of targets. In Section 2.3, we mathematically analyze the mean residence time under specific conditions. In Section 2.4, we conduct simulation experiments to evaluate the bionanosensor placement approaches in terms of the mean residence time of targets under various scenarios. Finally, we conclude this chapter in Section 2.5.

2.2 Problem Formulation

Table 2.1 shows the notations used to describe the model throughout this chapter. A target arrives at a point $\boldsymbol{x} \in A_{sig} \subseteq \mathcal{R}^n$, where n is the dimension considered. The arrival point $X \in \mathcal{R}^n$ follows *target arrival distribution* $a : \mathcal{R}^n \to \mathcal{R}$. $S = \{1, 2, 3, \cdots, |S|\}$ represents a set of indices of bionanosensors, $\boldsymbol{x}_p = (x_{p1}, x_{p2}, x_{p3}, \cdots, x_{pn})^T \in A_{nm} \subseteq \mathcal{R}^n$ represents the bionanosensor place-

ment for $p \in S$, and $\boldsymbol{X}_S = \left(\boldsymbol{x}_1, \boldsymbol{x}_2, \boldsymbol{x}_3, \cdots, \boldsymbol{x}_{|S|}\right) \in \mathcal{R}^{n \times |S|}$ represents a placement matrix of S. We assume that $A_{sig} = A_{nm} = [0, L]^n$.

A target arrives in the monitoring environment, travels via Brownian motion with the diffusion coefficient D_T, and is removed from the monitoring environment immediately after hitting a bionanosensor. The average amount of time that a target resides in the monitoring environment is called the mean residence time (MRT). MRT varies depending on the bionanosensor placement and therefore it is denoted as $MRT(\boldsymbol{X_S})$.

The goal of bionanosensor networks is to find the bionanosensor placement $\boldsymbol{X}_S$ that minimizes MRT. This is formulated as an optimization problem as follows.

$$\begin{aligned} \text{Minimize}: \quad & MRT(\boldsymbol{X}_S) \\ & = \int_{[0,L]^n} a(\boldsymbol{x}) \cdot w(\boldsymbol{x}, \boldsymbol{X}_S) d\boldsymbol{x} \\ \text{s.t.}: \quad & \boldsymbol{x}_p \in [0, L]^n, p \in \{1, 2, 3, \cdots, |S|\} \end{aligned} \tag{2.1}$$

where $w(\boldsymbol{x}, \boldsymbol{X_S})$ is the MRT for a target that arrives at $\boldsymbol{x}$. Note that the residence time used in this chapter is often referred to as first passage time (FPT) [77]. The concept of FPT has been applied in nano-scale communication problems in [24, 80]. Briefly, in a one-dimensional unbounded interval $x \in (-\infty, d]$, where a target signal arrives at $x = 0$ at time $t = 0$ and randomly walks in the interval with the diffusion coefficient D_T, the probability density function (pdf) of the FPT for a target location $x = d$ is given by

$$f(t; d) = \begin{cases} 0 & (t = 0) \\ \frac{d}{\sqrt{4\pi D_T t^3}} \exp\left(-\frac{d^2}{4 D_T t}\right) & (t > 0). \end{cases} \tag{2.2}$$

The mean of FPT (mFPT) is infinity (i.e., $\int_0^\infty tf(t)dt = \infty$). In a one-dimensional bounded interval, the pdf of FPT is not given by a closed-form expression, but the mFPT is known and finite. In two or higher dimensional space with multiple target locations (i.e., multiple bionanosensors), neither mFPT nor the pdf is known [22]. A common approach to compute mFPT is through discrete space and time random walk simulation.

2.2.1 Mean Residence Time in One Dimension

In the one-dimensional case ($n = 1$), the target arrival distribution $a(x)$ in (2.1) follows one-dimensional normal distribution with $x \in [0, L]$ (wrapped normal distribution):

$$\begin{aligned} a(x) &= \mathcal{N}_X(\mu, \sigma^2) \\ &= \begin{cases} \frac{1}{\sqrt{2\pi}\sigma} \exp\left(-\frac{(x-\mu)^2}{2\sigma^2}\right) & x \in [0, L] \\ 0 & otherwise \end{cases} \end{aligned} \tag{2.3}$$

In the one-dimensional case, the mean residence time $w(x, \boldsymbol{X}_S)$ in (2.1) is given as a closed-form expression [77], and thus, MRT for given bionanosensor placement $\boldsymbol{X_S}$ can be analytically calculated as follows.

Let the one-dimensional interval $A = [0, L]$ divided by bionanosensor locations into subintervals $A_i = [x_{i-1}, x_i]$ ($i = 1, 2, \cdots |S| + 1$) and $W_i(x)$ be the mean residence time of a target that arrives in A_i: i.e., $W_i(x) = w(x, (x_{i-1}, x_i))$ for $x \in A_i$ ($i = 1, 2, \cdots, |S| + 1$) where $x_0 = 0$ and $x_{|S|+1} = L$. In the one-dimensional case, a target in interval i will hit a bionanosensor on an either end of the interval. In this case, MRT is derived by adding up the weighted mean residence time of targets that arrive in each interval. $MRT(\boldsymbol{X_S})$ in (2.1) can be thus rewritten as follows.

$$MRT(\boldsymbol{X_S}) = \sum_{i=1}^{|S|+1} \int_{x_{i-1}}^{x_i} a(x) \cdot W_i(x) dx \tag{2.4}$$

where $X_S = \left(x_1, x_2, x_3, \cdots, x_{|S|}\right) \in [0, L]^{|S|}$, $0 \leq x_1 \leq x_2 \leq x_3 \leq \cdots \leq x_{|S|} \leq L$.

Assuming that a target at x moves to either $x - \delta$ or $x + \delta$ with the equal probability after a short period of time τ, we have

$$W_i(x) = \tau + \frac{1}{2}\left(W_i(x-\delta) + W_i(x+\delta)\right). \tag{2.5}$$

(2.5) is rewritten as, by subtracting $W_i(x)$ from both sides, and multiplying $2/\delta$,

$$\begin{aligned} \Leftrightarrow \quad & \frac{2\tau}{\delta} + \frac{1}{\delta}\left(W_i(x-\delta) - W_i(x)\right) \\ & -\frac{1}{\delta}\left(W_i(x) - W_i(x-\delta)\right) = 0, \end{aligned} \tag{2.6}$$

from the definition of partial derivative,

$$\Leftrightarrow \quad \frac{2\tau}{\delta} + \left.\frac{\partial W_i(x)}{\partial x}\right|_x - \left.\frac{\partial W_i(x)}{\partial x}\right|_{x-\delta} = 0, \tag{2.7}$$

and by multiplying $1/\delta$ and from the definition of partial derivative,

$$\begin{aligned} \Leftrightarrow \quad & \frac{2\tau}{\delta^2} + \frac{1}{\delta}\left(\left.\frac{\partial W_i(x)}{\partial x}\right|_x - \left.\frac{\partial W_i(x)}{\partial x}\right|_{x-\delta}\right) = 0 \\ \Leftrightarrow \quad & \frac{1}{D} + \frac{\partial^2 W_i(x)}{\partial x^2} = 0, \end{aligned} \tag{2.8}$$

where $2\tau/\delta^2 = 1/D$ is given by definition.

In solving (2.8), two cases for boundary conditions need to be considered: bionanosensors are placed on (A) both ends ($x = x_{i-1}$ and $x = x_i$), or (B) either end ($x = x_{i-1}$ or $x = x_i$). In (A), i.e., $i = 2, 3, \cdots, M$, we have

$$W_i(x_{i-1}) = W_i(x_i) = 0, \tag{2.9}$$

leading to

$$W_i(x) = \frac{1}{2D}\left\{(x_i - x_{i-1})(x - x_{i-1}) - (x - x_{i-1})^2\right\}. \tag{2.10}$$

In (B) with a bionanosensor on $x = x_i$, i.e., $i = 1$, we have

$$\left.\frac{\partial W_1(x)}{\partial x}\right|_{x=0} = 0, W_i(x_1) = 0, \tag{2.11}$$

leading to

$$W_1(x) = \frac{1}{2D}\left\{(x_1 - x_0)^2 - (x - x_0)^2\right\}. \tag{2.12}$$

Similarly, when $i = M + 1$, we have

$$W_{M+1}(x) = \frac{1}{2D}\left\{(x_{M+1} - x_M)^2 - (x_{M+1} - x)^2\right\}. \tag{2.13}$$

With (2.3), (2.4), (2.10), (2.12), and (2.13), the MRT for a given bionanosensor placement can be analytically computed.

2.2.2 Mean Residence Time in Higher Dimensions

In a higher dimensional case, for example, in a two-dimensional case ($n = 2$), the target arrival distribution $a(x)$ in (2.1) follows two-dimensional normal distribution:

$$a((x,y)^T) = \begin{cases} \mathcal{N}_X(\mu,\sigma^2)\cdot\mathcal{N}_Y(\mu,\sigma^2) & (x,y\in[0,L]) \\ 0 & otherwise \end{cases} \tag{2.14}$$

where $\mathcal{N}_X(\mu,\sigma^2)$ and $\mathcal{N}_Y(\mu,\sigma^2)$ are normal distribution in a one-dimensional interval. In this case, the mean residence time $w(\boldsymbol{x},\boldsymbol{X}_S)$ in (2.1) is not known as a closed-form expression [22], and thus the MRT cannot be given as a closed-form function of bionanosensor locations. To compute MRT, discrete time and space random walk simulation needs to be performed (see Section 2.4).

2.3 Analysis of Mean Residence Time

In this section, we assume that the variance σ^2 of target arrival distribution g is sufficiently large so that g is written as uniform distribution. Under this assumption, we describe an expression of the MRT or the lower bound of the MRT to show the impact of the two model parameters: the scale of the environment L and the number of bionanosensors $N_b = |S|$ on the MRT.

2.3.1 Mean Residence Time in One Dimension

For one dimension, assuming that $n = 1$ and $a(x) = \mathcal{U}(0,L)$, (2.4) can be rewritten as follows.

Minimize:

$$\frac{1}{12D_TL}\left\{4(x_1-x_0)^3+\sum_{i=2}^{|S|}(x_i-x_{i-1})^3+4(L-x_{|S|})^3\right\} \tag{2.15}$$

s.t.:

$$x_p \in [0, L], p \in \{1, 2, 3, \cdots, |S|\} \tag{2.16}$$

The optimal bionanosensor placement or the solution to (2.16) is uniquely found from the first derivative test: i.e.,

$$\frac{\partial w(x, X_S)}{\partial x_1} = -3(x_2 - 3x_1)(x_2 + x_1) \tag{2.17}$$

$$\frac{\partial w(x, X_S)}{\partial x_i} = -3(x_{i+1} - x_{i-1})(x_{i+1} + x_{i-1} - 2x_i) \tag{2.18}$$

$$\frac{\partial w(x, X_S)}{\partial x_{|S|}} = -3(x_{|S|} - x_{|S|-1} - 2L) \times (3x_{|S|} - x_{|S|-1} - 2L) \tag{2.19}$$

from which, we have

$$x_i^* = \frac{2i - 1}{2\,|S|} L. \tag{2.20}$$

By substituting (2.20) in (2.16), the mean residence time achieved by the optimal placement is given as

$$\min(MRT(\boldsymbol{X}_S)) = \frac{L^2}{12 D_T |S|^2}. \tag{2.21}$$

2.3.2 Mean Residence Time in Higher Dimensions

For higher dimensions, a closed form expression of the mean residence time is not known [22]. However, a lower bound expression has been proposed for discrete space and time random walk on finite lattices [21]. By applying the known equation to an n-dimensional regular lattice space, we have

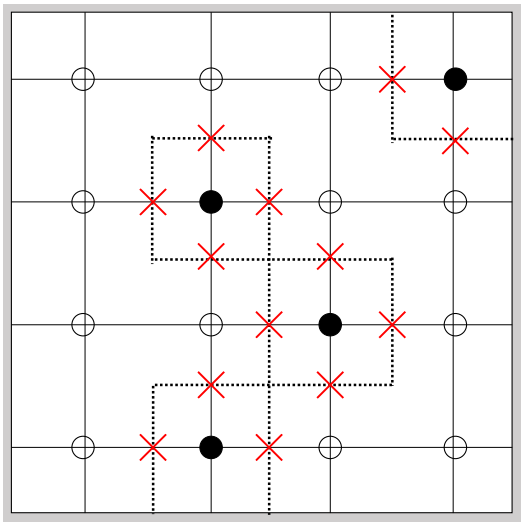


Figure 2.3: Example in a two-dimensional regular lattice area.

$$\inf(MRT(\boldsymbol{X}_S)) = (\frac{nV}{U} - \frac{1}{2})\tau, \tag{2.22}$$

$$= \left[\frac{n}{U}\left\{\left(\frac{L}{\delta}\right)^n - |S|^*\right\} - \frac{1}{2}\right]\tau, \tag{2.23}$$

where V is the number of sites that are not occupied with bionanosensors (and thus where a target moves), $|S|^*$ the number of sites occupied with bionanosensors (i.e., $V = \left(\frac{L}{\delta}\right)^n - |S|^*$), U the number of lines crossing the boundary between an unoccupied site and an occupied site, and τ ($= \frac{\delta^2}{2D_T}$) the time step length.

Fig. 2.3, for example, shows a two-dimensional regular lattice area ($n = 2$). A filled circle represents a site occupied with a bionanosensor, an open circle an unoccupied site, and a dashed line the boundary between an unoccupied site and an occupied site. A cross is placed on a line crossing a boundary. The area is surrounded by reflective walls. In this case, $|S|^* = 4$, $V = 12$, and $U = 13$.

2.4 Simulation Experiments

In a two dimensional environment, neither mFPT nor the pdf of FPT is known [22], and thus analytical solutions to the placement problem are not available. In this section, therefore, we perform discrete space and time random walk simulation to compute the mean residence time of several bionanosensor placements in two-dimensional environment.

2.4.1 Bionanosensor Placement Approaches

The three approaches are used to distribute bionanosensors (i.e., RAND, PROP, REG) as briefly described in Section 2.1. The three approaches determine the placement of bionanosensors $\boldsymbol{X_S}$ and MRT for a particular bionanosensor placement can then be computed analytically for the one-dimensional case (see Section 2.3) or through simulation for the two-dimensional case.

The three approaches are formally described as follows:

- *Random placement (RAND)*: bionanosensors are placed randomly over $[0, L]^n$. For each bionanosensor in S, a site is randomly selected from $[0, L]^n$ following uniform distribution, and the bionanosensor is placed on the site.

- *Proportional placement (PROP)*: bionanosensors are placed based on target arrival distribution. For each bionanosensor in S, a site is selected from $[0, L]^n$ following the target arrival distribution, and the bionanosensor is placed on the site.

- *Regular placement (REG)*: bionanosensors are placed with an equal interval on $[0, L]^n$ where the distance between two immediate bionanosensors is $L/\sqrt{|S|}$, and the distance between a bionanosensor on the edge and the area boundary is $L/2\sqrt{|S|}$.

Finding the optimal bionanosensor placement is computationally difficult. An exhaustive search needs to explore the solution space of $O(L^{n\times|S|})$ given the num-

Algorithm 1 Greedy bionanosensor placement

for all $m \in \{1, 2, 3, \cdots, |S|\}$ **do**
  MinMRT := MRT for the current bionanosensor location
  for all $n \in \{1, 2, 3, \cdots, m\}$ **do**
    for all $i \in \{1, 2, \cdots, n-1, n+1, \cdots, m\}$ **do**
      $\boldsymbol{x}_i^{(m)} := \boldsymbol{x}_i^{(m-1)}$
    end for
    $\boldsymbol{x}_n^{(m)} := \boldsymbol{x}$
    Find $\boldsymbol{x} = \boldsymbol{x}^*$ that minimizes MRT.
    NewMRT := MRT for new bionanosensor location
    if *NewMRT* $<$ *MinMRT* **then**
      MinMRT := *NewMRT*
      $\boldsymbol{x}_1^* := \boldsymbol{x}_1^{(m)}, \boldsymbol{x}_2^* := \boldsymbol{x}_2^{(m)}, \cdots, \boldsymbol{x}_m^* := \boldsymbol{x}_m^{(m)}$
    end if
  end for
  $\boldsymbol{x}_1^{(m)} := \boldsymbol{x}_1^*, \boldsymbol{x}_2^{(m)} := \boldsymbol{x}_2^*, \cdots, \boldsymbol{x}_m^{(m)} := \boldsymbol{x}_m^*,$
end for

ber of bionanosensors $|S|$. We thus use a simple heuristic, greedy placement (GRD), to obtain a candidate solution from the reduced search space of $O(|S|\, L^n)$:

- *Greedy placement (GRD)*: a bionanosensor is iteratively and optimally placed one by one until the number of bionanosensors reaches a given $|S|$. **Algorithm 1** shows a pseudo-code for the greedy placement.

Note that GRD is introduced for a comparison purpose and is used to evaluate MRT of the three approaches.

2.4.2 Simulation Model and Configurations

Simulation experiments are conducted to compare MRT of the four approaches: RAND, PROP, REG, and GRD. In the one-dimensional case, MRT can be analytically obtained when a placement is given (see Section 2.3). In the two-dimensional case, analytical calculation is not possible, and thus we conduct simulation experiments to calculate MRT. In simulation experiments, we discretize

the space and time for simulating Brownian motion of the target. At time $t = 0$ a target arrives on a lattice, following the target arrival distributions $a(\boldsymbol{x})$ in (2.3). At each time step, the target randomly chooses one of 2^n directions which are parallel to each axis to both positive and negative directions. The target moves to the adjacent lattice in the direction. When the target hits the boundary, the target steps back toward the opposite direction. Each simulation run records the number of time steps necessary for a target to first reach a site occupied with a bionanosensor. The MRT of a particular bionanosensor placement is then estimated based on the residence time obtained from 10000 simulation runs. We use arbitrary chosen default parameter values ($L = 100$, $|S| = 100$, $\mu = 50$, and $\sigma = 50/3$) and examine the impact of these parameter values on MRT.

2.4.3 Simulation Results

2.4.3.1 Impact of Number of Bionanosensors

First, we examine the impact of the number of bionanosensors on MRT. In this simulation, the number of bionanosensors is varied from 1 to 100. Fig. 2.4 shows MRT as a function of the number of bionanosensors for the four bionanosensor placement approaches in the two-dimensional case. The figure shows that MRT decreases exponentially as the number of bionanosensors increases in all the four approaches. The figure also shows that REG is comparable to GRD and outperforms PROP and RAND, representing a typical case under variates of conditions tested. In the one-dimensional case, MRT is roughly $1/100$ in the two-dimensional case, corresponding with the ratio of the number of sites that a target can move.

2.4.3.2 Impact of Target Arrival Distribution

The bionanosensor placement by PROP is affected by the target arrival distribution. To examine the impact of the target arrival distribution, we vary the standard deviation σ of $a(\boldsymbol{x})$ ((2.3) or (2.14)) from 0.1 to 1. The simulation results obtained

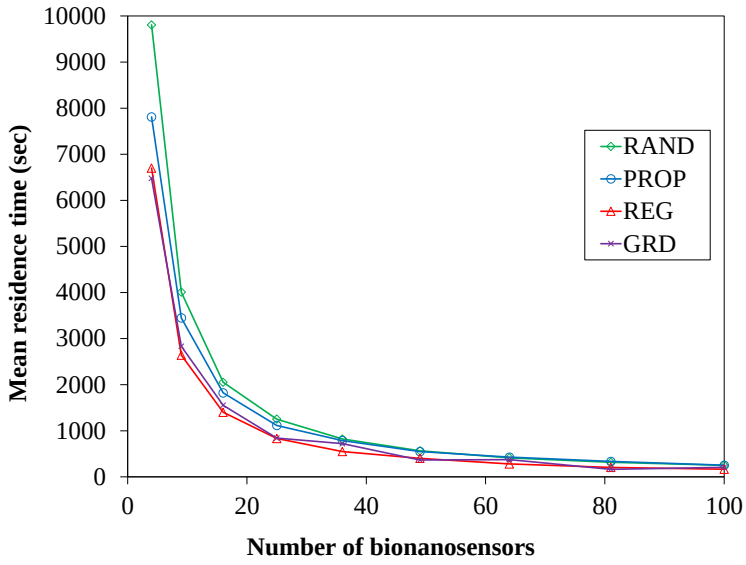


Figure 2.4: Mean residence time as a function of the number of bionanosensors in two dimension. $\sigma = 50/3$.

from the two-dimensional case are shown in Fig. 2.5 where MRT is plotted as a function of the standard deviation σ, showing that:

- PROP performs best with small σ where target arrival locations are highly skewed and concentrated around the center of the area. In this case, PROP distributes bionanosensors densely around the center to reduce MRT, while a target that arrives around the edges or a target that escapes from the center to the edges takes a very long journey to hit a bionanosensor, which leads to a large variance in MRT (3.72×10^6 when $\sigma = 0.1$). PROP increases MRT sharply and approaches RAND with large σ where the target arrival distribution approaches uniform distribution. In this case, PROP places bionanosensors more randomly becoming similar to RAND.

- REG achieves constant MRT with small variance (within 1.68×10^2 to 1.74×10^2 when σ varied) regardless of σ. When σ is large (> 0.5), REG outperforms PROP and becomes comparable to GRD. Since REG places

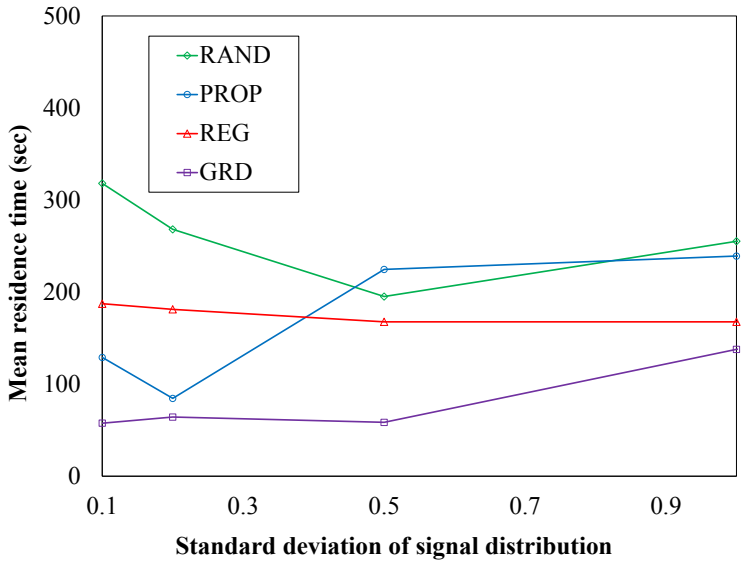


Figure 2.5: Mean residence time as a function of the standard deviation of the target arrival distribution in two dimension.

bionanosensors uniformly covering the entire environment, the arrival locations don't have much impact on MRT.

When σ is large (e.g., $\sigma \geq 100$), the target arrival distribution can be approximated as a uniform distribution. MRT achieved by REG is 164.76 when $\sigma = 100$, and 167.35 when $\sigma = 200$ while the lower bound calculated from (2.23) is 49.

2.4.3.3 Impact of Stochastic Sensing

In a small scale system with a limited number of molecules, the chemical reaction is influenced by the noise to be a stochastic process [29]. To examine the impact of noise in bionanosensor's sensing capability on MRT, we introduce the reaction probability, q. Under this scenario, a bionanosensor reacts with or detects a target with q when the target moves to a site occupied with the bionanosensor, and with $1 - q$, the target is not detected.

Fig. 2.6 shows MRT as a function of reaction probability in two dimensions.

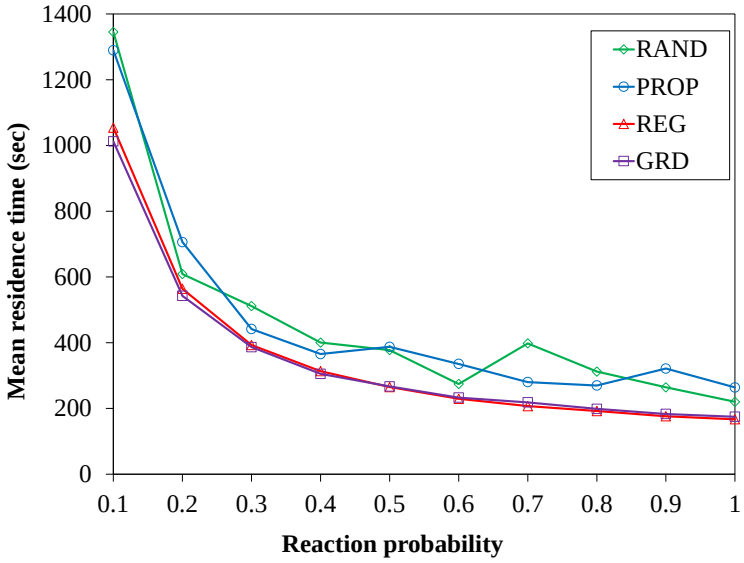


Figure 2.6: Mean residence time as a function of reaction probability in two dimension.

The figure shows that MRT exponentially decreases as q increases. The figure also shows that REG outperforms RAND and PROP, and is comparable to GRD as observed in the previous two cases.

2.4.3.4 Impact of Random Bionanosensor Failure

Bionanosensors are placed in an unpredictable environment and are always subject to unknown chemical compounds and mechanical stress. As a result, bionanosensors may fail or lose the sensing capability. In this scenario, unknown factors causing bionanosensor failure are uniformly distributed in the environment and bionanosensors fail at random. Under this assumption, we first use RAND, PROP, REG, or GRD to determine bionanosensor placement $\boldsymbol{X_S}$ and then repeatedly delete a randomly selected bionanosensor from $\boldsymbol{X_S}$ to measure MRT. Note that bionanosensors are not relocated after each bionanosensor failure, indicating that bionanosensor placement may no longer conform to the original placement.

Fig. 2.7 shows the impact of random bionanosensor failure on MRT in two

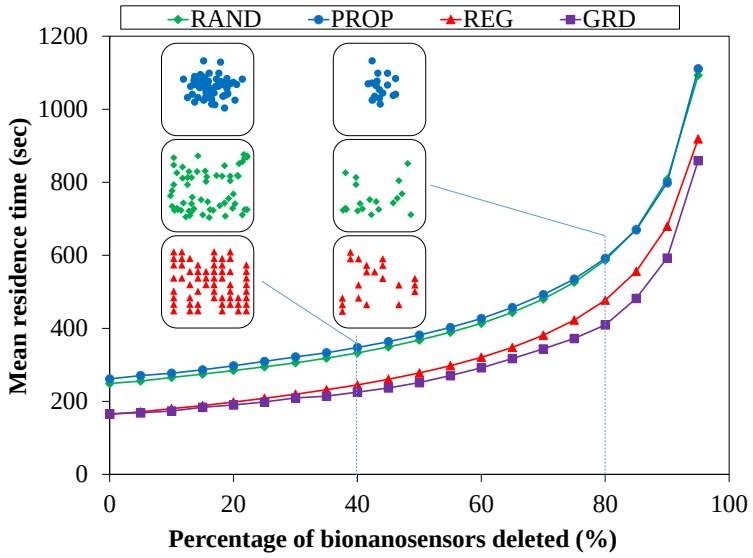


Figure 2.7: Impact of random bionanosensor failure on the mean residence time.

dimensions. The figure shows that MRT increases in a similar manner in all the four approaches as the number of bionanosensors deleted increases. This is observed under other scenarios considering bionanosensor failure to be presented in the rest of the section. The figure also shows that REG outperforms PROP and RAND as observed in all the previous cases (Figs. 2.4, 2.5, and 2.6). Moreover, the figure shows that REG increases MRT more rapidly than PROP and RAND, indicating that REG is the most impacted by random bionanosensor deletion. The increase of MRT relative to the MRT without bionanosensor deletion is 1.49 (REG), 1.33 (PROP), 1.34 (RAND) at 40% of bionanosensor failure, and 2.90 (REG), 2.26 (PROP), 2.36 (RAND) at 80% of bionanosensor failure. This is due to the fact that PROP and RAND place bionanosensors redundantly at the same site or nearby sites (e.g., around the center in the case of PROP (see the placements when 40% of bionanosensors fail in Fig. 2.7)), and more bionanosensors are removed from an area occupied with a larger number of bionanosensors because bionanosensors are removed at random (see the placements when 80% of bionanosensors fail in Fig. 2.7). The MRT of RAND and PROP is therefore not

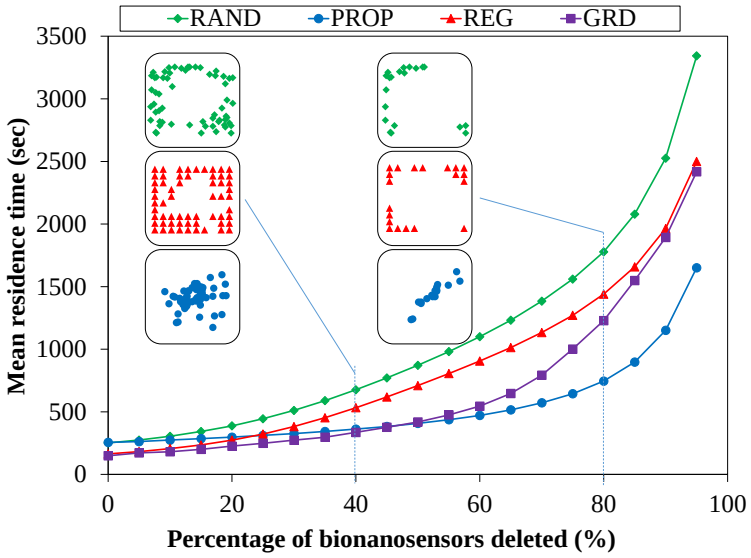


Figure 2.8: Impact of bionanosensor failure by target arrival distribution on the mean residence time. $\sigma = 50/3$ and $|S| = 100$.

affected as much by random bionanosensor failure.

2.4.3.5 Impact of Bionanosensor Failure by Target Arrival Distribution

Bionanosensors may also lose the sensing capability for targets after detecting the targets through the mechanism called adaptation. For instance, many biological cells become insensitive to chemical signals after exposed to the chemical signals through the receptor inactivation, sequestration, or down-regulation [4]. To examine the impact of bionanosensor adaptation on MRT, we first use one of the four placement approaches to determine bionanosensor placement $\boldsymbol{X_S}$, and then (1) select a target arrival site from the monitoring environment $[0, L]^n$ following the target arrival distribution, (2) delete the bionanosensor closest to the site from $\boldsymbol{X_S}$, assuming that the bionanosensor detects the target and becomes insensitive, and (3) measure MRT. Similar to the previous case, we repeatedly apply (1)-(3) to examine the impact of the number of bionanosensors that become adapted to the targets.

Fig. 2.8 shows the impact of the bionanosensor adaptation on MRT for the four approaches applied to the two dimensions ($\sigma = 50/3$ and $|S| = 100$). The figure shows that PROP is the most robust against bionanosensor adaptation and achieves the smallest MRT. This is because bionanosensors are densely located around the target arrival sites, and the deletion of bionanosensors around the target arrival sites has the smallest impact on MRT (compare the difference in placements by PROP between 40% and 80% of bionanosensors fail in Fig. 2.8). In other three approaches (i.e., RAND, REG, GRD), bionanosensors around the target arrival sites become sparse as more bionanosensors become insensitive, resulting in a large increase in MRT (compare the differences in placements by RAND, REG, and GRD, between 40% and 80% of bionanosensors fail in Fig. 2.8).

2.4.3.6 Impact of Bionanosensor Failure at Random Locations

Bionanosensors may also lose the sensing capability by reacting to inhibitory signals that appear in the monitoring environment, propagate, and bind to the bionanosensors. We assume that inhibitory signals arrive at random locations, and examine the impact on MRT for the four placement approaches. Given particular bionanosensor placement $\boldsymbol{X_S}$, we (1) randomly select a site from the monitoring environment $[0, L]^n$ where an inhibitory signal appears, (2) delete the bionanosensor closest to the site, assuming that the inhibitory signal binds to the bionanosensor, and (3) measure MRT. (1)-(3) are repeated to examine the impact of inhibitory signals as in the previous scenario.

Fig. 2.9 shows the impact of inhibitory signals on MRT of the four approaches in two dimension ($\sigma = 50/3$ and $|S| = 100$). The figure shows that REG is the most robust against inhibitory signals and PROP is the most vulnerable. Under this scenario, the sparse areas become more sparse as more bionanosensors are removed. The bionanosensor distribution in REG is initially uniform which slowly increases MRT, while that in PROP is biased and rapidly increases MRT (compare the differences in placements when 40% and 80% of bionanosensors fail in Fig. 2.9).

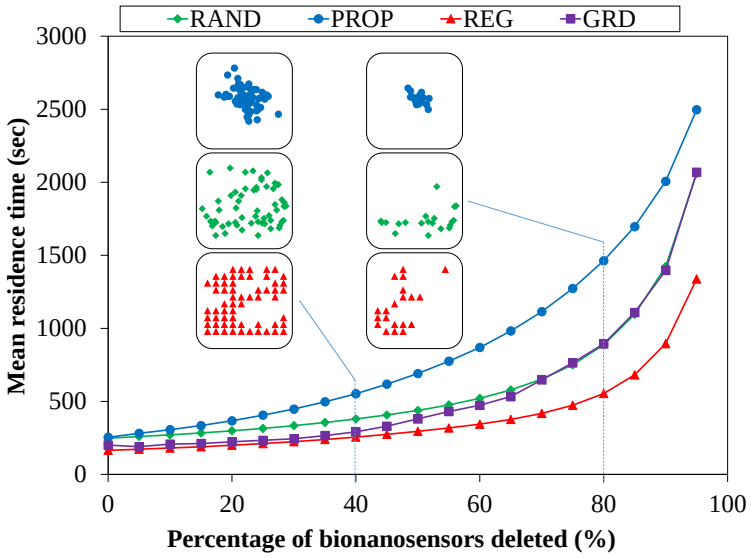


Figure 2.9: Impact of bionanosensor failure at random locations on the mean residence time. $\sigma = 50/3$ and $|S| = 100$.

2.5 Summary

In this chapter, we designed, modeled and evaluated the performance of a static bionanosensor network for target detecting. In the static bionanosensor network considered in this chapter, bionanosensors are placed in the environment to detect targets that randomly walk in the environment. We formulated the target detection problem as an optimization problem to find a spatial distribution of bionanosensors that can minimize mean residence time of targets (i.e., the amount of time from when a target appears in the environment to when it is detected by a bionanosensor). We then mathematically analyzed the problem under the condition that target arrival locations follow the uniform distribution: for one-dimensional environment, we found the optimal solution, and for n-dimensional environment ($n \geq 2$), we provided the lower bound expression. Furthermore, in a two-dimensional environment, where analytical approaches are not available, we assumed that target arrival locations follow the normal distribution and conducted

simulation experiments to compare the performance of several placement schemes (i.e., REG, RAND, and PROP) in terms of mean residence time.

Key results and findings described in this chapter are summarized below:

- When target arrival locations are uniformly distributed in a one-dimensional environment, placing bionanosensors at a constant spatial interval (i.e., REG) provides the optimal solution that can minimize mean residence time (Subsection 2.3.1). In more general cases, where target arrival locations are uniformly distributed in an n-dimensional environment ($n \geq 2$), finding optimal placement is intractable. For such cases, we provided the lower bound expression of mean residence time using key parameters such as the number of bionanosensors and the size of the environment (Subsection 2.3.2).

- When target arrival locations are normally distributed, mean residence time is highly affected by the deviation of the target arrival distribution function (Subsection 2.4.3). When the deviation is small, PROP performs best; however, when the deviation is large, REG outperforms PROP. When target arrival locations are not clearly known, i.e., normally distributed with a high deviation (> 0.5), REG is the best placement scheme out of the three placement schemes examined in this chapter (i.e., REG, PROP, and RAND). Additional simulation experiments however reveal that REG is vulnerable to a scenario where bionanosensors fail according to the target arrival distribution function while PROP is robust to such a scenario.

Our future work in static bionanosensor networks includes modeling complex network environments such as carbon nanotube networks [18] and microtubule networks [27] that affect how targets propagate in their environments. Our future work also includes modeling targets with more complex behavior such as viruses and bacteria that may grow, divide, and evolve while they migrate.

Chapter 3

Dynamic Bionanosensor Networks for Target Tracking

3.1 Overview

In this chapter, we consider a dynamic bionanosensor network for target tracking application. A bionanosensor network considered in this chapter consists of autonomous mobile bionanosensors. The dynamic bionanosensor network that exploits the mobility of bionanosensors has potential not only for quickly detecting targets, but also for tracking moving targets. The target tracking problem described in this chapter may apply to advanced targeted drug delivery, where sustained drug release is required for moving targets (e.g., pathogens, infectious micro-organisms, or chemical weapons). In such applications, bionanosensors storing drug molecules need to locate targets and keep track of targets as they move.

Fig. 3.1 shows a model of the dynamic bionanosensor network to be investigated in this chapter. Bionanosensors that constitute the dynamic bionanosensor network autonomously migrate in the monitoring environment. A target arrives and propagates in the monitoring environment. The specific task for the bionanosensors is to cooperatively locate a target and track the target as it moves.

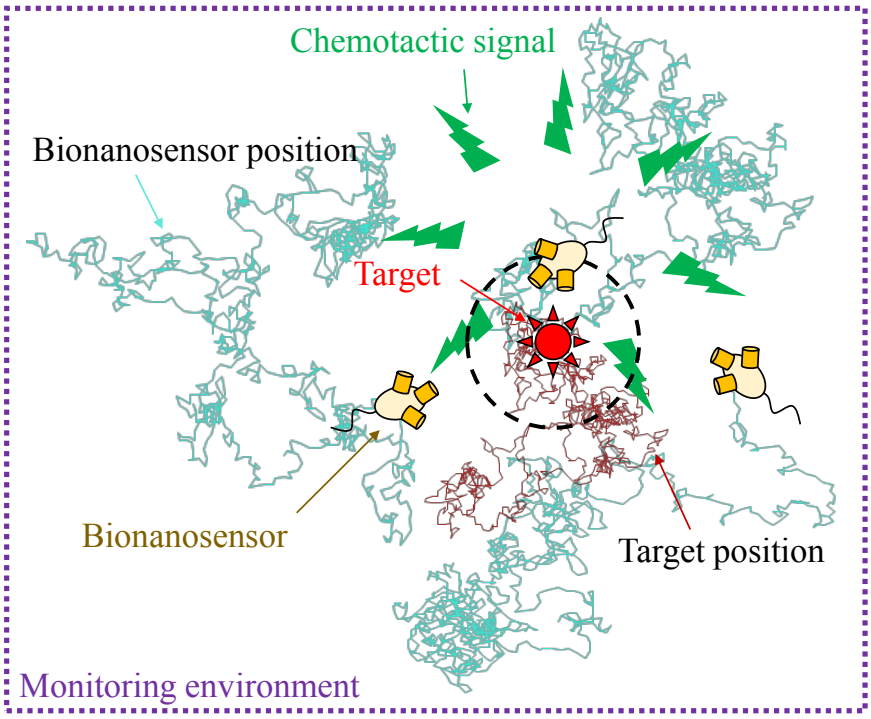


Figure 3.1: A dynamic bionanosensor network

For more detail of these model components, see Section 1.3.

A bionanosensor network considered in this chapter is dynamic in that bionanosensors autonomously move in the environment. In such a network, bionanosensors need to coordinate their movement to efficiently locate and detect targets. In this chapter, we consider that bionanosensors use two types of signaling molecules to coordinate their movement: repellents and attractants. In search of a target, bionanosensors release repellents to quickly spread over the environment; the released repellents form the concentration gradient in the environment, bionanosensors move toward lower concentrations of repellents and therefore they move away from each other to help their search processes. Upon detecting a target, they release attractants to recruit other bionanosensors in the environment toward the target location; the released attractants also form the concentration gradient in the environment, and bionanosensors move toward higher concentrations of

attractants, namely toward the target location.

Figs. 3.2 and 3.3 exemplify a target tracking processes, i.e., how the repellents and attractants work in locating and tracking a single moving target. Fig. 3.2 illustrates the processes as spatial-temporal distributions of bionanosensors, and Fig. 3.3 shows the processes as a dynamics of the number of bionanosensors in the proximity of the target. (The number of bionanosensors found within the red open circle.) Here (a) a group of bionanosensors is placed in the monitoring environment where a target exists, (b) the group of bionanosensors first spreads over the environment using repellents, and as a result one of the bionanosensors detects the target, (c) this bionanosensor, upon detecting the target, starts releasing attractants and nearby bionanosensors are thus attracted to the location of the bionanosensor (i.e., near the target), and (d) as the target moves, the group of bionanosensors uses repellents and attractants in the same manner to move and track the target.

The remainder of this chapter is organized as follows. In Section 3.2, we model dynamic bionanosensor networks for target tracking using a set of partial differential equations (PDEs). In Section 3.3, we conduct numerical experiments to understand how parameters for interactions among bionanosensors impact on the target tracking performance. Finally, we conclude this chapter in Section 3.4.

3.2 PDE-based Model

In the bionanosensor networks, a set of bionanosensors collectively moves through *simple* interactions with repellents and attractants. Simplicity is a key requirement in bionanosensor design in general. With this point in mind, we design a bionanosensor that emits attractants and repellents as follows.

- A bionanosensor continuously emits repellents.
- A bionanosensor emits attractants only when it detects the target, i.e., bionanosensor stays at the target site.

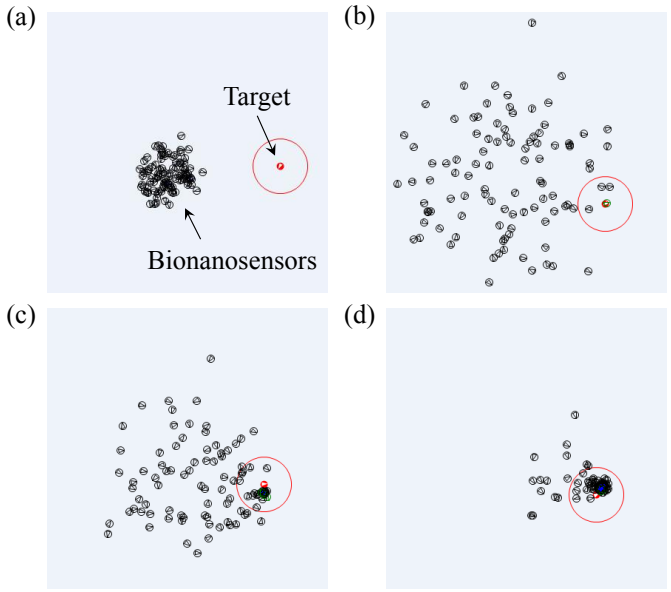


Figure 3.2: Spatial-temporal distributions of bionanosensors [66, 68].

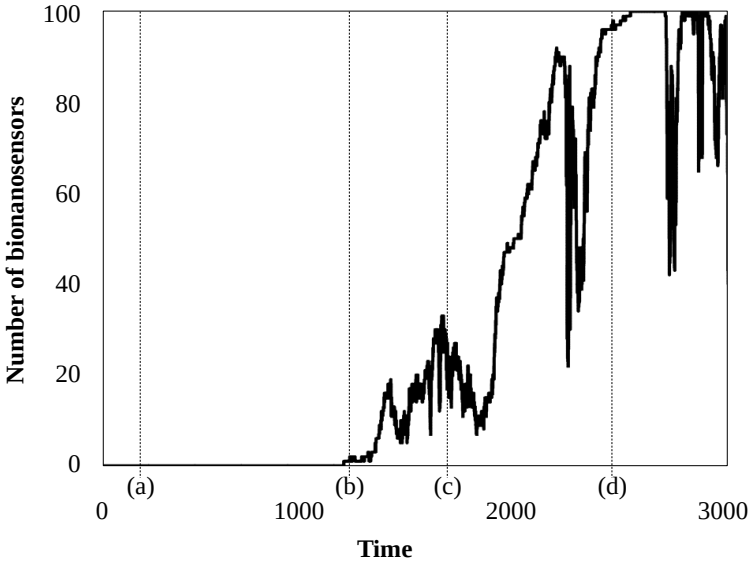


Figure 3.3: Number of bionanosensors in the proximity of the target.

The mobility of a given bionanosensor is affected by the concentrations (i.e., density of molecules) and concentration gradients of attractants and repellents

at its location. Following the classical model of bacterial chemotaxis [40], we assume that a bionanosensor is able to sense concentrations and concentration gradients of repellents and attractants at its location, and changes its moving direction toward a lower concentration of repellents and/or a higher concentration of attractants.

The model shown in this section describes the rates of changes in concentrations of bionanosensors, attractants and repellents, respectively denoted as C_b, C_a, and C_r. In this section, we describe a two-dimensional model and thus $C_b\,(= C_b(x, y, t))$, $C_a\,(= C_a(x, y, t))$ and $C_r\,(= C_r(x, y, t))$. Note that the model can be easily extended to one-dimension [67] or three-dimension as needed.

The objective is to maximize the concentration of bionanosensors at the target location.

$$\text{Maximize}: \quad C_b(x, y, t) \cdot c_T(x, y, t) \tag{3.1}$$

3.2.1 Dynamics of Bionanosensor Concentration

Bionanosensors diffuse based on the concentration gradients of attractants and repellents in the two-dimensional area. Bionanosensors are not produced nor lost in the area. The rate of change in C_b in this case is described using the partial differential equation below.

$$\frac{\partial C_b}{\partial t} \;=\; D_b \left(\frac{\partial^2 C_b}{\partial x^2} + \frac{\partial^2 C_b}{\partial y^2} \right) - \left(\frac{\partial f\, C_b}{\partial x} + \frac{\partial f\, C_b}{\partial y} \right) \tag{3.2}$$

The first term on the right hand side of (3.2) describes the diffusion of bionanosensors according to the diffusion coefficient D_b and the second term the drift effect or biased diffusion determined by the function f.

The drift effect f is modeled as a linear combination of the two individual drift effects f_a by attractants and f_r by repellents: i.e.,

Table 3.1: Notations

Symbol	Description
L	Half length of the area along an axis
C_b	Concentration of bionanosensors
C_r	Concentration of attractants
C_a	Concentration of repellents
C_T	Concentration of targets
D_b	Diffusion coefficient of bionanosensors
D_a	Diffusion coefficient of attractants
D_r	Diffusion coefficient of repellents
k_a	Decay rate constant of attractants
v	Production rate constant of repellents
k_r	Decay rate constant of repellents
V_a	Attraction coefficient
K_a	Sensitivity to the attractant concentration
V_r	Repulsion coefficient
K_r	Sensitivity to the repellent concentration
V	Maximum attractant production rate
K_1	Parameter for attractant production
K_2	Parameter for attractant production
N_b	Number of bionanosensors in the area
N_T	Number of targets in the area
g_a	Production rate of attractants
g_r	Production rate of repellents

$$f = f_a - f_r, \tag{3.3}$$

$$f_a = \frac{V_a\, C_a}{K_a + C_a}\left(\frac{\partial C_a}{\partial x} + \frac{\partial C_a}{\partial y}\right), \tag{3.4}$$

$$f_r = \frac{V_r\, C_r}{K_r + C_r}\left(\frac{\partial C_r}{\partial x} + \frac{\partial C_r}{\partial y}\right). \tag{3.5}$$

See Table 3.1 for parameters (V_a, V_r, K_a and K_r) used above.

The initial distribution of bionanosensors over the two-dimensional area is

described by C_{b0}, and the boundaries of the two-dimensional area are set to be reflecting for bionanosensors (i.e., bionanosensors do not diffuse away from the area). Thus, the initial condition and boundary conditions become

$$C_b = C_{b0} \quad \text{at} \quad t = 0, \tag{3.6}$$

$$\frac{\partial C_b}{\partial x} = 0 \quad \text{at} \quad x = -L \text{ and } L, \tag{3.7}$$

$$\frac{\partial C_b}{\partial y} = 0 \quad \text{at} \quad x = -L \text{ and } L. \tag{3.8}$$

3.2.2 Dynamics of Attractant Concentration

Bionanosensors use attractants to communicate the location information of targets. Without loss of generality, we assume that attractants diffuse in the monitoring area while they are produced and broken down. Thus, the rate of change in C_b is given by

$$\frac{\partial C_a}{\partial t} = D_a \left(\frac{\partial^2 C_b}{\partial x^2} + \frac{\partial^2 C_b}{\partial y^2} \right) + g_a - k_a C_a, \tag{3.9}$$

where D_a is the diffusion coefficient of attractants, g_a the production rate of attractants, and k_a the decay rate constant of attractants.

Assuming that bionanosensors are the only source of producing attractants and that they release attractants upon detecting targets, the production rate g_a is written as

$$g_a = \frac{V C_b C_T}{(K_1 + C_b)(K_2 + C_T)}, \tag{3.10}$$

where C_T is the concentration of targets at location (x, y) and at time t. V, K_1, and K_2 are parameters; see Table 3.1.

Assuming further that attractants do not exist in the monitoring area initially

and that they diffuse within the area (i.e., they do not diffuse away at the boundaries of the area), the initial condition and boundary conditions for attractants become

$$C_a = 0 \quad \text{at} \quad t = 0, \tag{3.11}$$
$$\frac{\partial C_a}{\partial x} = 0 \quad \text{at} \quad x = -L \text{ and } L, \tag{3.12}$$
$$\frac{\partial C_a}{\partial y} = 0 \quad \text{at} \quad x = -L \text{ and } L. \tag{3.13}$$

3.2.3 Dynamics of Repellent Concentration

Bionanosensors use repellents to distribute over the monitoring area. Similar to (3.9), the rate of change in C_r is given by

$$\frac{\partial C_r}{\partial t} = D_r \left(\frac{\partial^2 C_r}{\partial x^2} + \frac{\partial^2 C_r}{\partial y^2} \right) + g_r - k_r \, C_r, \tag{3.14}$$

where D_r is the diffusion coefficient of repellents, g_r the production rate of repellents, and k_r the decay rate constant of repellents. When the production rate of repellents is constant per bionanosensor, we describe g_r as

$$g_r = v \, C_b. \tag{3.15}$$

Applying the same assumptions made to the attractants, the initial condition and boundary conditions for repellents become

$$C_r = 0 \quad \text{at} \quad t = 0, \tag{3.16}$$
$$\frac{\partial C_r}{\partial x} = 0 \quad \text{at} \quad x = -L \text{ and } L, \tag{3.17}$$
$$\frac{\partial C_r}{\partial y} = 0 \quad \text{at} \quad y = -L \text{ and } L. \tag{3.18}$$

3.3 Numerical Experiments

The set of PDEs described in the previous section, namely (3.2), (3.9) and (3.14), are numerically integrated to compute the concentrations of bionanosensors, attractants and repellents. In the first set of numerical experiments, we examine the effect of attractants in recruiting distributed bionanosensors to a single location, where no repellents are used. We then examine, in the second set of experiments, the effect of repellents without using attractants, in spreading bionanosensors from a single location over the monitoring area. In the last set of experiments, we examine the combined effects of attractants and repellents in tracking moving targets.

In numerical experiments, we set the following parameter values as default unless otherwise noted: $L = 50$, $D_a = 10$, $D_b = 5$, $D_r = 2$, $k_a = 0.5$, $k_r = 0.2$, $v = 0.2$, $K_a = 0.1$, $K_r = 0.1$, $V = 1$, $K_1 = 0.1$, $K_2 = 0.1$, $N_b = 100$ (units are arbitrary). Note that we performed preliminary experiments and determined these parameter values based on the experimental results. Note also that values for V_a and V_r are given in each set of experiments described in this section.

3.3.1 Numerical Method

To numerically find the solution for a set of PDEs, we adopt a method of finite difference. In this method, domain of a function is subdivided into a set of finite subdomains. The derivative of the function is approximated as the difference between the function values at neighboring subdomains divided by the sizes of subdomains. For instance, the first partial derivative of a function $f(x,t)$ at $x = x_i$ is calculated as

$$\left.\frac{\partial f(x,t)}{\partial x}\right|_{x=x_i} = \frac{f(x_{i+1},t) - f(x_i,t)}{x_{i+1} - x_i}, \tag{3.19}$$

and the second partial derivative of $f(x,t)$ at $x = x_i$ as

$$\left.\frac{\partial^2 f(x,t)}{\partial x^2}\right|_{x=x_i} = \frac{1}{x_{i+1}-x_i}\left\{\left.\frac{\partial f(x,t)}{\partial x}\right|_{x=x_{i+1}} - \left.\frac{\partial f(x,t)}{\partial x}\right|_{x=x_i}\right\}. \quad (3.20)$$

By approximating the derivatives of functions, finite difference method constructs the set of PDEs considered. In practice, our set of PDEs considered in this chapter consists of first-order PDEs with respect to time variable. In this case, the discretization is applied only on the spatial variables leaving time variable t continuous, so that we can apply an approximation method for ordinary differential equations, known as "numerical integration." Starting from the initial time $t = t_0$, the solution for the set of PDEs is sequentially calculated.

3.3.2 Impact of Attractants

The attractants allow bionanosensors, upon detecting a target, to direct other bionanosensors in the monitoring area towards the location of the target. Without attractants, a group of bionanosensors moves through non-directional diffusion, eventually forming a uniform distribution over the area (i.e., $C_b = N_b/(2L)^2$).

To understand the effect of the attractants, we distribute bionanosensors uniformly in a two-dimensional area, place one static target at the center of the area, and observe how the bionanosensors are attracted to the target location. We therefore apply the following conditions.

$$C_{b0} = \frac{N_b}{(2L)^2} \quad (3.21)$$

$$C_T = \delta(x)\,\delta(y) \quad (3.22)$$

Note that no repellents are produced (i.e., $g_r = 0$) in this set of numerical experiments.

Fig. 3.4 shows how the mean square distances between bionanosensors and the

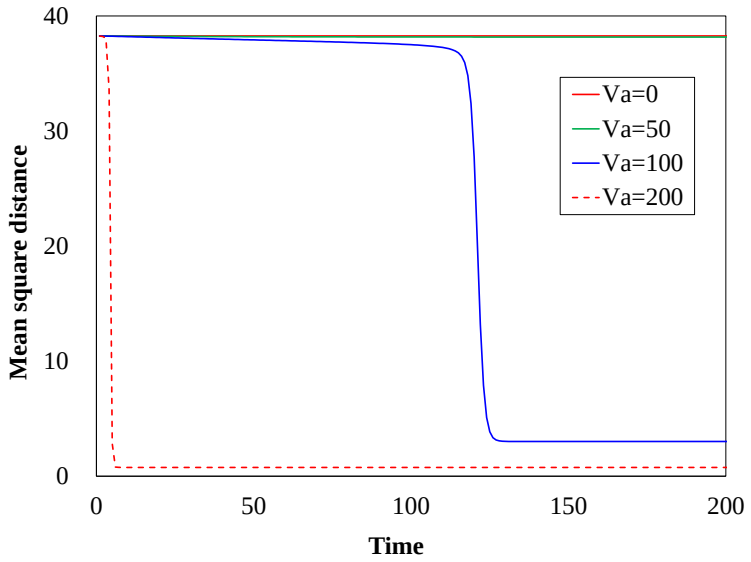


Figure 3.4: Impact of the attraction coefficient (V_a) on the mean square distance between bionanosensors and the target.

target change over time for different attraction coefficients $V_a \in \{0, 50, 100, 200\}$. As shown in the figure, the mean square distance drops sharply when a large V_a is used (e.g., $V_a = 200$), while being unchanged for a small V_a (e.g., $V_a = 50$). Note that $V_a = 0$ represents the case without attractants; in this case, bionanosensors remain uniformly distributed and the mean square distance never decreases. The figure also shows that the mean square distance converges after a sufficiently long time elapses, indicating that the distribution of bionanosensors over the area reaches its steady state.

Fig. 3.5 shows the steady-state distributions of bionanosensors along the x-axis of the area obtained at $t = 1000$ for different attraction coefficients $V_a \in \{0, 50, 100, 200\}$. The figure shows that, as V_a increases from $V_a = 50$ to 100 and 200, the steady-state concentration of bionanosensors becomes higher around the target location, indicating that the steady-state concentration of bionanosensors becomes lower at locations far from the target (see also Figs. 3.6 – 3.9 below). Note that, when attractants are not used ($V_a = 0$), the concentration of

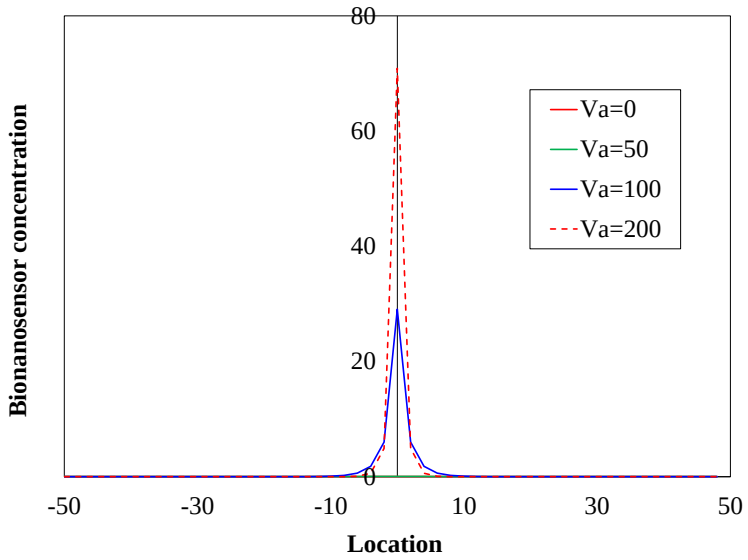


Figure 3.5: Impact of the attraction coefficient (V_a) on the steady-state distribution of bionanosensors.

bionanosensors is unchanged and $C_b = 0.04$.

Figs. 3.6 – 3.9 show how the concentrations of bionanosensors measured at different locations $(x, 0)$ change over time ($x \in \{0, 4, 10, 20\}$). When a small V_a is used (e.g., $V_a = 50$), the concentration of bionanosensors remains almost unchanged (i.e., $C_b = 0.04$) as also observed in Fig. 3.5. When a large V_a is used (e.g., $V_a = 100$ or 200), the concentration of bionanosensors at locations closer to the target increases over time to reach a concentration higher than the initial concentration of $C_b = 0.04$ (e.g., $x = 0$ and 4 for $V_a = 200$, $x = 0$, 4 and 10 for $V_a = 100$), while the concentration far from the target decreases, indicating that bionanosensors initially distributed uniformly over the monitoring area move towards the target.

Figs. 3.10 and 3.11 show the spatio-temporal dynamics of the bionanosensor concentration and of attractant concentration, when attractants are used, illustrating how the attractants spread in the area and how bionanosensors gather based on the distribution of attractants in the area. In these figures, horizontal axis rep-

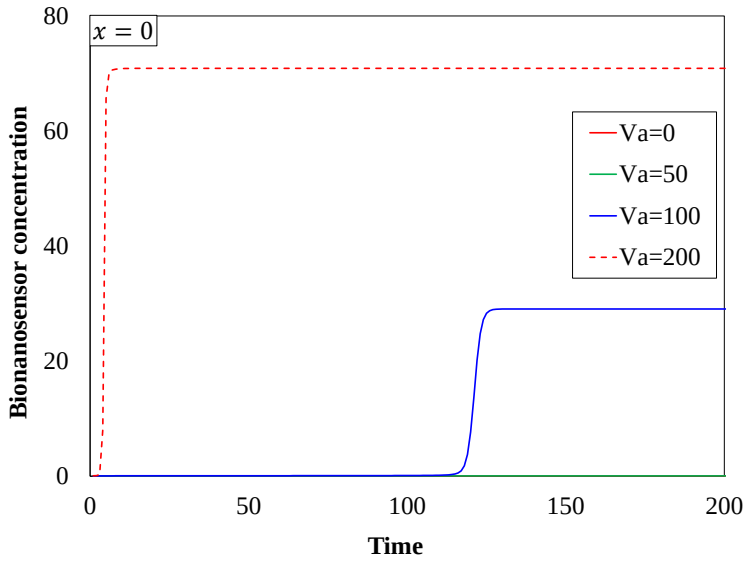


Figure 3.6: Impact of the attraction coefficient (V_a) on the concentrations of bionanosensors at location $x = 0$.

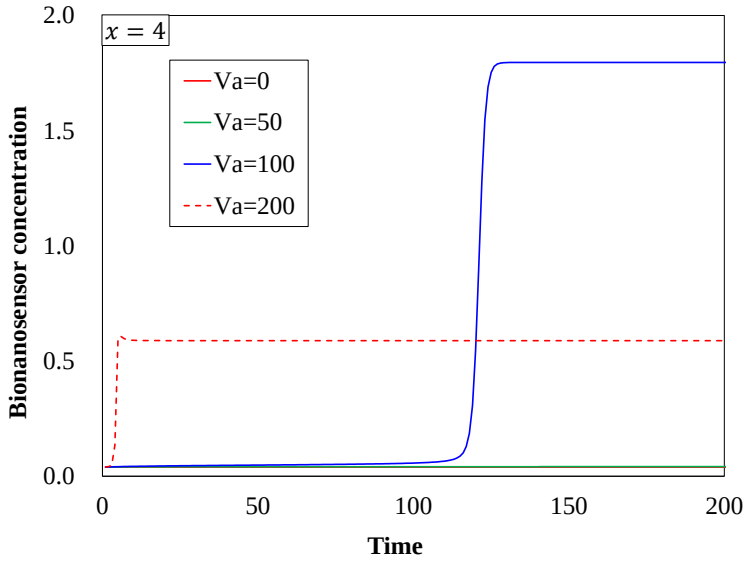


Figure 3.7: Impact of the attraction coefficient (V_a) on the concentrations of bionanosensors at location $x = 4$.

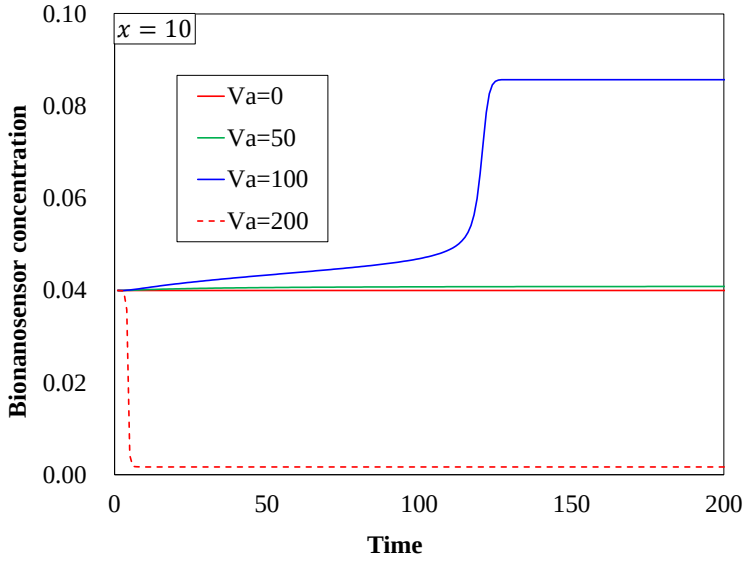


Figure 3.8: Impact of the attraction coefficient (V_a) on the concentrations of bionanosensors at location $x = 10$.

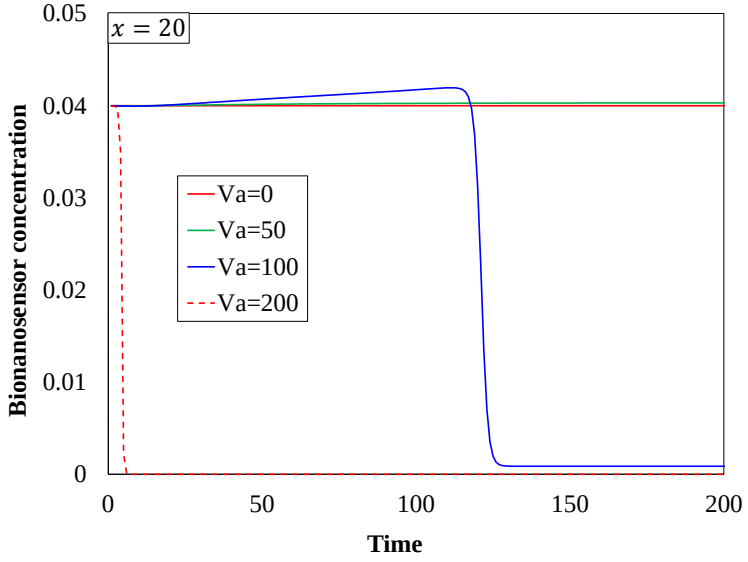


Figure 3.9: Impact of the attraction coefficient (V_a) on the concentrations of bionanosensors at location $x = 20$.

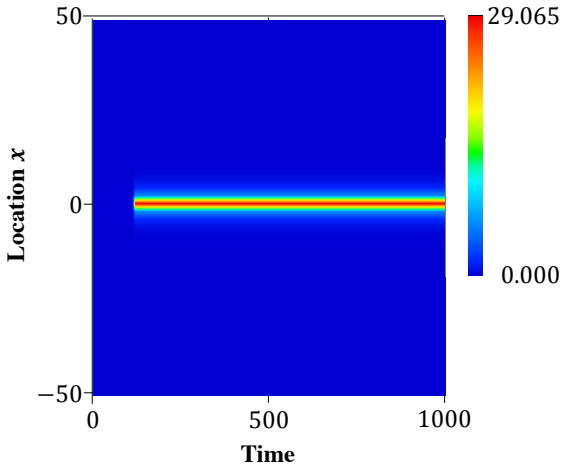


Figure 3.10: The spatio-temporal dynamics of the bionanosensor concentration for $V_a = 100$, where color bar represents the concentration of bionanosensors.

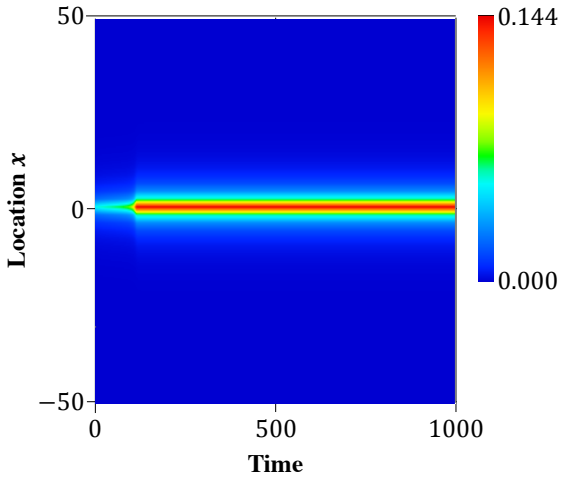


Figure 3.11: The spatio-temporal dynamics of the attractant concentration for $V_a = 100$, where color bar represents the concentration of attractants.

resents time, vertical axis corresponds to location $(x, 0)$, and the color legend the bionanosensor / attractants concentration.

3.3.3 Impact of Repellents

The repellents facilitate the spread of bionanosensors, and become useful to locate a target that is distant from the bionanosensors or when the monitoring area is large. Without repellents, a group of bionanosensors at a location spreads based on non-directional diffusion, which can be a slow-spreading process. The mean square of the distance from the origin to a bionanosensor in the absence of repellents increases in proportion to the time ($<x^2>+<y^2> = 4D_b t$), indicating that a significantly long time is taken for bionanosensors to distribute in the area.

To understand the effect of the repellents, we place bionanosensors at the center of a two-dimensional area (i.e., the origin) and observe how they spread over the area in the absence of targets: i.e., we apply the following conditions.

$$C_{b0} = N_b\,\delta(x)\,\delta(y), \tag{3.23}$$

$$C_T = 0. \tag{3.24}$$

Note that targets do not exist in the area and thus no attractants are produced in this set of numerical experiments.

Fig. 3.12 shows how the mean square distances between bionanosensors and the origin increase over time for different repulsion coefficients $V_r = \{0, 1, 10\}$. As expected, the mean square distance increases based on repulsive forces as V_r increases. Note that the mean square distance reaches a plateau or its steady-state after a sufficiently long time elapses since the area is bounded.

Figs. 3.13 – 3.16 show how the concentrations of bionanosensors measured at different locations $(x, 0)$ change over time ($x = \{0, 4, 10, 20\}$). The figures show that, when repellents are used ($V_r = 1$ or 10), the concentration of bionanosensors quickly decreases around the origin (i.e., $x = 0$) while it increases at locations far from the origin (e.g., $x = 10$ and 20) compared to the case without repellents ($V_r = 0$). The quick increase in bionanosensor concentration at locations far from the target may indicate that bionanosensors detect a target quicker and with

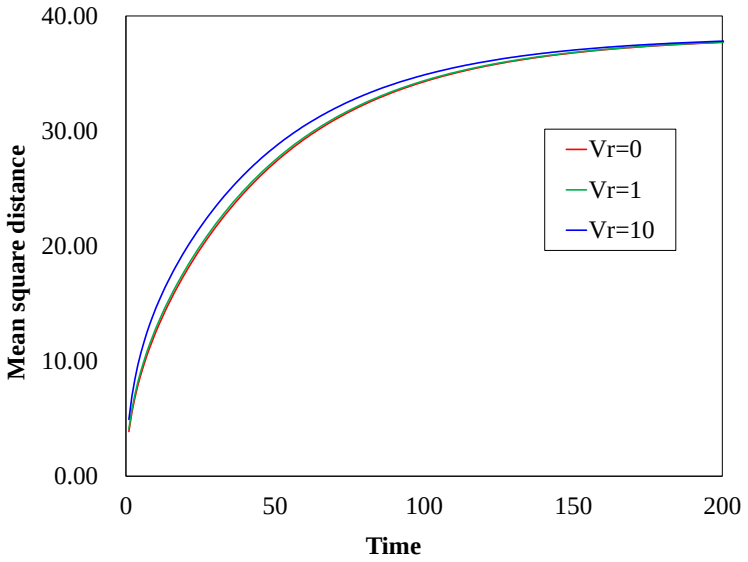


Figure 3.12: Impact of the repulsion coefficient (V_r) on the mean square distance between bionanosensors and the target.

a higher probability when repellents are used, (see also Section 3.3.4.2).

Fig. 3.17 shows the spatio-temporal dynamics of the bionanosensor concentration when repellents are not used ($V_r = 0$) and Fig. 3.18 when repellents are used ($V_r = 10$), illustrating the effect of repellents. In these figures, the horizontal axis represents time, the vertical axis represents location $(x, 0)$, and the color bar shows the bionanosensor concentration. When repellents are used, the bionanosensors concentrated at the target location $(0, 0)$ quickly move away from the target location, split into two groups, and eventually distributed uniformly in the environment. Fig. 3.19 shows the spatio-temporal dynamics of repellent concentration when repellents are used ($V_r = 10$).

3.3.4 Target Tracking

In the last set of numerical experiments, we demonstrate that a group of bionanosensors is able to track moving targets using attractants and repellents. We

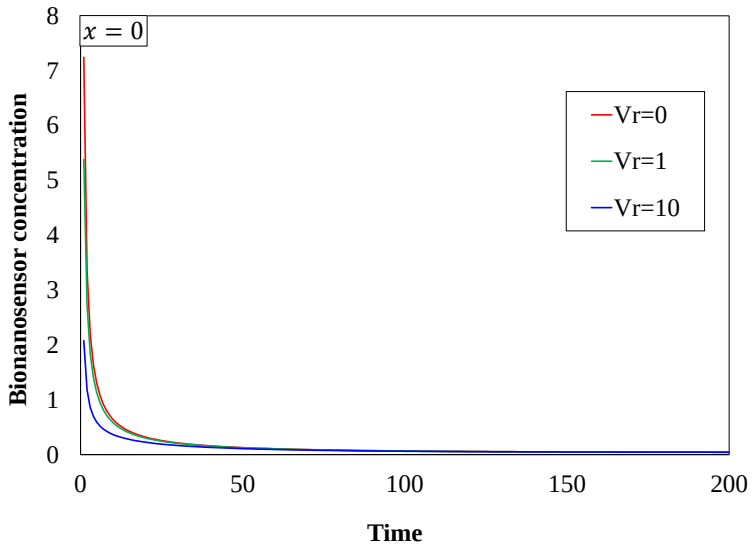


Figure 3.13: Impact of the repulsion coefficient (V_r) on the concentrations of bionanosensors at location $x = 0$.

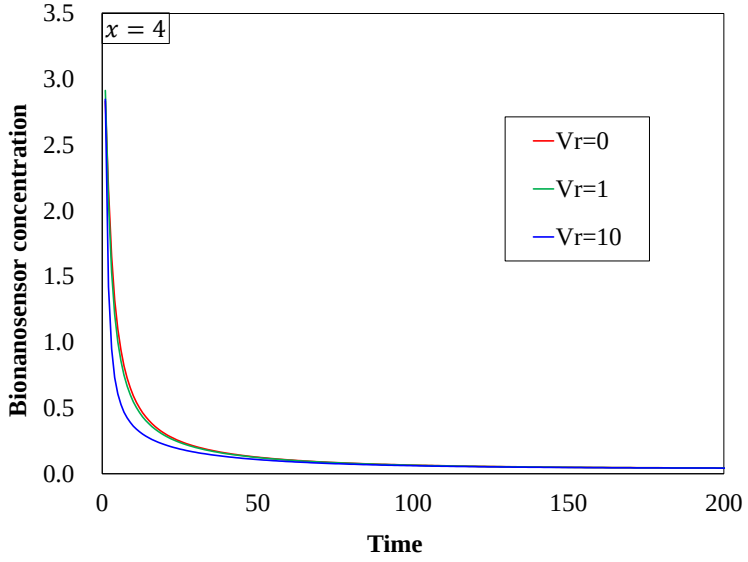


Figure 3.14: Impact of the repulsion coefficient (V_r) on the concentrations of bionanosensors at location $x = 4$.

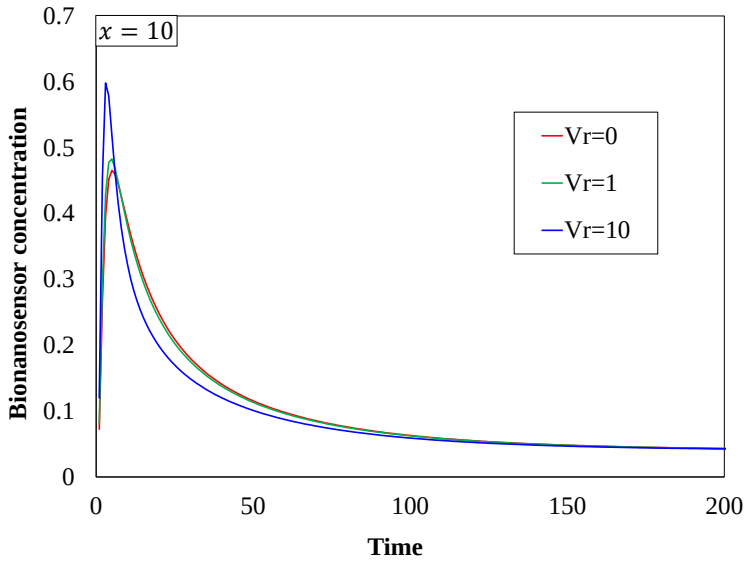


Figure 3.15: Impact of the repulsion coefficient (V_r) on the concentrations of bionanosensors at location $x = 10$.

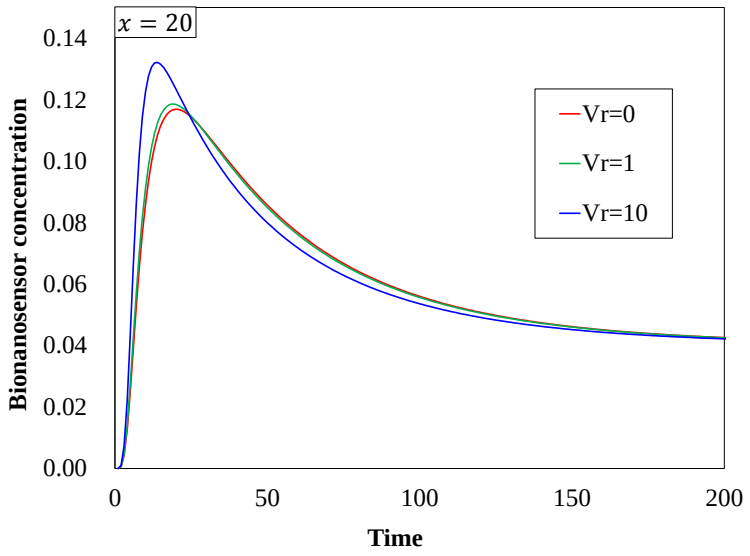


Figure 3.16: Impact of the repulsion coefficient (V_r) on the concentrations of bionanosensors at location $x = 20$.

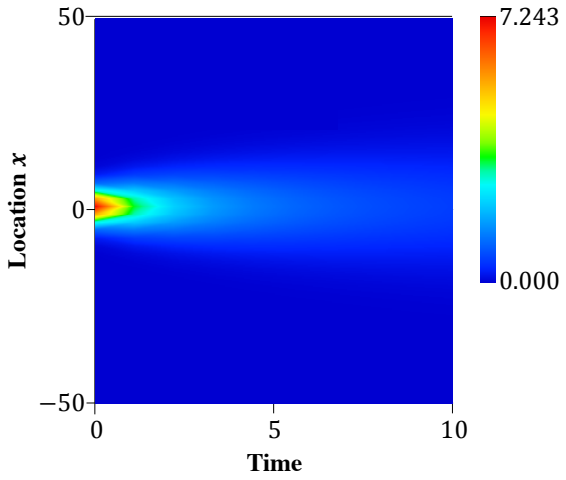


Figure 3.17: The spatio-temporal dynamics of the bionanosensor concentration for $V_r = 0$. Color bar represents the concentration of bionanosensors.

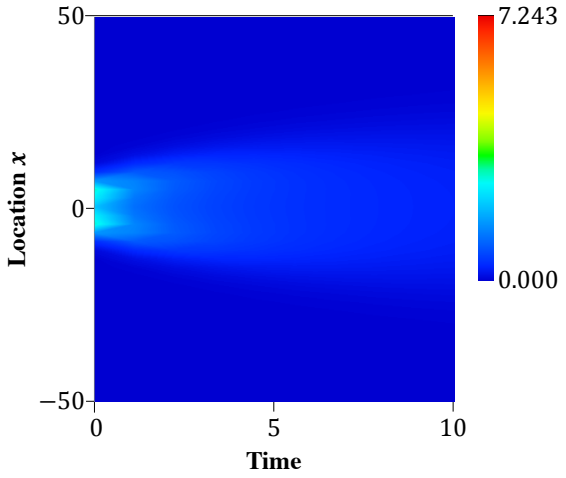


Figure 3.18: The spatio-temporal dynamics of the bionanosensor concentration for $V_r = 10$. Color bar represents the concentration of bionanosensors.

first show that attractants are used to track a moving target (in Section 3.3.4.1). We then show that the combined use of attractants and repellents may also be useful to track a moving target (in Section 3.3.4.2).

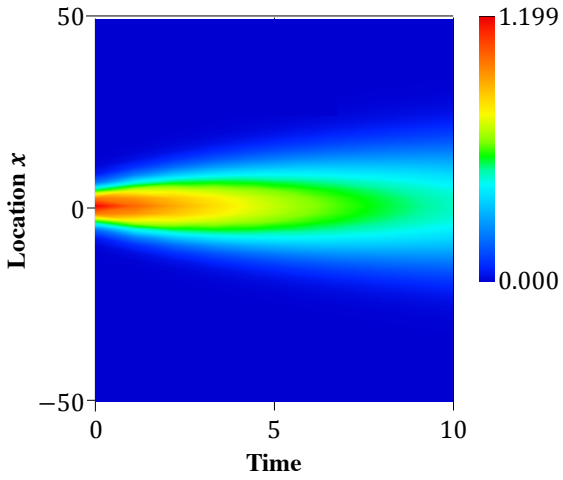


Figure 3.19: The spatio-temporal dynamics of the repellent concentration for $V_r = 10$. Color bar represents the concentration of repellents.

3.3.4.1 Using Attractants for Target Tracking

To examine the effect of attractants to track a moving target, we introduce a single target that performs circular motion, leading to

$$C_T = \delta\left(x - \frac{3L}{5}\cos\omega t\right)\,\delta\left(y - \frac{3L}{5}\sin\omega t\right), \tag{3.25}$$

where ω is the angular velocity of the moving target. For the initial condition of the bionanosensor concentration, we use (3.21) (i.e., uniform distribution), although the initial condition appears to have no impact on results shown below.

Figs. 3.20 – 3.22 show the concentrations of bionanosensors at the target location for different angular velocities of the moving target $\omega \in \{0, \pi/400, \pi/200\}$, respectively, showing that a larger V_a is needed to successfully track the moving target as the target moves faster (i.e., as ω increases). Fig. 3.23 shows whether a particular combination of the attraction coefficient and the angular velocity of the moving target achieves "successful" tracking. In this figure, '$\circ$' represents a successful case where the bionanosensor concentration at the target location is maintained at higher than 10 and '$\times$' represents an unsuccessful case. (Note that

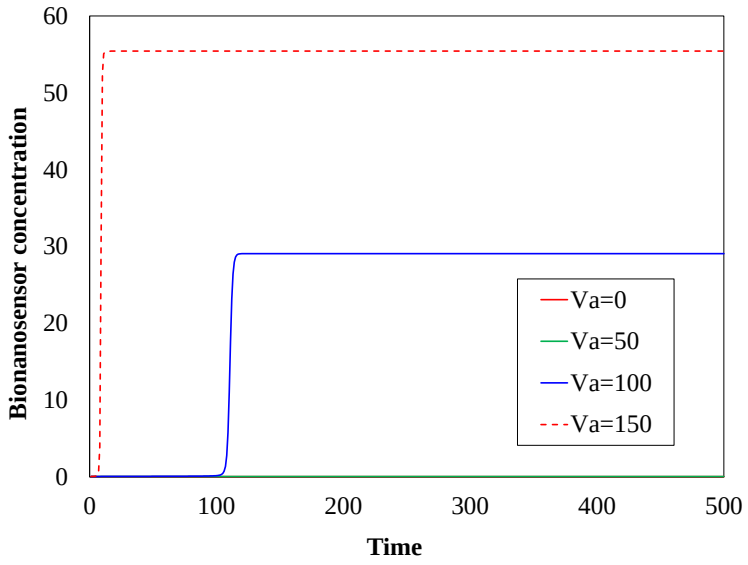


Figure 3.20: Concentration of bionanosensors at the target that is static, i.e., $\omega = 0$. $V_a = \{0, 50, 100, 150\}$. $V_r = 0$.

$C_b = 0.04$ when bionanosensors are uniformly distributed.) Fig. 3.24 shows two example cases of target tracking: a successful case ($V_a = 100$ and $\omega = \pi/400$) and an unsuccessful case ($V_a = 100$ and $\omega = \pi/200$). As shown in the figure, in a successful case, most of the bionanosensors are found at the target and (almost) no bionanosensors are found at non-target locations, while in an unsuccessful case the bionanosensors are distributed around the target location and only a small number of bionanosensors are found at the target location.

3.3.4.2 Combined Use of Attractants and Repellents

The combined use of attractants and repellents becomes useful when the target moves fast or irregularly. To demonstrate the role of repellents in target tracking, we simulate a scenario where a single target is present at the origin in the area from time $t = 0$ to 500, moves to location $(d, 0)$ at $t = 500$, and stays at the location. For the initial condition of the bionanosensor concentration, we use (3.21) (i.e., uniform distribution), although the initial condition appears to have no impact on

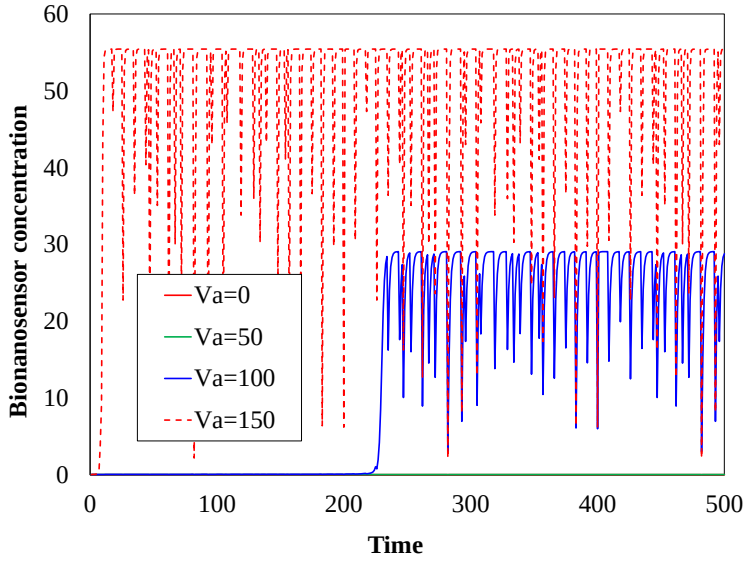


Figure 3.21: Concentration of bionanosensors at the target that moves with an angular velocity $\omega = \pi/400$. $V_a = \{0, 50, 100, 150\}$. $V_r = 0$.

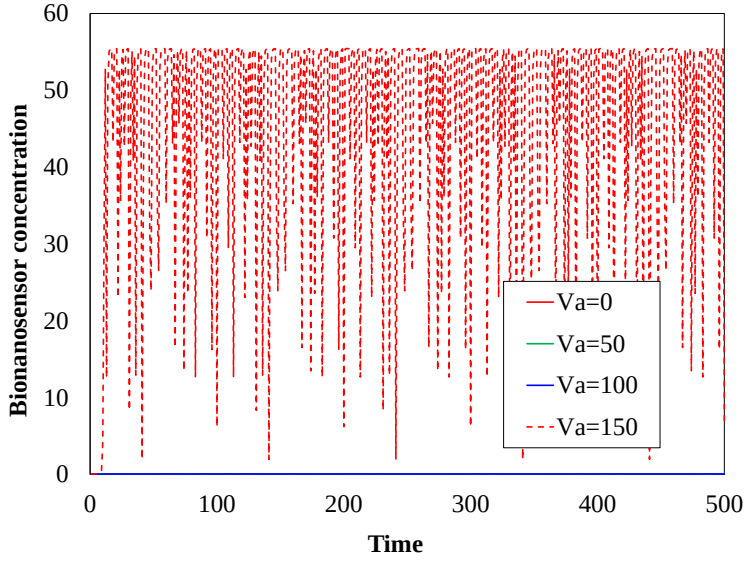


Figure 3.22: Concentration of bionanosensors at the target that moves with an angular velocity $\omega = \pi/200$. $V_a = \{0, 50, 100, 150\}$. $V_r = 0$.

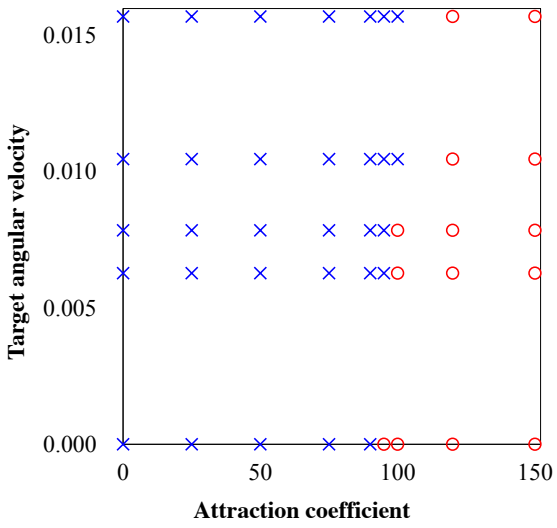


Figure 3.23: The combinations of the attraction coefficient and the target angular velocity: ○ represents a successful case and × an unsuccessful case.

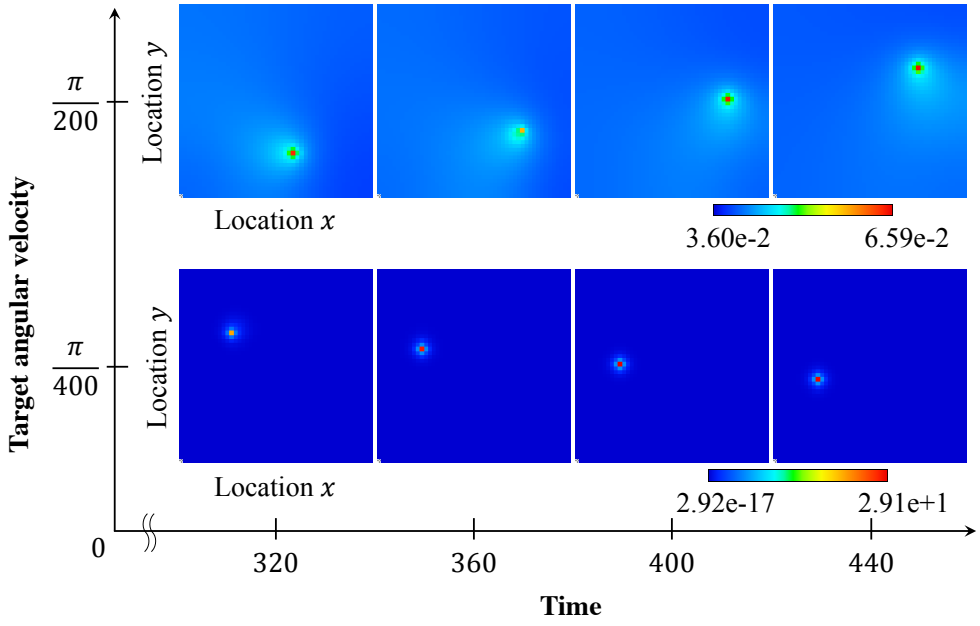


Figure 3.24: Representative target tracking processes.

results shown below.

Figs. 3.25 – 3.27 show the concentrations of bionanosensors at different locations $(d, 0)$ ($d = \{4, 10, 20\}$) and Figs. 3.28 – 3.30 show the first location times of a moving target obtained from Figs. 3.25 – 3.27 with $V_a = 100$ and $V_r \in \{0, 1, 10\}$. The first location time is defined as the time taken for the concentration of bionanosensors to reach the threshold concentration θ at the target location. The first location time indicates how long it takes for bionanosensors to detect a target and start releasing attractants, once the target is lost during the process of target tracking. As shown in the figures, the repellents can decrease the first location time for large d.

Fig. 3.31 shows the target tracking performance measured by the time average of the percentage of bionanosensors around the moving target. As shown in the figure, the target tracking performance is maximized when the attractant coefficient is large and the repellent coefficient is small, demonstrating that repellents negatively impact the target tracking performance. This is probably because repellents tend to prohibit bionanosensors from gathering at the same location (e.g., the target location) although they are useful to decrease the first location time of a target. We consider that in the PDE-based model, target detection is a trivial task for bionanosensors because of the continuum nature of the model and the role of repellents becomes less significant. As we will see in next chapter, when an individual-based, desecrated model of bionanosensors is used, both attractants and repellents become useful for target tracking.

3.4 Summary

In this chapter, we designed, modeled and evaluated the performance of a dynamic bionanosensor network for target tracking. In the dynamic bionanosensor network considered in this chapter, bionanosensors use repellents and attractants to detect and track a moving target. Bionanosensors release repellents to spread over the monitoring environment in search of targets, while they release attrac-

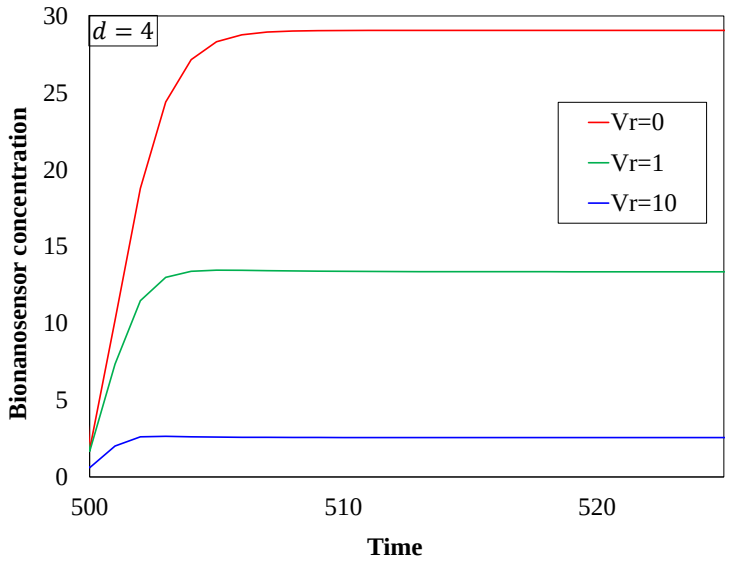


Figure 3.25: Impact of combined use of attractants and repellents on the concentrations of bionanosensors at the target location with $d = 4$.

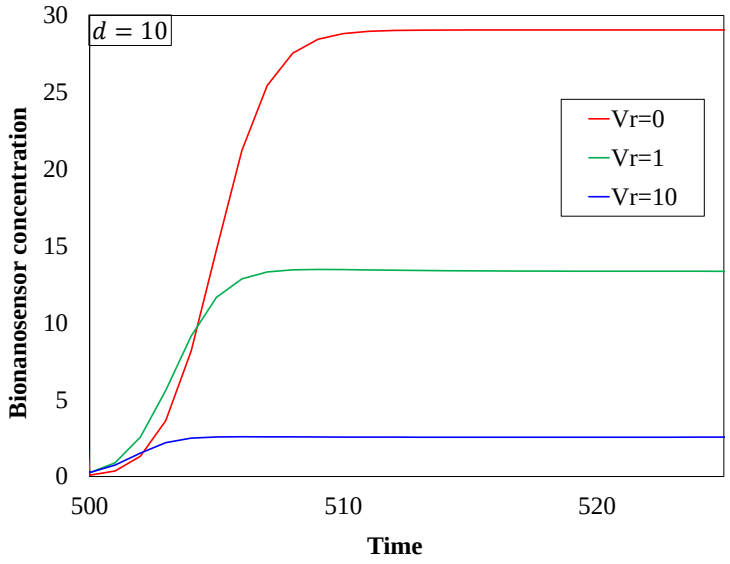


Figure 3.26: Impact of combined use of attractants and repellents on the concentrations of bionanosensors at the target location with $d = 10$.

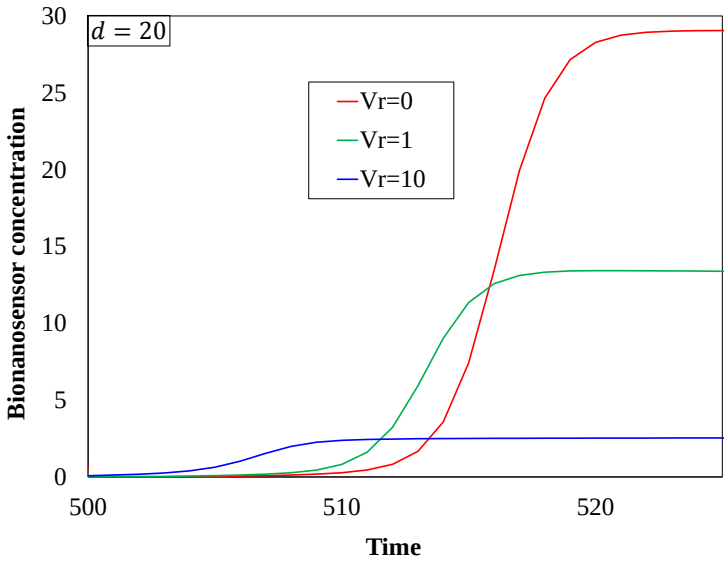


Figure 3.27: Impact of combined use of attractants and repellents on the concentrations of bionanosensors at the target location with $d = 20$.

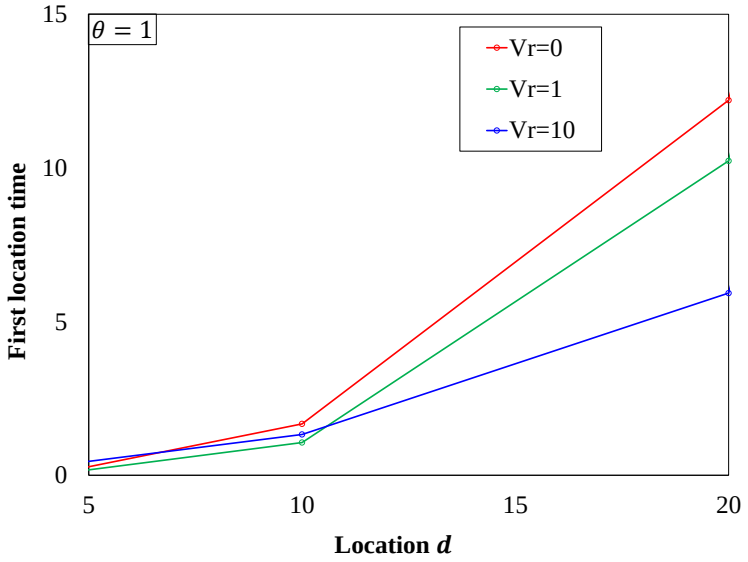


Figure 3.28: First location time with the threshold concentration $\theta = 1$.

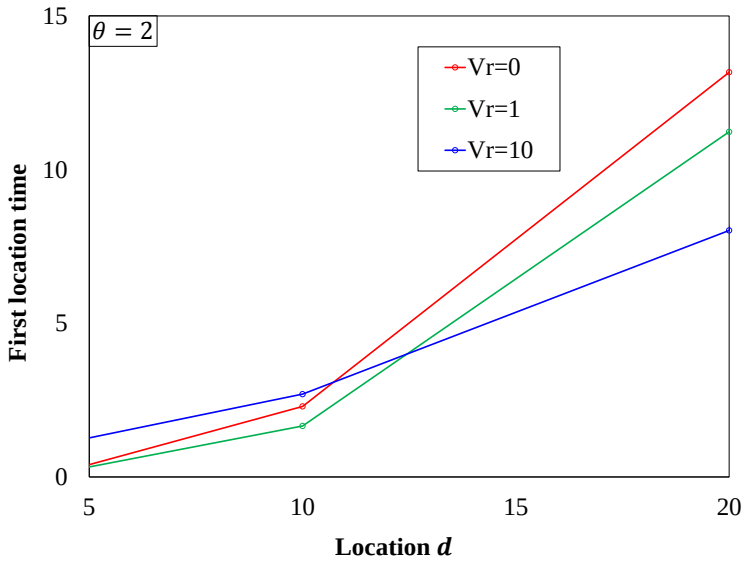


Figure 3.29: First location time with the threshold concentration $\theta = 2$.

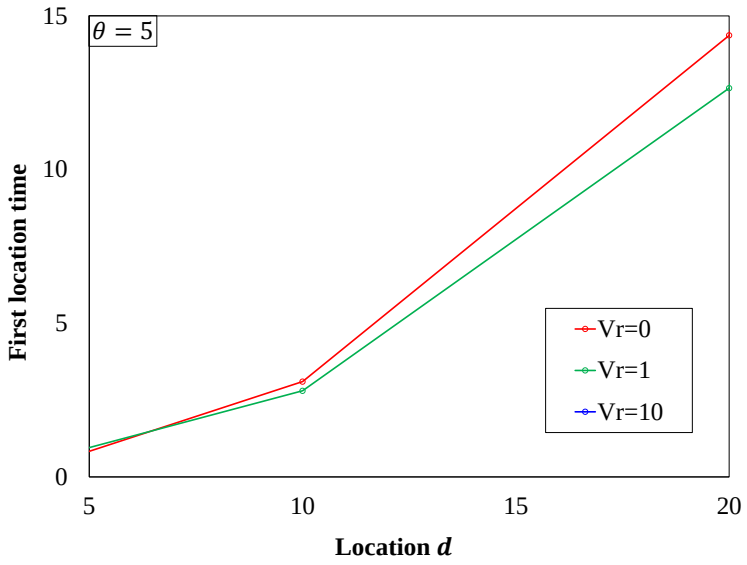


Figure 3.30: First location time with the threshold concentration $\theta = 5$.

tants to gather in a specific location (e.g., around a target). We used a set of partial differential equations to describe the spatial-temporal dynamics of the concentra-

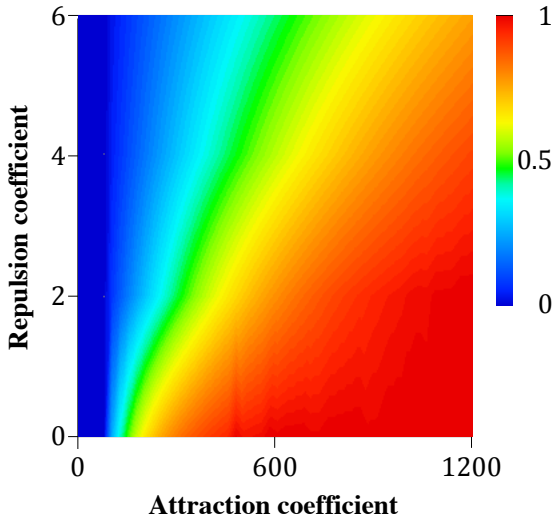


Figure 3.31: Impact of combined use of attractants and repellents.

tions of bionanosensors. We then numerically integrate the set of partial differential equations to demonstrate the ability of the dynamic bionanosensor network to locate and track targets under varieties of settings.

Key results and findings described in this chapter are the following:

- When attractants are used, bionanosensors decrease effectively the mean square distance to a target location in the monitoring environment (Subsection 3.3.2). On the other hand, when attractants are not used, bionanosensors move through non-directional diffusion, eventually forming a uniform distribution over the monitoring environment.

- When repellents are used, bionanosensors increase effectively the mean square distance from their original location, indicating that repellents are useful to facilitate the spread of bionanosensors (Subsection 3.3.3). When repellents are not used, on the other hand, bionanosensors spread slowly based on non-directional diffusion.

- For target tracking, attractants are useful to direct bionanosensors to the proximity of a moving target (Subsection 3.3.4). Repellents are also useful

for target tracking to detect a moving target in the first place. When attractants and repellents are used together, however, repellents negatively impact the target tracking performance measured by the number of bionanosensors in the proximity of a moving target.

Our future work investigates multiple-target tracking problems. The simulation experiments described in this chapter are limited to the tracking of a single target. In practical environments, multiple targets may appear, and a group of bionanosensors needs to locate and track all these targets. Therefore, we plan to extend the model of attractant- and repellent-based interactions for multiple-target tracking, showing that model parameters such as attractant and repellent threshold concentrations can be adjusted so that a group of bionanosensors splits up and tracks multiple targets.

Chapter 4

Bacterium-based Bionanosensor Networks for Target Tracking

4.1 Overview

In this chapter, we investigate the feasibility of using bacteria as bionanosensors to form a dynamic bionanosensor network for target tracking. Bacteria are promising materials to implement bionanosensors for target tracking because they are small (in the order of micrometers in length [14]), they are able to sense chemical conditions in the environment, and they have mobility known as *chemotaxis* that allows bacteria to move based on concentration gradients of molecules in the environment.

Bacteria in nature use chemotaxis to find a favorable environment containing attractants and to avoid a harmful environment with repellents. Examples of attractants are nutrients that are necessary for bacteria to enter into cell division, while repellents could be toxic molecules (see Table 4.1). Bacteria determine concentration gradients of these molecules through temporal sensing [72] or spatial sensing [82]. In temporal sensing [72], bacteria remember the concentration of a certain type of molecule they detected, and compare with the concentration to be detected after they move, therefore they learn whether the concentration is

Table 4.1: Known attractants and repellents [14]

Attractants
Amino acids (e.g., aspartate, serine)
Dipeptides
Salts at low concentrations
Sugars and sugar alcohols (e.g., fructose, galgacitol, galgactose)
Repellents
Alcohols (e.g., ethanol, isopropanol)
Amino acids (e.g., leucine, isoleucine, valine)
Glycerol or ethylene glycol at high concentrations

increasing or decreasing. In spatial sensing, bacteria have enough volumes (or lengths) for sensing a concentration gradient [82].

Fig. 4.1 shows a signaling network found in bacterial species *Escherichia coli* (*E. coli*) [16]. The network involves a number of membrane receptors and intracellular proteins such as CheA, CheW, CheY, and CheZ. The binding of extracellular molecules to the receptors leads to protein-protein interactions through which the flagellar motors rotate either *clockwise to tumble* (i.e., change the moving direction) or *counterclockwise to run* (i.e., maintain the moving direction). For instance, the binding of a repellent to a membrane receptor causes the intracellular protein kinase CheA attached to the CheW protein to become phosphorylated. The phosphate group in the phospholylated CheA (CheAp) is then passed to the CheY. This phosphorylated form of CheY, namely, CheYp, then diffuses and binds to the flagellar motor, which in turn rotates clockwise, causing the flagellar bundle to become disorganized. This causes the bacterium to tumble and avoid moving toward the source of the repellent. The binding of an attractant to a membrane receptor, on the other hand, dephosphorylates CheA and CheY, which causes the flagella motor to rotate counterclockwise. This allows the bacterium to run continuously toward the source of the attractant. The CheZ accelerates the dephosphorylation of CheYp to enable the bacterium to quickly respond to changes in the environment.

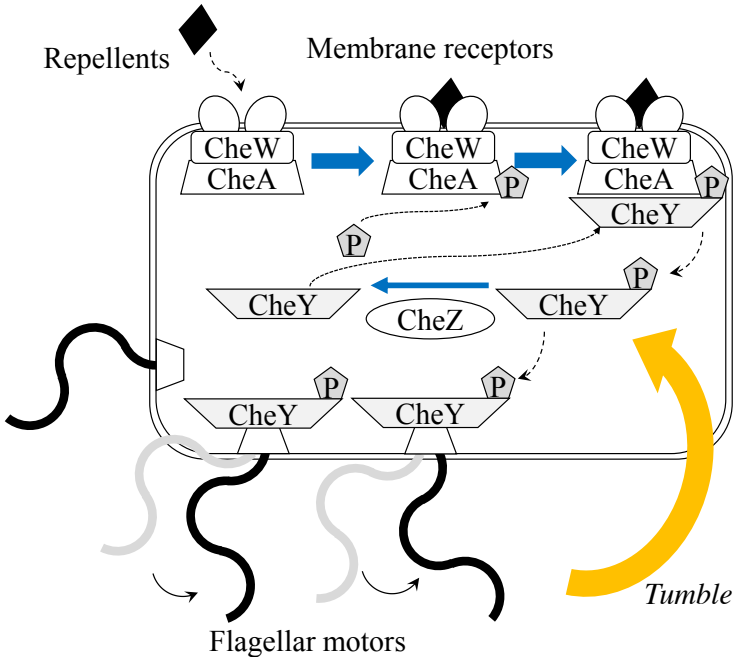


Figure 4.1: *E. coli*'s signaling network for chemotaxis [16].

The bacterium-based autonomous bionanosensors assumed in this chapter are hypothetical in that they emit repellents and attractants for target tracking. The bacterium-based autonomous bionanosensors may be genetically engineered from bacteria in order to produce attractants and repellents as needed, or to exhibit modified chemotactic responses to specific molecules that they produce, with these molecules thus acting as attractants or repellents. In this way, the hypothetical bionanosensors in search of the target emit repellents to facilitate the spread of nearby bionanosensors over the environment; and they emit attractants upon detecting a target, thereby attracting other bionanosensors toward the target.

The remainder of this chapter is organized as follows. In Section 4.2, we develop the mobility model of bacterium-based autonomous bionanosensors. In Section 4.3, we conduct simulation experiments to find optimal parameters for tracking a moving target. Finally, we conclude this chapter in Section 4.4.

Table 4.2: Notations

Symbol	Description
S	Set of bionanosensors
L	Linear length of the two-dimensional monitoring area
τ	Time interval
ϕ	Step angle
v_b	Moving velocity of the bionanosensor
θ	Moving direction of the bionanosensor
R_b	Rotational diffusion coefficient of the bionanosensor
d_t	Detectable distance to the target
T_A	Time duration to emit attractants
ψ_A	Maximum drift angles to move toward attractants
ψ_R	Maximum drift angles to move away from repellents
H_A	Threshold concentration to detect attractants
H_R	Threshold concentration to detect repellents

4.2 Model of Bacterium-based Bionanosensors

In this section, we apply the principle of bacterial rotational diffusion [13] to develop a basic mobility model of bacterium-based autonomous bionanosensors (Section 4.2.1). We then extend the model to incorporate interactions among bionanosensors through attractants and repellents (Section 4.2.2). Different from the model in Chapter 3 that describes the swarm behavior of a group of bionanosensors, the model in this section provides flexibility in modeling individual behaviors of bionanosensors. The major notations used in this section are summarized in Table 4.2.

4.2.1 Mobility Model

A set of bacterium-based bionanosensors S is distributed over an $L \times L$ two-dimensional bounded area for tracking a single moving target. A bionanosensor and the target are modeled as points in the area. Time is divided into time intervals of equal length τ, and a bionanosensor at the beginning of each time interval

moves from its current location (x, y) to the next location $(x + \Delta x, y + \Delta y)$ such that

$$\begin{aligned} \Delta x &= v_b \tau \cos\theta, \\ \Delta y &= v_b \tau \sin\theta, \end{aligned} \tag{4.1}$$

where v_b is the moving velocity of the bionanosensor, and θ is the moving direction. At boundaries, the law of reflection is applied to determine the new location of the bionanosensor (i.e., the angle of incidence is equal to that of reflection).

At each time step, a bionanosensor changes its moving direction from θ to $\theta + \Delta\theta$ (Fig. 4.2). Following the bacterial rotational diffusion model [13], we use

$$\Delta\theta = \Phi, \tag{4.2}$$

where a random variable Φ chooses $+\phi$ or $-\phi$ with equal probabilities. Therefore, the mean and variance of θ at time t are given as

$$\mathrm{E}[\theta] = \theta_0, \tag{4.3}$$

$$\mathrm{VAR}[\theta] = 2R_b t, \tag{4.4}$$

where θ_0 is the moving direction of the bionanosensor at time $t = 0$ and R_b is the rotational diffusion coefficient of the bionanosensor defined by

$$R_b = \frac{\phi^2}{2\tau}. \tag{4.5}$$

The rotational diffusion coefficient R_b affects the mobility pattern of a bionanosensor. As shown in Figs. 4.3 (a) and (b), a bionanosensor with small

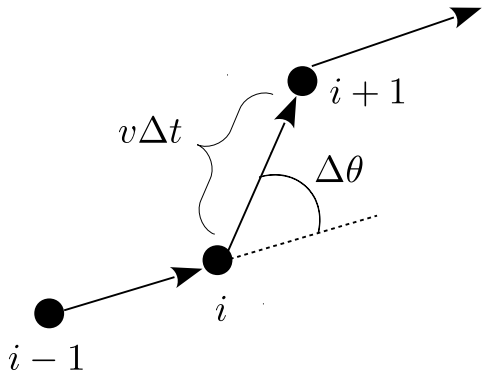


Figure 4.2: Locations of a bionanosensor at time steps $i-1$, i, and $i+1$

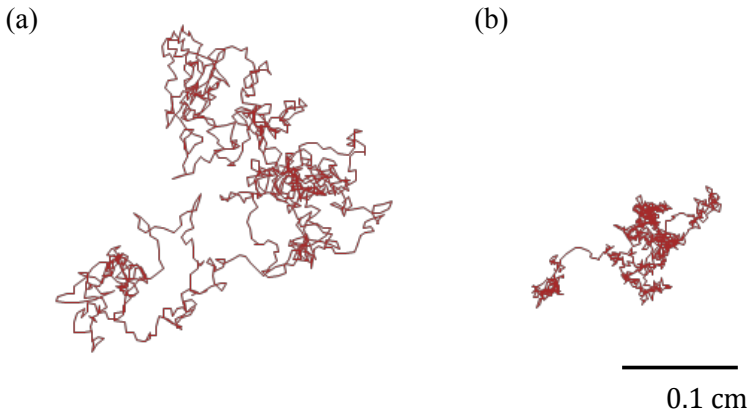


Figure 4.3: Mobility patterns produced from the basic model. (a) $R_b = 1$ $(\mathrm{rad}^2/\mathrm{s})$ and (b) $R_b = 5$ $(\mathrm{rad}^2/\mathrm{s})$. $v_b = 5.0 \times 10^{-3}$ (cm/s) for 2000 seconds.

R_b tends to maintain its moving direction to move away from the original location, while a bionanosensor with large R_b randomly changes its direction to stay around the original location. When R_b approaches 0, a bionanosensor moves in a straight line, and thus the distance from the original location increases in proportion to time (t). When R_b is sufficiently large, a bionanosensor performs two-dimensional random walk and thus the distance from the original location increases in proportion to the square root of time $\left(\sqrt{t}\right)$.

4.2.2 Interactions among Bionanosensors

As described in Section 3.2, interactions among bionanosensors take place through simple use of repellents and attractants. The model in this chapter allows flexibility to describe more details about the interactions as follows.

- A bionanosensor continuously emits repellents.
- A bionanosensor starts emitting attractants when it approaches the target within a detectable distance d_t from the target, and stops emitting attractants after the time duration of T_A.

The mobility of a given bionanosensor is affected by the concentrations of attractants and repellents in its vicinity, and is modeled by modifying $\Delta\theta$ as follows.

$$\Delta\theta \;=\; \Phi \;+\; \Psi_R + \Psi_A \tag{4.6}$$

Parameters Ψ_A and Ψ_R describe step drift angles reflecting repulsion and attraction forces due to repellents and attractants. These two parameters are determined based on the concentrations of repellents and attractants observed by the bionanosensor:

$$\Psi_R = \arg\min_{\psi \in \mathcal{D}_R} C_R(x_\psi, y_\psi), \tag{4.7}$$

$$\Psi_A = \arg\max_{\psi \in \mathcal{D}_A} C_A(x_\psi, y_\psi), \tag{4.8}$$

where $\mathcal{D}_A = [-\psi_A, \psi_A]$ and $\mathcal{D}_R = [-\psi_R, \psi_R]$ are ranges of drift angles for repellents and attractants, from which the bionanosensor chooses one angle to move toward the lowest concentration of repellents and the other angle to move toward the highest concentration of attractants. ψ_A and ψ_R are the maximum drift angles that the bionanosensor can choose for repellents and attractants, respectively.

$C_R(x_\psi, y_\psi)$ and $C_A(x_\psi, y_\psi)$ are the concentrations of repellents and attractants detected by a bionanosensor if the bionanosensor changes its moving direction by ψ and moves by $v_b\tau$: i.e.,

$$\begin{aligned} x_\psi &= x + v_b\,\tau\,\cos(\theta+\psi), \\ y_\psi &= y + v_b\,\tau\,\sin(\theta+\psi). \end{aligned} \tag{4.9}$$

Note that, in (4.7) and (4.8), we use $\Psi_R = 0$ when $C_R(x_\psi, y_\psi) = 0$ for $\forall\psi \in \mathcal{D}_R$, and $\Psi_A = 0$ when $C_A(x_\psi, y_\psi) = 0$ for $\forall\psi \in \mathcal{D}_A$.

The concentration of either type of molecule detected by a bionanosensor $C(\psi)$, namely, $C_R(\psi)$ in (4.7) or $C_A(\psi)$ in (4.8), depends on the sensitivity of the bionanosensor:

$$C(x,y) = \begin{array}{ll} c(x,y) & (c(x,y) \geq H) \\ 0 & (otherwise), \end{array} \tag{4.10}$$

where $c(x, y)$ is the concentration of either type of molecule at location (x, y), and H is the threshold concentration (H_A for attractants and H_R for repellents), this being the minimum concentration that is required for a bionanosensor to detect the type of molecule.

To reduce the complexity of the model, we assume that the molecule diffuses so quickly that the molecule concentration reaches the steady state immediately, then the concentration of either type of molecule is approximated as exponentially decreasing with respect to the square distance from the source emitting the molecule. To further simplify the model, we also assume that molecules released at time t quickly dissipate and thus do not impact the concentration of molecule after time $t + \tau$. Based on this simplification, we describe $c(x, y)$ in (4.10) as follows.

$$c\,(x,y) \;=\; \sum_{i\in U} \exp\left(-d_i(x,y)^2\right), \tag{4.11}$$

where U is a set of bionanosensors emitting either type of molecule and $d_i(x,y)$ is the distance from location (x,y) to bionanosensor i.

4.3 Simulation Experiments

In this section, we demonstrate using the mobility model described in Section 4.2 that a group of bionanosensors interacts through repellents and attractants to track a moving target.

4.3.1 Simulation Algorithms

Pseudocode 2 shows the algorithm we used to simulate target tracking processes based on the model described in Section 4.2. In each simulation, a set of bionanosensors is placed at the same location where the single target is initially present. When a simulation begins, the target performs circular motion around the origin of the two-dimensional area, and its location (x_T, y_T) change according to

$$\begin{aligned} x_T &= \frac{L}{5}\cos\left(\omega_T\, t\right), \\ y_T &= \frac{L}{5}\sin\left(\omega_T\, t\right). \end{aligned} \tag{4.12}$$

where ω_T $(\mathrm{rad}\,/\mathrm{s})$ is the angular velocity of the moving target. Default parameter values are set as follows: $\tau = 2.0 \times 10^{-2}$ (s), $|S| = 100$, $L = 1$ (cm^2), $v_b = 5.0 \times 10^{-3}$ (cm/s) [13], $R_b = 5$ (rad^2/s), $\psi_A = 3.49 \times 10^{-2}$ (rad), $\psi_R = 3.49 \times 10^{-3}$ (rad), $T_A = 40$ (s), $H_A = H_R = 0$ $(1/\mathrm{cm}^3)$, $d_l = 5.0 \times 10^2$ (cm).

Pseudocode 2 Target Tracking Simulation

```
Set time t := 0
Place a set of bionanosensors S and a target T in a L × L two-dimensional space
while true do
    Move T based on (4.12)
    for all bionanosensor s ∈ S do
        Move s based on (4.1)
        Compute the drift angle for repellents (4.7)
        Compute the drift angle for attractants (4.8)
        Update s's moving direction based on (4.6)
        if s detects T in previous T_A steps then
            Emit attractants
        end if
        Emit repellents
    end for
    Measure the number of bionanosensors within the distance d_l from T
    Update time t := t + τ
end while
```

Note that we performed preliminary experiments and determined these parameter values based on the experimental results, except for those parameter values that are available in the literature.

Simple interactions through repellents and attractants introduced in the previous section can induce collective movement in a group of bionanosensors. In this section, we perform preliminary experiments without placing a moving target in order to understand the impact of repellents and attractants on the collective movement of a group of bionanosensors.

4.3.2 Impact of Repellents

Repellents facilitate the spread of a group of bionanosensors over the monitoring area and are useful to locate a target in a large area. Without repellents, a group of bionanosensors needs to distribute itself based on rotational diffusion, which can

be a slow-spreading process (Fig. 4.3).

To understand the impact of the repellents, we place 100 bionanosensors at the origin in the two-dimensional area and observe how the bionanosensors spread over the area using repellents. For this, we measure the mean square distance (MSD) of the bionanosensors from the origin and the percentage P_d of bionanosensors within distance d_l from location $(d, 0)$, where $d = 1.0 \times 10^{-1}$ (cm) and $d_l = 5.0 \times 10^{-2}$ (cm). No attractants are used. Default parameter values are $N = 100$, $H_R = 0$ $(1/\text{cm}^3)$, $\psi_R = 3.49 \times 10^{-3}$ (rad), $L = 1$ (cm), $R_b = 5$ (rad^2/s) and $v_b = 5.0 \times 10^{-3}$ (cm/s). The following set of figures show the ensemble average of 10 independent simulation runs.

Figs. 4.4 and 4.5 show how the ensemble averages of MSD and P_d ($\langle\text{MSD}\rangle$ and $\langle P_d\rangle$) change over time when $\psi_R \in \{0, 1.74 \times 10^{-3}, 3.49 \times 10^{-3}\}$ (rad) is used. Fig. 4.4 indicates that the $\langle\text{MSD}\rangle$ increases faster as ψ_R increases due to the repulsive forces among bionanosensors. Fig. 4.5 shows that $\langle P_d\rangle$ quickly increases to reach its peak, indicating that a distant target may be detected in a shorter period of time. This figure also shows that $\langle P_d\rangle$ drops quickly after it reaches the peak, indicating that it may take a significantly long time to detect a target if the target is not found in earlier time. Note that, in these figures, $\psi_R = 0$ (rad) represents the case where repellents are not used.

Figs. 4.6 and 4.7 show the impact of the threshold concentration H_R on the $\langle\text{MSD}\rangle$ and $\langle P_d\rangle$ when $H_R \in \{99.900, 99.925, 99.950\}$ $(1/\text{cm}^3)$ is used for a fixed $\psi_R = 3.49 \times 10^{-3}$ (rad). These figures show that, when the threshold concentration is high (i.e., $H_R \in \{99.925, 99.950\}$ $(1/\text{cm}^3)$), a group of bionanosensors spreads slowly over the area.[1] This is expected since the high threshold concentration indicates that bionanosensors have low sensitivity for repellents and become unable to detect the concentration.

Figs. 4.8 and 4.9 show the impact of the rotational diffusion coefficient R_b on the $\langle\text{MSD}\rangle$ and $\langle P_d\rangle$ when $R_b \in \{1, 10, 100\}$ (rad^2/s) is used again for a

[1]The two cases from $H_R = 99.925$ and 99.950 result in the very similar $\langle\text{MSD}\rangle$ and $\langle P_d\rangle$ at the scales used in Figs. 4.6 and 4.7.

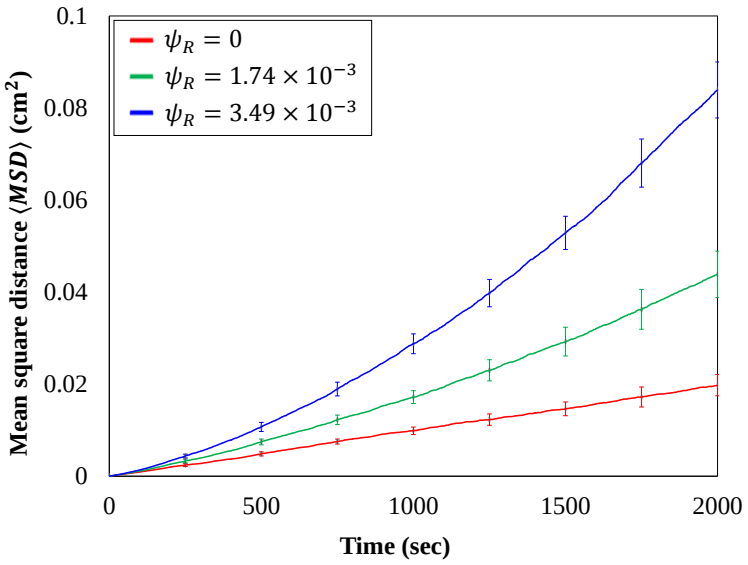


Figure 4.4: Impact of maximum drift angle for repellents (ψ_R) on the mean square distance.

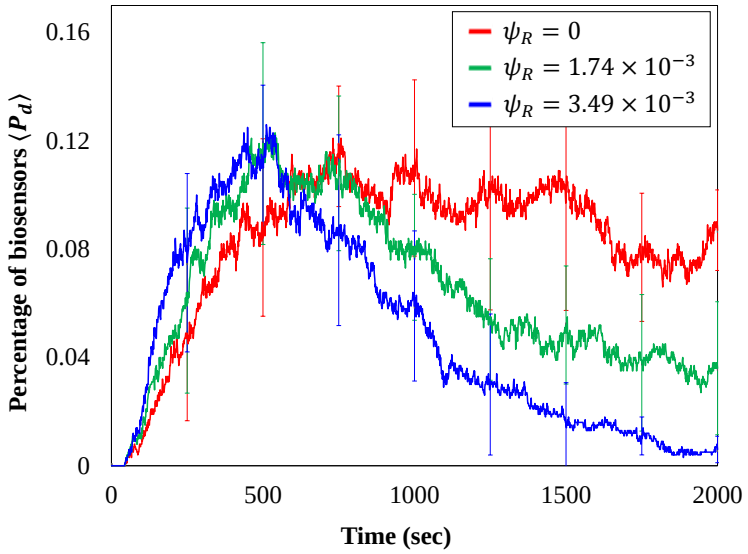


Figure 4.5: Impact of maximum drift angle for repellents (ψ_R) on the percentage of bionanosensors at location $(0, d)$.

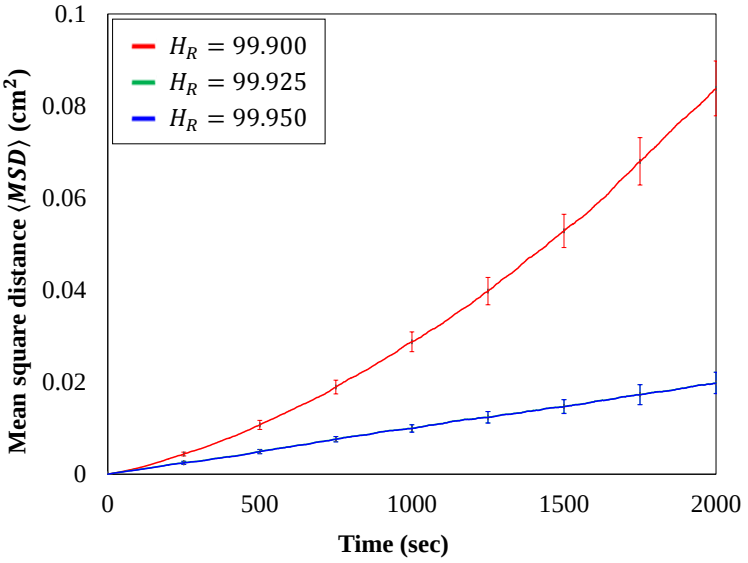


Figure 4.6: Impact of threshold concentration for repellents (H_R) on the mean square distance.

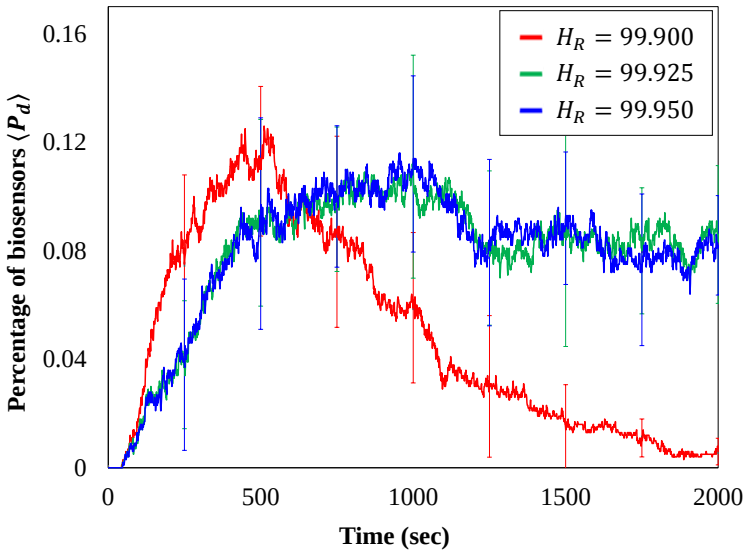


Figure 4.7: Impact of threshold concentration for repellents (H_R) on the percentage of bionanosensors at location $(0, d)$.

fixed $\psi_R = 3.49 \times 10^{-3}$ (rad). These figures show that the spreading process of bionanosensors becomes quicker when R_b is smaller while it remains slow if R_b is large (e.g., $R_b = 100$ (rad^2 /s)) even when repellents are used. This is because, as R_b increases, the drift angle caused by repellents becomes more negligible compared to the effect of rotational diffusion. When $R_b = 100$ (rad^2 /s), for instance, the maximum drift angle caused by repellents is 3.49×10^{-3} (rad) per simulation step, while the step angle by the rotational diffusion is 2.0 (rad) and over 570 times larger the maximum drift angle.

4.3.3 Impact of Attractants

Attractants allow a bionanosensor, upon detecting a target, to direct other bionanosensors in the monitoring area toward the location of the target. Without attractants, the detection of a target by a bionanosensor becomes opportunistic and it takes a significantly long time for a group of bionanosensors to gather around the target.

To understand the impact of the attractants, we place a static target at the origin in the two-dimensional area, one bionanosensor also at the origin as an initial source of attractants, and 99 bionanosensors at randomly selected locations. We then observe how the bionanosensors are attracted toward the origin by measuring the MSD from the origin and the percentage P_d of bionanosensors within distance d_l from the origin, where $d = 1.0 \times 10^{-1}$ (cm) and $d_l = 5.0 \times 10^{-2}$ (cm) (i.e., $P_d = P_0$). We use only attractants in this set of experiments. Default parameter values are $N = 100$, $H_A = 0$ (1/cm^3), $\psi_A = 3.49 \times 10^{-2}$ (rad), $T_A = 40$ (s),$L = 1$ (cm), $R_b = 5$ (rad^2 /s) and $v_b = 5.0 \times 10^{-3}$ (cm/s). The following set of figures show the ensemble average of 10 independent simulation runs.

Figs. 4.10 and 4.11 show how the ensemble averages of MSD and P_0 ($\langle$MSD$\rangle$ and $\langle P_d \rangle$) change over time when $\psi_A \in \{0, 1.74 \times 10^{-2}, 3.49 \times 10^{-2}\}$ (rad) is used. Fig. 4.10 indicates that $\langle$MSD$\rangle$ decreases faster as ψ_A increases due to the attractive forces among bionanosensors. Fig. 4.11 shows that $\langle P_0 \rangle$ quickly increases as ψ_A increases, indicating that bionanosensors distributed over the area

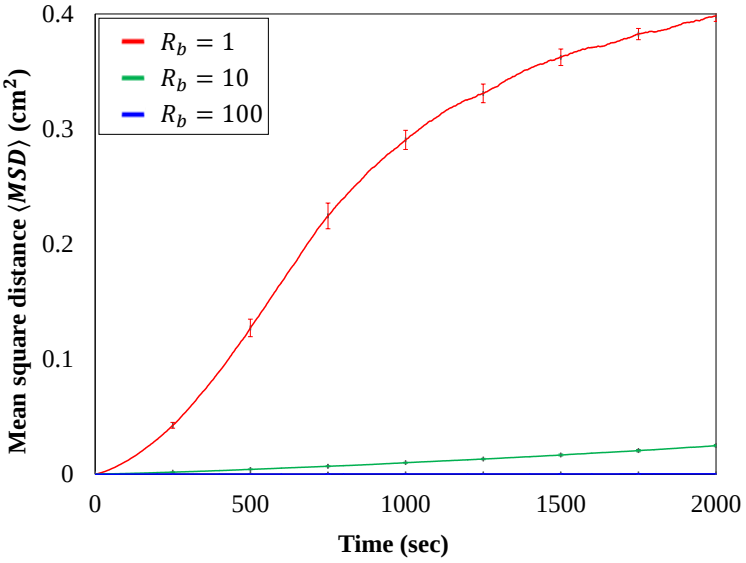


Figure 4.8: Impact of rotational diffusion coefficient (R_b) on the mean square distance.

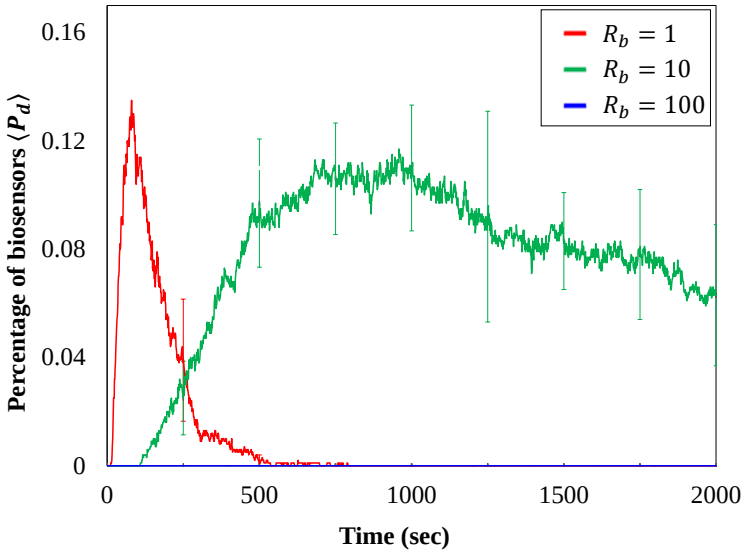


Figure 4.9: Impact of rotational diffusion coefficient (R_b) on the percentage of bionanosensors at location $(0, d)$.

are attracted to the target location in a shorter period of time. Note that, in these figures, $\psi_A = 0$ (rad) represents the case where attractants are not used.

Figs. 4.12 and 4.13 show the impact of threshold concentration for attractants (H_A) on $\langle$MSD$\rangle$ and $\langle P_0 \rangle$ when $H_A = \{0.5, 0.95, 1\}$ ($1/\text{cm}^3$) is used for a fixed $\psi_A = 3.49 \times 10^{-2}$ (rad). As shown in the figure, when the threshold concentration is high (i.e., $H_A = 1$ ($1/\text{cm}^3$)), bionanosensors are unable to detect the concentration of attractants and remain distributed over the area.

Figs. 4.14 and 4.15 show the impact of the time duration to release attractants (T_A) (namely, the time duration in which a bionanosensor releases attractants after it detects the target) on $\langle$MSD$\rangle$ and $\langle P_0 \rangle$ when $T_A = \{80, 160, 2000\}$ (s) for a fixed $\psi_A = 3.49 \times 10^{-2}$ (rad). These figures show that more bionanosensors are attracted to the origin when T_A is larger (i.e., $T_A \in \{160, 2000\}$ (s)). These figures also show that a very large T_A (i.e., $T_A = 2000$ (s)) is not required. This is because a very large T_A negatively impacts the attraction processes; a bionanosensor that probabilistically moves away from the origin keeps releasing attractants and other bionanosensors can be attracted to a location where the target is absent.

Figs. 4.16 and 4.17 show the impact of the rotational diffusion coefficient R_b on $\langle$MSD$\rangle$ and $\langle P_0 \rangle$ when $R_b \in \{1, 10, 100\}$ (rad^2/s) is used again for a fixed $\psi_A = 3.49 \times 10^{-2}$ (rad). These figures show that attractants become less effective as R_b increases. This is because, as R_b increases, the drift angle caused by attractants becomes more negligible compared to the effect of rotational diffusion.

Numerical results shown in Figs. 4.10 through 4.17 exhibit high variance because of the probabilistic nature of the experiments. In one case, the bionanosensor initially placed at the origin attracts a sufficient number of bionanosensors to create a "stable" concentration gradient of attractants. In this case, the remaining bionanosensors are successfully attracted to the origin, leading to $\langle$MSD$\rangle = 0$ and $\langle P_0 \rangle = 1$. In another case, the bionanosensor initially placed at the origin fails to attract a sufficient number of bionanosensors to the origin (e.g., because it moves away from the origin or it stops releasing attractants). In this case, no concentration gradient of attractants is formed and all bionanosensors randomly

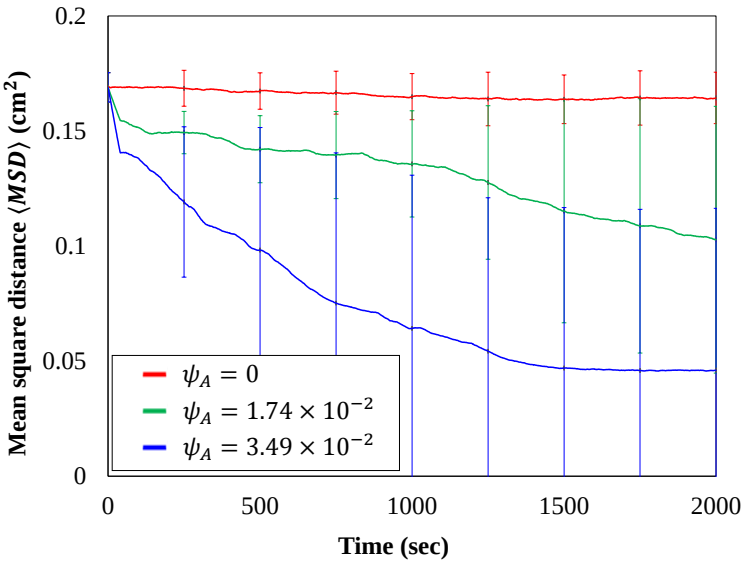


Figure 4.10: Impact of maximum drift angle for attractants (ψ_A) on the mean square distance.

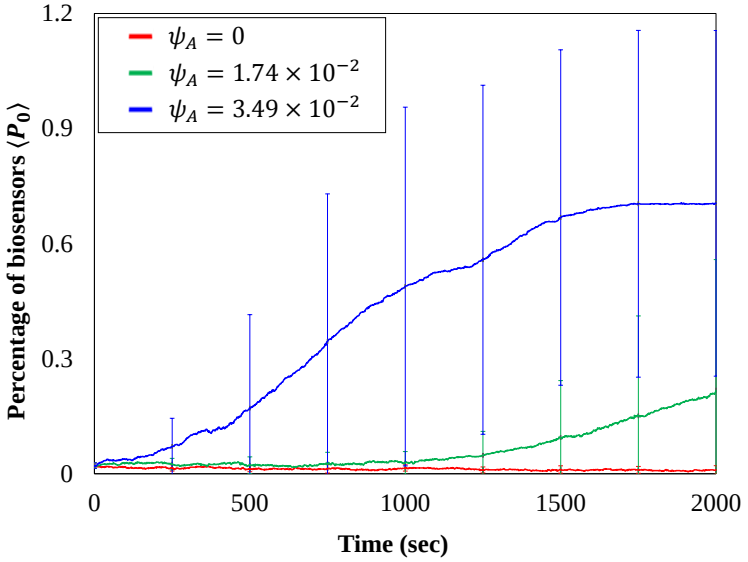


Figure 4.11: Impact of maximum drift angle for attractants (ψ_A) on the percentage of bionanosensors around the origin.

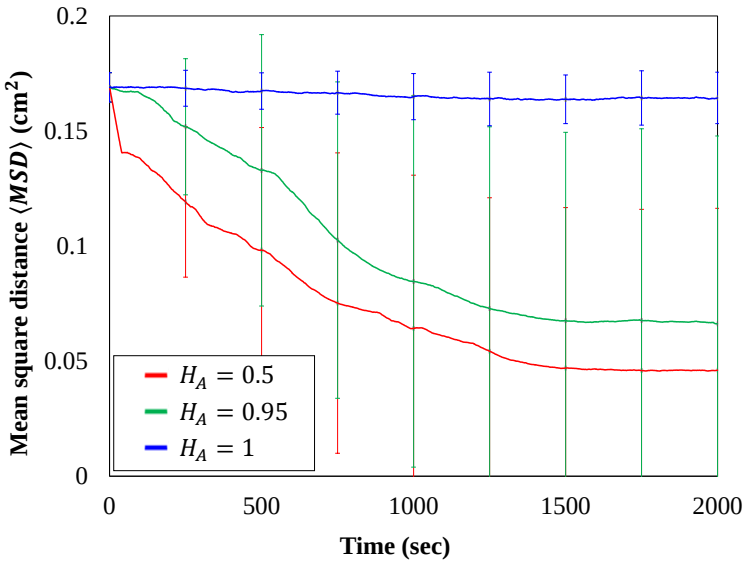


Figure 4.12: Impact of threshold concentration for attractants (H_A) on the mean square distance.

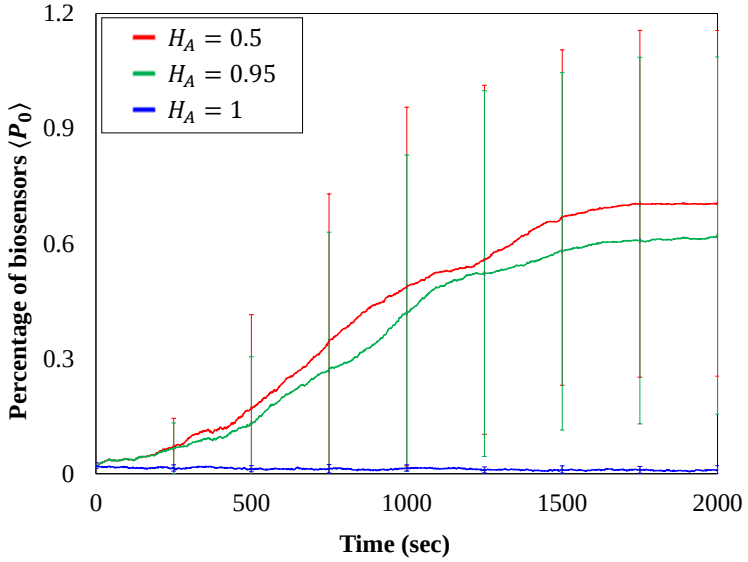


Figure 4.13: Impact of threshold concentration for attractants (H_A) on the percentage of bionanosensors around the origin.

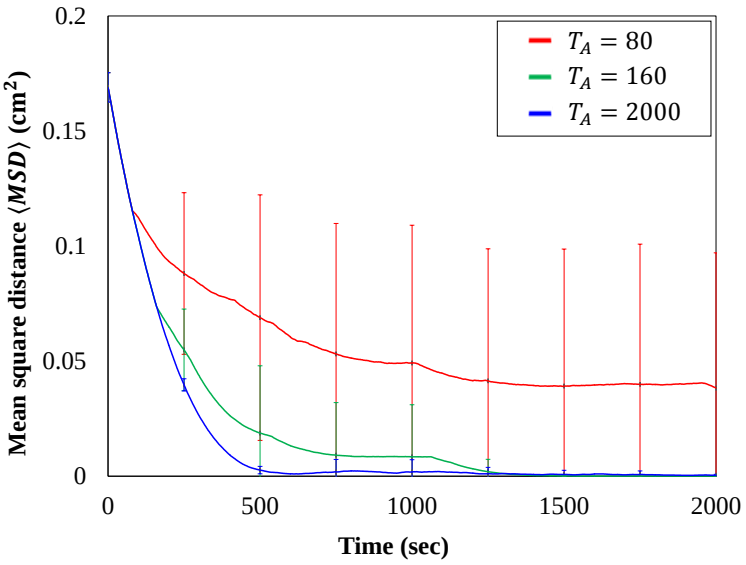


Figure 4.14: Impact of time duration to release attractants (T_A) on the mean square distance.

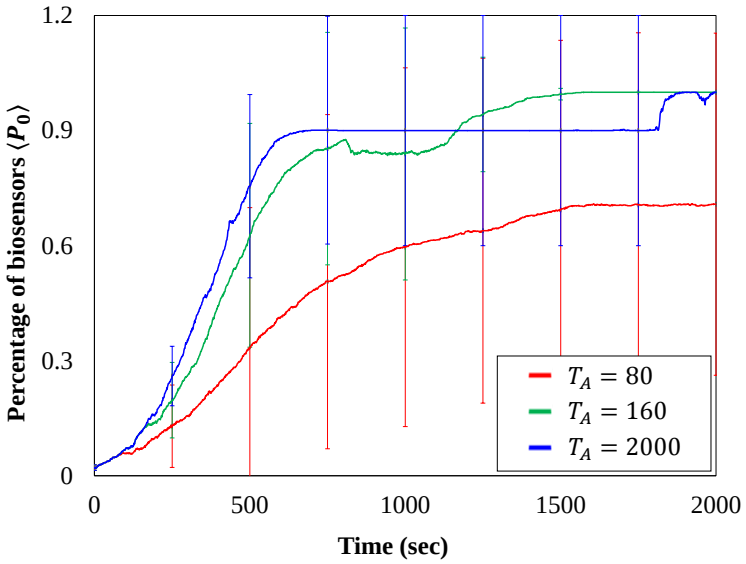


Figure 4.15: Impact of time duration to release attractants (T_A) on the percentage of bionanosensors around the origin.

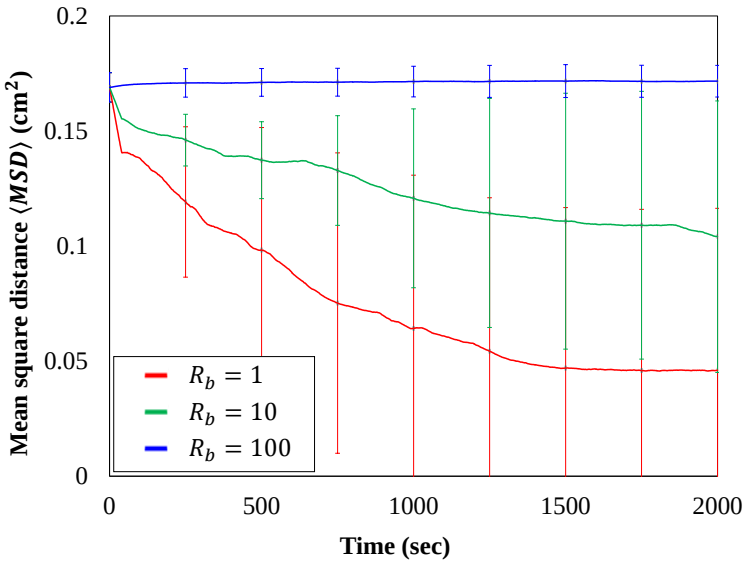


Figure 4.16: Impact of rotational diffusion coefficient (R_b) on the mean square distance.

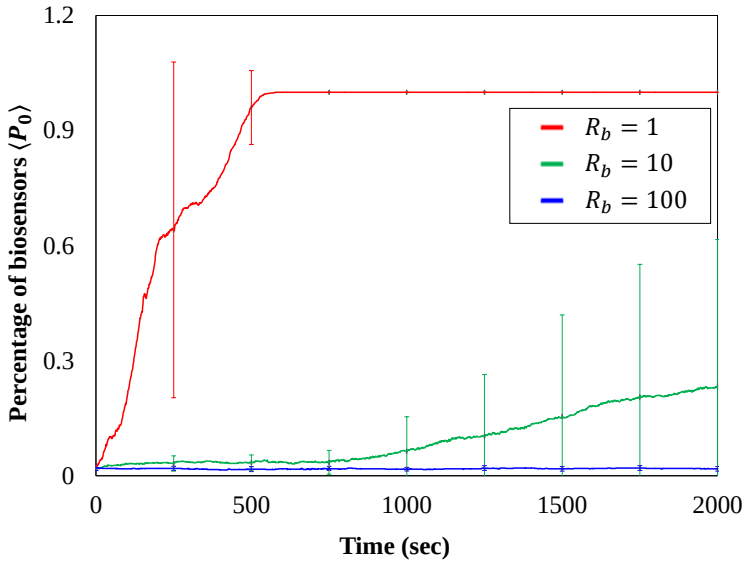


Figure 4.17: Impact of rotational diffusion coefficient (R_b) on the percentage of bionanosensors around the origin.

move based on the rotational diffusion, and thus $\langle \text{MSD} \rangle$ remains large and $\langle P_0 \rangle$ small. These two cases are observed in most of numerical results in Figs. 4.10 through 4.17, where the variance is high.

4.3.4 Target Tracking

The percentage of bionanosensors around the target P is impacted upon by the model parameters used. Our simulation experiments focus on the optimization of the two key parameters, maximum drift angles for repellents and attractants (ψ_R and ψ_A). Our simulation experiments also examine the impact of the angular velocity of the moving target (ω_T) on P.

Figs. 4.18 (a), (b) and (c) show three target tracking processes often observed in simulations. In Fig. 4.18 (a), a group of bionanosensors continuously tracks the moving target and thus $\langle P \rangle$ is maintained around 1.0. In Fig. 4.18 (b), a group of bionanosensors starts losing the target in the middle of target tracking but soon recovers to track the target. In Fig. 4.18 (c), a group of bionanosensors loses the target and it starts spreading over the environment.

Fig. 4.19 shows the impact of ψ_R on the time average of $\langle P \rangle$, (i.e., $\overline{\langle P \rangle}$) where ψ_A is fixed to 3.49×10^{-2} (rad) and Fig. 4.20 the impact of ψ_A on $\overline{\langle P \rangle}$ where ψ_R is fixed to 3.49×10^{-3} (rad). Each figure also shows two cases where the target moves slow ($\omega_T = 0.002$ (rad/s)) and fast ($\omega_T = 0.005$ (rad/s)). From these figures, we observe that:

- A group of bionanosensors is able to track the slow moving target when ψ_R or ψ_A is properly tuned. It may however fail to track the fast moving target.

- Fig. 4.19 shows that $\overline{\langle P \rangle}$ is maximized at $\psi_R = 1.40 \times 10^{-2}$ (rad), indicating that repulsive forces can be useful to track a moving target. When ψ_R is smaller, bionanosensors spread over the environment too slowly to locate a target and $\overline{\langle P \rangle}$ tends to be small. This is often observed when bionanosensors lose the target "after" they gather around the target; all bionanosensors

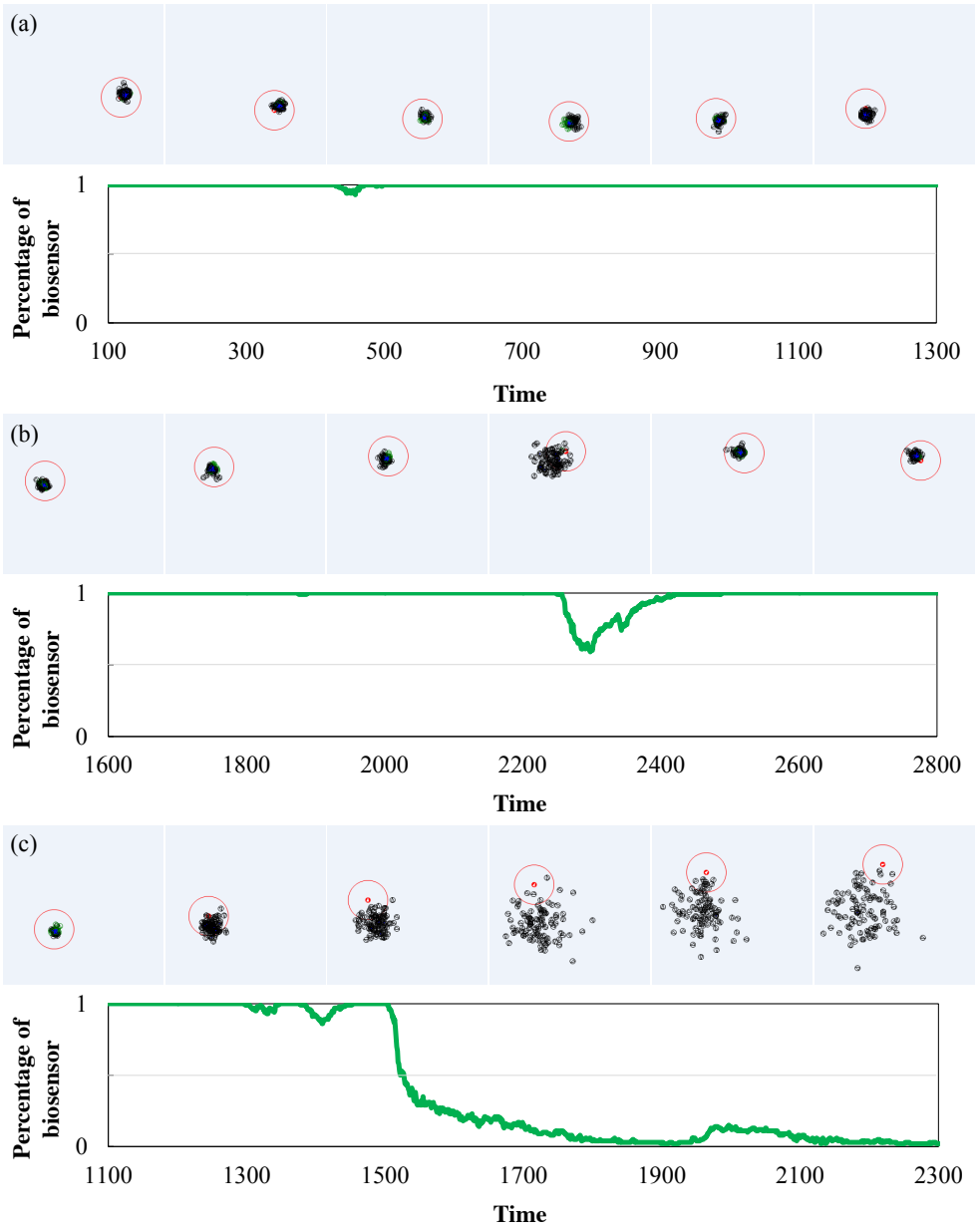


Figure 4.18: Target tracking processes: (a) successful target tracking, (b) a loss of a target and recovery, and (c) a loss of a target and failure in tracking.

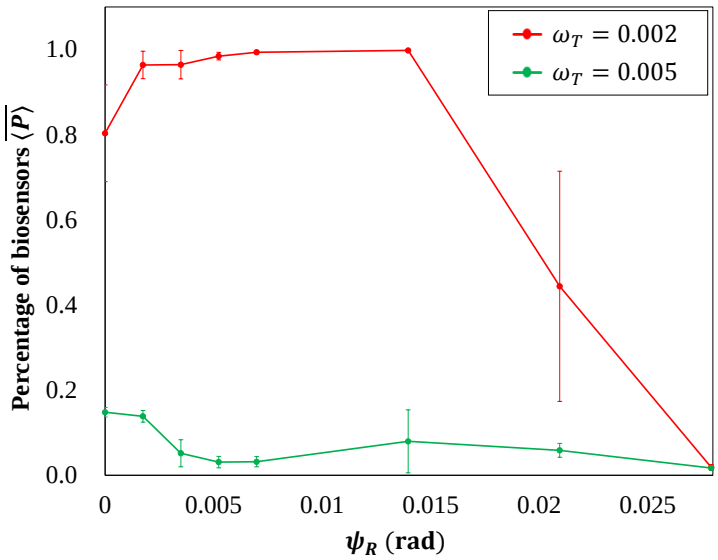


Figure 4.19: Impact of repellent related parameter (ψ_R) on the target tracking performance

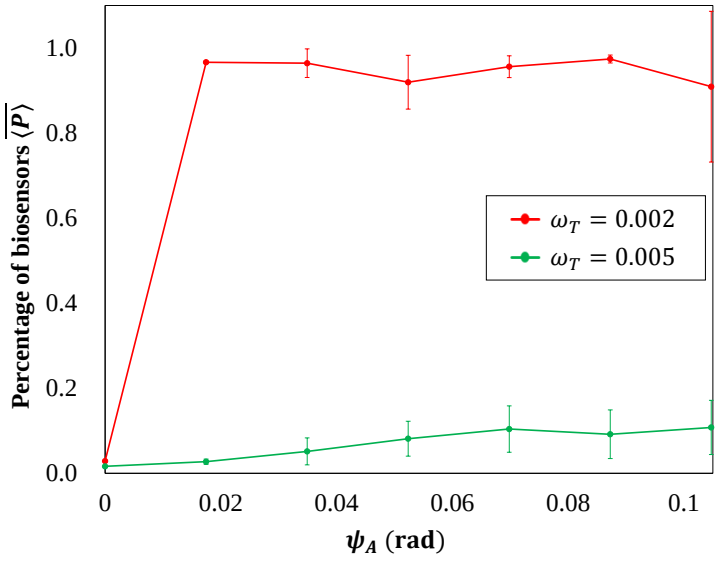


Figure 4.20: Impact of attractant related parameter (ψ_A) on the target tracking performance

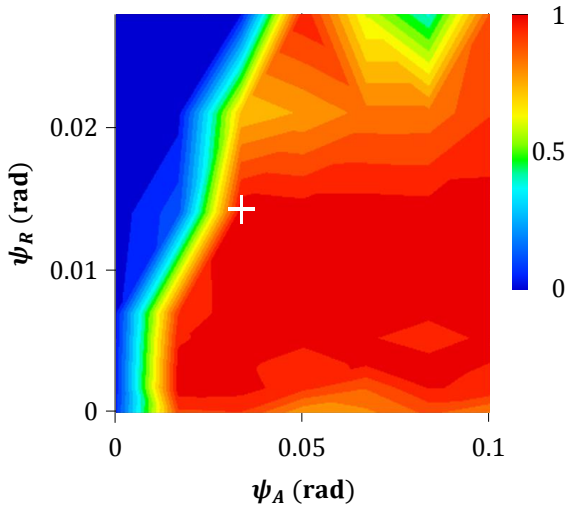


Figure 4.21: Impact of repellent and attractant related parameters (ψ_R and ψ_A) on the target tracking performance

stay together and the target cannot be located again. When ψ_R is larger, bionanosensors repel each other and thus it becomes difficult to stay together around the target (i.e., to maintain a large $\overline{\langle P \rangle}$.)

- Fig. 4.20 shows that $\overline{\langle P \rangle}$ increases as ψ_A increases and thus attractive forces are useful in target tracking.

Fig. 4.21 shows the combined impact of ψ_R and ψ_A on $\overline{\langle P \rangle}$ where $\omega_T = 0.002$ (rad/s). Within the ranges of ψ_R and ψ_A examined, $\overline{\langle P \rangle}$ is maximized when $\psi_R = 1.40 \times 10^{-2}$ and $\psi_A = 3.49 \times 10^{-2}$ (indicated by the white cross in the figure.) The figure shows that repellents and attractants both are useful to track a moving target.

In this chapter, repellents are found useful when they are used together with attractants. This is not observed in Chapter 3 where repellents negatively impact the target tracking performance when they are used together with attractants (Subsection 3.3.4). This is due to the following reasons.

1. In the model described in Chapter 3, attractants are always secreted from

bionanosensors that are in the vicinity of a target while in the model described in this chapter, attractants may be secreted from bionanosensors that are apart from a target (because bionanosensors releasing attractants may move away from a target). In the model described in this chapter, repellents may help alleviate the negative effects of attractants.

2. Also, in the model described in Chapter 3, bionanosensors are distributed over the environment probabilistically, meaning that bionanosensors always exist at the location of a target. In this case, detecting a target is a trivial task for bionanosensors and repellents are useless. In the model described in this chapter, on the other hand, bionanosensors need to detect a target. In this case, repellents are helpful to spread bionanosensors over the environment to increase the probability to detect a target.

4.4 Summary

In this chapter, we investigated through in silico experiments the feasibility of using bacteria as bionanosensors to form a dynamic bionanosensor network for target tracking. We developed first a mobility model of bacterium-based bionanosensors, and then evaluated the ability of bacterium-based bionanosensors to locate and track moving targets.

Key results and findings described in this chapter are the following:

- Repellents are useful for bacterium-based bionanosensors to increase the mean square distance from their original location (Subsection 4.3.2), while attractants are useful to decrease the mean square distance to a target location in the monitoring environment (Subsection 4.3.3). These results are consistent with previous results described in Chapter 3. This chapter uses a model of bacterium-based bionanosensors and gives detailed insight into the impact of individual model parameters associated with bacterium-based bionanosensors such as drift angles for repellents and attractants.

- Bacterium-based bionanosensors are able to track a moving target when the combined use of attractants and repellents is employed (Section 4.3.4). Unlike previous results described in Chapter 3, this chapter shows that both attractants and repellents are useful for target tracking and that an optimal combination of drift angles for repellents and attractants exists for tracking a moving target.

On-going work is to develop a more realistic model of bionanosensors [71]. In this chapter, the mobility of bionanosensors was modeled after flagellated bacteria [13]; the simple rotational diffusion model of chemotactic bacteria was modified to incorporate interactions through attractants and repellents. In more biologically realistic models, such as [17, 26, 84], the intracellular signaling dynamics (Fig. 4.1) are modeled deterministically using ordinary differential equations (ODEs) or simulated stochastically. The extracellular concentrations of attractants or repellents in those models affect the signaling dynamics within the bacteria, which determines how the flagellar motors rotate and how the bacteria migrate (i.e., run or tumble).

Future work involves more detailed modeling of the dynamics and properties of attractant and repellent molecules. This is necessary to understand how parameter values such as the diffusion coefficients of attractants and repellents impact the mobility patterns of bionanosensors and to identify the types of molecule that would be suitable as attractants and repellents. Future work also addresses practical aspects of bacterium-based bionanosensor networks. For example, the individual behavior and functionalities of bacterium-based autonomous bionanosensors (e.g., their sensitivity to attractants) may differ due to phenotypic differences, which need to be considered in the design of collective behavior. Also, bacterium-based autonomous bionanosensors may grow, divide and die during the target tracking operation, meaning that such population dynamics need to be considered.

Chapter 5

Conclusion

5.1 Summary of Thesis

In this thesis, we consider two major classes of problems in nanomedical applications of bionanosensor networks: target detection and target tracking. Targets in such applications can be disease sites or infectious microorganisms that represent potential threat to the environment, and timely detection of targets and tracking of targets are important to provide immediate treatments or further analysis of the environment. In this thesis, we design two types of bionanosensor networks: static and dynamic to attack the target detection or tracking problem. Here a static bionanosensor network consists of bionanosensors that are immobilized to perform application functionality, while a dynamic bionanosensor network consists of bionanosensors that autonomously migrate to perform application functionality.

In Chapter 1, we described the background of bionanosensor network research. We then introduced research challenges in bionanosensor networks and defined objectives of this thesis. We also illustrated an architecture of bionanosensor networks and reviewed related work to highlight contributions of this thesis.

In Chapter 2, we considered a static bionanosensor network for target detection application. In this type of bionanosensor network, bionanosensors are statically placed in the monitoring environment to detect targets that randomly walk in

the environment. We formulated the target detection problem as an optimization problem to find a spatial distribution of bionanosensors that can minimize mean residence time of targets. We then mathematically analyzed the problem under the condition that target arrival locations follow the uniform distribution: for one-dimensional environment, we found the optimal solution, and for n-dimensional environment ($n \geq 2$), we provided the lower bound expression. Furthermore, in a two-dimensional environment, where analytical approaches are not available, we assumed that target arrival locations follow the normal distribution and conducted simulation experiments to compare the performance of several placement schemes in terms of mean residence time.

In Chapter 3, we considered a dynamic bionanosensor network for target tracking. In this type of bionanosensor network, autonomous mobile bionanosensors use repellents and attractants to detect and track a moving target. Bionanosensors release repellents to spread over the monitoring environment in search of targets, while they release attractants to gather around a target location. We developed a mathematical model to describe the spatio-temporal dynamics of bionanosensors, repellents, and attractants, and demonstrated through numerical experiments that the dynamic bionanosensor network is able to locate and track a moving target under varieties of settings.

In Chapter 4, we investigated through in silico experiments the feasibility of using bacteria as bionanosensors to form a dynamic bionanosensor network. A bacterium is an microscale organism capable of sensing environmental conditions, producing chemical substances, and actively moving in the environment. Also, it can be genetically engineered to modify these functionalities. We first developed a mobility model of bacterium-based bionanosensors, and then evaluated the ability of bacterium-based bionanosensors to locate and track moving targets. Simulation results demonstrated that a group of bacterium-based bionanosensors is able to track a moving target when the combined use of attractants and repellents is employed, indicating that bacteria are promising materials to implement bionanosensors for target tracking.

In summary, we investigated for the first time in the literature two key problems in nanomedical applications of bionanosensor networks: target detection and target tracking. We believe that methods and results described in this thesis provide a basis for further studies toward development and deployment of bionanosensor networks for practical applications.

5.2 Future Work

The area of bionanosensor networks is still in its infancy. In the following, we discuss open research issues that need to be addressed in future work.

5.2.1 Wet Laboratory Experiments

An open research issue is to demonstrate bionanosensor networks in wet laboratory experiments. Research efforts in this area so far have been theoretical, and wet laboratory experiments need to be conducted to demonstrate the feasibility of bionanosensor networks, identify practical issues, and gain insight into the design of bionanosensor networks. In wet laboratory experiments, bionanosensors may be implemented using biomaterials such as bacteria (as we assumed in Chapter 4), other motile cells, and artificial cells [78], and their collective behavior is demonstrated for a specific application such as target detection and target tracking.

5.2.2 Robust Molecular Communication Methods

Another open research issue is to design and develop robust molecular communication methods through which bionanosensors can coordinate their behaviors in practical environments such as inside the human body. Methods of molecular communication we used in Chapters 3 and 4 are diffusion-based molecular communication in which bionanosensors communicate by propagating molecules in the environment [51]. Diffusion-based molecular communication may not however apply to an environment where molecules disperse quickly because in such

an environment the concentration of a molecule decreases quickly before it is detected by bionanosensors. Diffusion-based molecular communication is also vulnerable to the disturbance of the environment such as the blood flow. To address these issues, non-diffusion-based molecular communication may be utilized [62]. In non-diffusion-based molecular communication, bionanosensors may release adhesive molecules that bind to a surface in the environment to form a stable concentration gradient on the surface, allowing bionanosensors to communicate more robustly. Future work thus needs to be conducted to determine an appropriate method of molecular communication for a given environment.

5.2.3 Protocols and Architectures

Another open research issue is to define a set of protocols and generic architecture that can help design and develop practical applications of bionanosensor networks [57, 61]. A layered architecture traditionally used in computer networks [81] may provide a starting point for discussions. Based on a layered architecture, for instance, we may organize various research issues and design concerns in bionanosensor networks into layers that are relatively independent of each other in order to accelerate research and development in each layer.

5.2.4 Interfaces with External Devices

Another open research issue is to establish interfaces to interconnect bionanosensor networks deployed inside the human body and external devices that may be placed on or outside the human body [53, 54]. Such interfaces allow external devices to control bionanosensor networks and expand the capability and potential of bionanosensor networks as well as existing communication networks [3, 10]. For instance, bionanosensor networks deployed inside the human body may timely relay the information about the environmental conditions to an external device and enable real-time visualization [19]. Bionanosensor networks may be controlled from external devices via the Internet by a medical doctor for remote therapy or

tissue engineering [53]. Establishing such interfaces is also a first step toward developing fully autonomous bionanosensor networks that do not require external control.

5.2.5 Noise Effects

Another open research issue is to overcome noise effects. In Chapter 4, bionanosensors move based on the rotational random walk model due to noise effects, and as a result, target tracking performance exhibits large variance (Figs. 4.10 – 4.16). This may not be desirable depending on applications and we need to consider a robust design that can overcome noise effects. One method to overcome noise effects is to rely on a large number of bionanosensors. Another method is to utilize noise effects to improve system performance (e.g., based on stochastic resonance to enhance a signal-to-noise ratio as in neural information processing [43]). Future work needs to develop biologically implementable methods for bionanosensor networks to overcome noise effects.

Acknowledgment

Upon the completion of this thesis, I would like to borrow this opportunity to express my sincerest gratitude to those who have offered me assistances to the thesis.

First and foremost, I am deeply indebted to my honors supervisor, Prof. Shojiro Nishio, who not only accepted me as his student, but gave me insightful guidance to my research work and great encouragement to overcome all the obstacles I encountered. This thesis would never have been completed without his unfailingly wise advice and support.

Meanwhile, it is my pleasure and fortunate that Associate Prof. Takahiro Hara and Associate Prof. Tadashi Nakano become my direct advisors, assisting me to overcome the limitation of my knowledge and converting me into a researcher in this pioneering research field, as well as providing me invaluable advice and guidance throughout doctoral research work.

I would like to express my appreciation to Prof. Shinji Shimojo at Osaka University (Cybermedia Center) for his valuable advices and discussions as doctoral advisories.

I would also like to acknowledge the committee members of my thesis, Prof. Norihisa Komoda, Prof. Toru Fujiwara, and Prof. Makoto Onizuka at the Department of Multimedia Engineering of the Graduate School of Information Science and Technology of Osaka University. Their insightful and constructive comments considerably improved the quality of the thesis.

I am very grateful for the help and support from Prof. Yasushi Hiraoka at Os-

aka University, Prof. Tokuko Haraguchi at National Institute of Information and Communications Technology, Associate Prof. Jun Suzuki at University of Massachusetts Boston, Associate Prof. Kaname Harumoto at Osaka University, Associate Prof. Tomoki Yoshihisa at Osaka University, Associate Prof. Kazufumi Hosoda at Osaka University, Assistant Prof. Masumi Shirakawa at Osaka University, Associate Prof. Akimitsu Kanzaki at Shimane University, Dr. Tatsuya Suda at at the University Netgroup Incorporated, Dr. Jian-Qin Liu at National Institute of Information and Communications Technology, Dr. Michael John Moore at Qualcomm Incorporated, Dr. Shohei Kobayashi at National Institute of Information and Communications Technology, and Dr. Hiroyuki Hamada at Nisshin Giken.

I also would like to thank my team member, Takuya Obuchi with whom I had many discussions concerning the research and made good progress on research work.

With pleasure of studying and working with a number of very talented and warm hearted people at Nishio laboratory, I would like to express thanks to them.

Last but by no means least it gives me immense pleasure to offer my hearty thanks to my family and friends. No words can fully express my appreciation to their support and love in my life.

Finally, with all my best wishes to those wonderful people who ever gave me assistances, supports and encouragements throughout my research experience.

Bibliography

[1] N. Agoulmine, K. Kim, S. Kim, T. Rim, J. Lee, and M. Meyyappan. Enabling communication and cooperation in bio-nanosensor networks: toward innovative healthcare solutions. *IEEE Wireless Communications*, 19(5):42–51, 2012.

[2] I. F. Akyildiz, F. Brunetti, and C. Blazquez. Nanonetworks: a new communication paradigm. *Computer Networks*, 52:2260–2279, 2008.

[3] I. F. Akyildiz and J. M. Jornet. The internet of nano-things. *IEEE Wireless Communications*, 17(6):58–63, 2010.

[4] B. Alberts, A. Johnson, J. Lewis, M. Raff, K. Roberts, and P. Walter. *Molecular Biology of the Cell, Fifth Edition*. Garland Science, 2007.

[5] U. Alon. *An Introduction to Systems Biology: Design Principles of Biological Circuits*. Chapman and Hall, 1 edition, 2006.

[6] B. Atakan and O. B. Akan. On molecular multiple-access, broadcast and relay channels in nanonetworks. In *International Conference on Bio-Inspired Models of Network, Information, and Computing Systems (BIONETICS 2008)*, 2008.

[7] B. Atakan and O. B. Akan. Deterministic capacity of information flow in molecular nanonetworks. *Nano Communication Networks*, 1:31–42, 2010.

[8] B. Atakan, O. B. Akan, and S. Balasubramaniam. Body area nanonetworks with molecular communications in nanomedicine. *IEEE Communications Magazine*, 50(1):28–34, 2012.

[9] Y. Bae, N. Nishiyama, S. Fukushima, H. Koyama, M. Yasuhiro, and K. Kataoka. Preparation and biological characterization of polymetric micelle drug carriers with intracellular ph-triggered drug release property: Tumor permeability, controlled subcellular drug distribution, and enhanced in vivo antitumor efficacy. *Bioconjugate Chemistry*, 16:122–130, 2005.

[10] S. Balasubramaniam and J. Kangasha. Realizing the internet of nano things: Challenges, solutions, and applications. *Comuter*, 46(2):62–68, 2013.

[11] S. Basu, Y. Gerchman, C. H. Collins, F. H. Arnold, and R. Weiss. A synthetic multicellular system for programmed pattern formation. *Nature*, 434:1130–1134, 2005.

[12] Y. Benenson, B. Gil, U. Ben-Dor, R. Adar, and E. Shapiro. An autonomous molecular computer for logical control of gene expression. *Nature*, 429(6990):423–429, 2004.

[13] H. C. Berg. *Random Walks in Biology*. Princeton University Press, 1993.

[14] H. C. Berg. *E. coli in motion*. Springer, 2003.

[15] P. Bogdan, G. Wei, and R. Marculescu. Modeling populations of microrobots for biological applications. In *IEEE International Conference on Communications (ICC) Workshop on Molecular and Nano-scale Communications (MoNaCom 2012)*, 2012.

[16] D. Bray. Protein molecules as computational elements in living cells. *Nature*, 376:307–312, 2012.

[17] D. Bray, M. D. Levin, and K. Lipkow. The chemotactic behavior of computer-based surrogate bacteria. *Current Biology*, 17:12–19, 2007.

[18] S. F. Bush and S. Goel. Graph spectra of carbon nanotube networks. In *1st International Conference on Nano-Networks (NanoNet 2006)*, 2006.

[19] Y. Chen, P. Kosmas, P. S. Anwar, and L. Huang. A touch-communication model of tatarget drug delivery. In *Asia-Pacific Microwave Conference*, pages 528–530, 2014.

[20] L. C. Cobo and I. F. Akyildiz. Bacteria-based communication in nanonetworks. *Nano Communication Networks*, 1(4):244–256, 2010.

[21] S. Condamin, O. Benichou, and M. Moreau. First-exit times and residence times for discrete random walks on finite lattices. *Physics Review E*, 72(1), 2005.

[22] S. Condamin, O. Benichou, and M. Moreau. First-passage times for random walks in bounded domains. *Physical Review Letters*, 95, 2005.

[23] M. Csete and J. Doyle. Bow ties, metabolism and disease. *Trends in Biotechnology*, 9:446 – 450, 2004.

[24] A. W. Eckford. Nanoscale communication with brownian motion. *Proceedings of the 41st Annual Conference on Information Sciences and Systems*, pages 160–165, 2007.

[25] A. W. Eckford, N. Farsad, S. Hiyama, and Y. Moritani. Microchannel molecular communication with nanoscale carriers: Brownian motion versus active transport. In *IEEE International Conference on Nanotechnology*, pages 854–858, 2010.

[26] T. Emonet, C. M. Macal, M. J. North, C. E. Wickersham, and P. Cluzel. AgentCell: a digital single-cell assay for bacterial chemotaxis. *Bioinformatics*, 21(11):2714–2721, 2005.

[27] A. Enomoto, M. Moore, T. Nakano, and T. Suda. Stochastic cargo transport by molecular motors in molecular communication. In *2012 IEEE International Conference on Communications (ICC) Workshop on Molecular and Nano-scale Communications (MoNaCom 2012)*, pages 6142–6145, 2012.

[28] R. F. Fakhrullin, A. I. Zamaleeva, R. T. Minullina, S. A. Konnova, and V. N. Paunov. Cyborg cells: functionalisation of living cells with polymers and nanomaterials. *The Royal Society of Chemistry Review*, 41:4189–4206, 2012.

[29] D. T. Gillespie. Exact stochastic simulation of coupled chemical reactions. *The Journal of Physical Chemistry*, 81(25):2340–2361, 1977.

[30] A. Goel and V. Vogel. Harnessing biological motors to engineer systems for nanoscale transport and assembly. *Nature Nanotechnology*, 3:465–475, 2008.

[31] B. M. Gumbiner. Cell adhesion: The molecular basis of tissue architecture and morphogenesis. *Cell*, 84:345 – 357, 1996.

[32] A. Guney, B. Atakan, and O. B. Akan. Mobile ad hoc nanonetworks with collision-based molecular communication. *IEEE Transactions on Mobile Computing*, 11(3):353–366, 2011.

[33] H. Hayashi, K. Kono, and T. Takagishi. Temperature-controlled release property of phospholipid vesicles bearing a thermo-sensitive polymer. *Biochimica et Biophysica Acta*, 1280:127–134, 1996.

[34] S. Hiyama and Y. Moritani. Molecular communication: harnessing biochemical materials to engineer biomimetic communication systems. *Nano Communication Networks*, 1(1):20–30, 2010.

[35] C. T. Ho, R. Z. Lin, W. Y. Chang, H. Y. Chang, and C. H. Liu. Rapid heterogeneous liver-cell on-chip patterning via the enhanced field-induced dielectrophoresis trap. *The Royal Society of Chemistry*, 6:724–734, 2006.

[36] W. D. Jang, N. Nishiyama, G. D. Zhang, A. Harada, D. L. Jiang, S. Kawauchi, Y. Morimoto, M. Kikuchi, H. Koyama, T. Aida, and K. Kataoka. Supramolecular nanocarrier of anionic dendrimer porphyrins with cationic block copolymers modified with polyethylene glycol to enhance intracellular photodynamic efficacy. *Angewandte Chemie International Edition*, 44(3):419–423, 2005.

[37] S. Kadloor, R. S. Adve, and A. W. Eckford. Molecular communication using brownian motion with drift. *IEEE Transactions on NanoBioscience*, 11(2):89–99, 2012.

[38] H. Karl and A. Willig. *Protocols and Architectures for Wireless Sensor Networks*. Wiley, 2005.

[39] K. Kataoka, H. Miyazaki, M. Bunya, T. Okano, and Y. Sakurai. Totally synthetic polymer gels responding to external glucose concentration: Their preparation and application to on - off regulation of insulin release. *Journal of American Chemical Society*, 120:12694–12695, 1998.

[40] E. F. Keller and L. A. Segel. Model for chemotaxis. *Journal of Theoritical Biology*, 30:225–234, 1971.

[41] A. Kiourti, K. A. Psathas, and K. S. Nikita. Implantable and ingestible medical devices with wireless telemetry functionalities: A review of current status and challenges. *Bioelectromagnetics*, 35(1):1–15, 2014.

[42] H. T. Kung and D. Vlah. Efficient location tracking using sensor networks. In *IEEE Wireless Communications and Networking Conference (WCNC)*, 2003.

[43] L. Laer, M. Kloppstech, C. Schofl, T. J. Sejnowski, G. Brabant, and K. Prank. Noise enhanced hormonal signal transduction through intracellular calcium oscillations. *Biophysical Chemistry*, 91:157 – 166, 2001.

[44] K. Ma, Y. Zhang, and W. Trappe. Managing the mobility of a mobile sensor network using network dynamics. *IEEE Transactions on Parallel and Distributed Systems*, 19(1):106–120, 2008.

[45] M. U. Mahfuz, D. Makrakis, and H. T. Mouftah. On the characterization of binary concentration-encoded molecular communication in nanonetworks. *Nano Communication Networks*, 1(4):289–300, 2010.

[46] Y. Matsumura and H. Maeda. A new concept for macromolecular therapeutics in cancer chemotherapy: mechanism of tumoritropic accumulation of proteins and the antitumor agent smancs. *Cancer Research*, 46:6387–6392, 1986.

[47] M. J. Moore and T. Nakano. Addressing by beacon distances using molecular communication. *Nano Communication Networks*, 2(2-3):161–173, 2011.

[48] M. J. Moore and T. Nakano. Synchronization of inhibitory molecular spike oscillators. In *International Conference on Bio-Inspired Models of Network, Information, and Computing Systems (BIONETICS 2011)*, pages 183–195, 2011.

[49] M. J. Moore, T. Nakano, A. Enomoto, and T. Suda. Measuring distance from single spike feedback signals in molecular communication. *IEEE Transactions on Signal Processing*, 60(7):3576–3587, 2012.

[50] M. J. Moore, T. Suda, and K. Oiwa. Molecular communication: modeling noise effects on information rate. *IEEE Transactions on NanoBioscience*, 8(2):169–180, 2009.

[51] T. Nakano, A. Eckford, and T. Haraguchi. *Molecular Communication*. Cambridge University Press, 2013.

[52] T. Nakano, T. Hara, Y. Okaie, T. Obuchi, and S. Nishio. Mobile bionanosensor networks through molecular communication. In *Asia-Pacific Microwave Conference (APMC 2014)*, pages 525–527, November 2014.

[53] T. Nakano, S. Kobayashi, T. Suda, Y. Okaie, Y. Hiraoka, and T. Haraguchi. Externally controllable molecular communication. *IEEE Journal of Selected Areas in Communication (JSAC)*, 32(12):1–15, December 2014.

[54] T. Nakano, S. Kobayashi, T. Suda, Y. Okaie, Y. Hiraoka, and T. Haraguchi. Externally controllable molecular communication systems for pattern formation. In *Proc. 1st ACM International Conference on Nanoscale Computing and Communication*, 2014.

[55] T. Nakano and J. Q. Liu. Design and analysis of molecular relay channels: An information theoretic approach. *IEEE Transactions on NanoBioscience*, 9(3):213–221, 2010.

[56] T. Nakano, M. Moore, F. Wei, A. V. Vasilakos, and J. W. Shuai. Molecular communication and networking: opportunities and challenges. *IEEE Transactions on NanoBioscience*, 11(2):135–148, 2012.

[57] T. Nakano, M. J. Moore, Y. Okaie, and A. Enomoto. Cooperative drug delivery through molecular communication among biological nanomachines. In *IEEE International Conference on Communications (ICC 2013)*, June 2013.

[58] T. Nakano, M. J. Moore, Y. Okaie, A. Enomoto, and T. Suda. Swarming biological nanomachines through molecular communication for targeted drug. In *6th International Conference on Soft Computing and Intelligent Systems & The 13th International Symposium on Advanced Intelligent Systems (SCIS-ISIS 2012)*, pages 2317–2320, November 2012.

[59] T. Nakano, Y. Okaie, and J. Q. Liu. Channel model and capacity analysis of molecular communication with brownian motion. *IEEE Communications Letters*, 16(6):797–800, 2012.

[60] T. Nakano and J. Shuai. Repeater design and modeling for molecular communication networks. *Proceedings IEEE INFOCOM (International Con-*

ference on Computer Communications) Workshop on Molecular and Nanoscale Communications (MoNaCom 2011), pages 501–506, 2011.

[61] T. Nakano, T. Suda, Y. Okaie, M. J. Moore, and A. V. Vasilakos. Molecular communication among biological nanomachines: A layered architecture and research issues. *IEEE Transactions on NanoBioscience*, 13(3):169–197, 2014.

[62] T. Obuchi, Y. Okaie, T. Nakano, T. Hara, and S. Nishio. Inbody mobile bionanosensor networks through non-diffusion-based molecular communication. (submitted).

[63] Y. Okaie. Nanomachine distribution problems in nanonetworks: Optimization and heuristics. In *IEEE International Workshop on Molecular and Nanoscale Communication (MoNaCom 2012)*, June 2012.

[64] Y. Okaie and T. Nakano. Propagation delay of brownian molecules in nanobiosensor networks. In *6th International Conference on Bio-Inspired Models of Network, Information, and Computing Systems (BIONETICS 2011)*, December 2011.

[65] Y. Okaie and T. Nakano. Sensor placement strategies for detecting brownian molecules in nanonetworks. In *IEEE Wireless Communications and Networking Conference (WCNC 2012)*, pages 1777–1781, 2012.

[66] Y. Okaie, T. Nakano, T. Hara, K. Hosoda, Y. Hiraoka, and S. Nishio. Cooperative target tracking by a bacterium-based mobile sensor network. *IEEE Transactions on NanoBioscience*, 13(3):1–11, September 2014.

[67] Y. Okaie, T. Nakano, T. Hara, K. Hosoda, Y. Hiraoka, and S. Nishio. Modeling and performance evaluation of mobile bionanosensor networks for target tracking. In *IEEE Internatinoal Conference on Communications (ICC 2014)*, pages 3980–3985, June 2014.

[68] Y. Okaie, T. Nakano, T. Hara, and S. Nishio. Single target tracking in bionanosensor networks: Preliminary simulation results. In *8th International Conference on Body Area Networks (BODYNETS 2013)*, pages 476–477, October 2013.

[69] Y. Okaie, T. Nakano, T. Hara, and S. Nishio. Autonomous mobile bionanosensor networks for target tracking: A two-dimensional model. *Nano Communication Networks*, 5(3):63–71, September 2014.

[70] Y. Okaie, T. Nakano, T. Hara, and S. Nishio. Distributing nanomachines for minimizing mean residence time of molecular signals in bionanosensor networks. *IEEE Sensors Journal*, 14(1):218–227, January 2014.

[71] Y. Okaie, T. Nakano, T. Obuchi, T. Hara, and S. Nishio. Bacterium-based mobile bionanosensor networks for target tracking: A biologically realistic model. In *8th International Conference on Bio-Inspired Information and Communications Technologies*, December 2014.

[72] R. Phillips, J. Kondev, and J. Theriot. *Physical Biology of the Cell*. Garland Science, 2008.

[73] M. Pierobon and I. F. Akyildiz. A physical end-to-end model for molecular communication in nanonetworks. *IEEE Journal on selected areas in communications*, 28(4):602–611, 2010.

[74] M. Pierobon and I. F. Akyildiz. Diffusion-based noise analysis for molecular communication in nanonetworks. *IEEE Transactions on Signal Processing*, 59:2532–2547, 2011.

[75] P. E. M. Purnick and R. Weiss. The second wave of synthetic biology from modules to systems. *Nature Review Molecular Cell Biology*, 10:410–422, 2009.

[76] R. Rao and G. Kesidis. Purposeful mobility for relaying and surveillance in mobile ad hoc sensor networks. *IEEE Transactions on Mobile Computing*, 3(3):225–232, 2004.

[77] S. Redner. *A Guide to First-Passage Processes*. Cambridge University Press, 2010.

[78] Y. Sasaki, Y. Shioyama, W. J. Tian, J. Kikuchi, S. Hiyama, Y. Moritani, and T. Suda. A nanosensory device fabricated on a liposome for detection of chemical signals. *Biotechnology and Bioengineering*, 105(1), 2010.

[79] K. Sohraby, D. Minoli, and T. Znati. *Wireless Sensor Networks: Technology, Protocols, and Applications*. Wiley, 2007.

[80] K. V. Srinivas, R. S. Adve, and A. W. Eckford. Molecular communication in fluid media: the additive inverse gaussian noise channel. *IEEE Transactions on Information Theory*, 58(7):4678–4692, 2012.

[81] A. S. Tanenbaum and D. J. Wetherall. *Computer Networks*. Prentice Hall, 5th ed edition, 2010.

[82] R. Thar and M. Kuhl. Bacteria are not too small for spatial sensing of chemical gradients: An experimental evidence. *Proceedings of the National Academy of Sciences (PNAS)*, 100(10):5748–5453, 2003.

[83] V. P. Torchilin. Recent advances with lliposome as pharmaceutical carriers. *Nature Review Drug Discovery*, 4(2):145–160, 2005.

[84] N. Vladimirov, L. Løvdok, D. Lebiedz, and V. Sourjik. Dependence of bacterial chemotaxis on gradient shape and adaptation rate. *PLoS Computational Biology*, 4(12), 2008.

[85] G. Wei, P. Bogdan, and R. Marculescu. Bumpy rides: Modeling the dynamics of chemotactic interacting bacteria. *IEEE Journal of Selected Areas in Communication (JSAC)*, 31(12):879–890, 2013.

[86] G. Wei, P. Bogdan, and R. Marculescu. Efficient modeling and simulation of bacteria-based nanonetworks with bnsim. *IEEE Journal on Selected Areas in Communications (JSAC)*, 31(12):868–878, 2013.

[87] R. Weiss, S. Basu, S. Hooshangi, A. Kalmbach, D. Karig, R. Mehreja, and I. Netravali. Genetic circuit building blocks for cellular computation, communications, and signal processing. *Natural Computing*, 2(1):47–84, 2003.

[88] E. Xu, Z. Ding, and S. Dasgupta. Target tracking and mobile sensor navigation in wireless sensor networks. *IEEE Transactions on Mobile Computing*, 12(1):177–186, 2013.

[89] Y. Xu, J. Winter, and W. C. Lee. Prediction-based strategies for energy saving in object tracking sensor networks. In *IEEE International Conference on Mobile Data Management (MDM'04)*, 2004.

[90] J. W. Yoo, D. J. Irvine, D. E. Discher, and S. Mitragotri. Bio-inspired, bioengineered and biomimetic drug delivery carriers. *Nature Reviews Drug Discovery*, 10(7):521–535, 2011.

[91] R. Yoshida, Y. Kaneko, K. Sakai, K. Okano, Y. SakY. Sakurai. H. Bae, and S. W. Kim. Positive thermosensitive pulsatile drug release using negative thermosensitive hydrogels. *Journal of Controlled Release*, 32:97–102, 1994.

[92] L. You, R. S. Cox III, R. Weiss, and F. H. Arnold. Programmed population control by cellcell communication and regulated killing. *Nature*, 428:868 – 871, 2004.

[93] M. Younis and K. Akkaya. Strategies and techniques for node placement in wireless sensor networks: A survey. *Ad Hoc Networks*, 6:621–655, 2008.

[94] W. Zhang and G. Cao. Dctc: Dynamic convoy tree-based collaboration for target tracking in sensor networks. *IEEE Transactions on Wireless Communications*, 3(5):1689–1701, 2004.

[95] Y. Zou and K. Chakrabarty. Distributed mobility management for target tracking in mobile sensor networks. *IEEE Transactions on Mobile Computing*, 6(8):872–887, 2007.